Comparison of GLDAS, GLEAM, FLUXCOM and LSA-SAF Against ICOS Observations

Evaluation of evapotranspiration and turbulent energy fluxes during Belgian drought events

Technical report – MSc Internship

Supervisor
Prof.dr. Kwinten Van Weverberg

MSc student
Iva Pogarcic

Affiliations
Royal Meteorological Institute of Belgium
University of Ghent

July, 2026

Introduction

The increasing frequency, duration and severity of droughts across many regions of Europe have become an important topic in the context of climate change, particularly because of the increasing occurence of compound drought-heat events (Ionita et al., 2021; Bastos et al., 2022). Despite Belgium historically being considered a humid temperate region, recent years have been characterised by several severe droughts and heatwaves, increasing water stress and posing new challenges for ecosystems, agriculture and water management. Land–atmosphere interactions provide the physical background for the relationship between heat and drought. During drought, soil moisture becomes limiting, reducing evapotranspiration. Changes in evapotranspiration alter the partitioning of available energy between latent and sensible heat. These feedbacks influence surface temperature, boundary layer development, and weather and climate processes. As droughts become more frequent, accurately representing land–atmosphere interactions becomes increasingly important. Land surface variables such as evapotranspiration and turbulent heat fluxes cannot be measured everywhere. Therefore, they are estimated using different approaches, including land surface models, satellite remote sensing, machine-learning products, and products combining observations and modelling. These products are widely used in hydrology, weather forecasting, climate research and many other environmental applications. Different products often provide notably different estimates of the same variable, and their performance may change during drought, when land–atmosphere interactions become more complex. It is therefore important to understand whether, why and to what extent these products differ. This study compares several evapotranspiration and turbulent heat flux products against ICOS flux tower observations during drought conditions in Belgium. By identifying agreements, discrepancies and the potential causes of these differences, the study aims to evaluate the suitability of these products for drought-related research and applications.

Data preprocessing

Collection and preparation

The study combines in situ observations, gridded evapotranspiration products, drought indices , turbulent fluxes, land cover data and soil information to evaluate performance of different evapotranspiration products over Belgium.

Reference dataset were ICOS observations. Variables including latent heat flux (LE) , sensible heat flux (H), air temperature, soil water content, incoming shortwave radiation and percipitation were extracted for the selected Belgian stations.

Gridded data was obtained from LSA-SAF, GLEAM, GLDAS and FLUXCOM. These datasets were preprocessed and extracted for ICOS station locations as CSV files. Additional datasets describing land cover, soil characteristics were also included. ECOCLIMAP was used to characterize the land cover surrounding each station footprint, HWSD provided soil information, and SPI, SPEI, EDDI and SSI were used to describe drought conditions. Prior to the statystical analysis, all datasets were preprocessed to ensure consistency and comparability. This includes temporal and spatial harmonization, and quality control. Missing values resulting from data gaps or unavailable observations were excluded from the analysis. Performance metrics were calculated only for observations where both ICOS measurements and the corresponding product estimates were available.

Temporal harmonization

Because of different temporal resolutions, all datasets were harmonized to a common temporal resolution prior to comparison with the ICOS observation.

Daily analyses – For the daily analyses, all subdaily datasets were converted to daily values. They were then matched to ICOS daily observations. Daily temporal resolution was chosen as an agreement between the datasets with different temporal resolutions to much the most robust one – GLEAM.

Subdaily analyses – For the subdaily analyses, all datasets were harmonized to a common 3-hourly temporal resolution. Datasets with a finer temporal resolution were converted accordingly. 3-hourly temporal resolution was chosen based on the most robust resolution – GLDAS in order to observe subdaily behaviour of the fluxes. In this case, GLEAM was excluded from the analysis because of its daily resolution.

Spatial representativeness

One of the main challenges of product comparison was validating gridded products against point measurements. Because gridded products represent the average conditions within a grid cell, the comparison assumes that the ICOS observations are representative of the corresponding grid cell. To enable comparison, the gridded products were converted to station-based time series by associating each ICOS site with the corresponding grid cell by assigning each tower to the nearest grid cell using a nearest-neighbour approach. The resulting dataset was used to create time series that were compared to ICOS time series.

Data processing

The prepared datasets were aligned by station and observation date to obtain daily observations for each data product and the corresponding ICOS measurements. Time series were generated for the period 2015–2025, combining turbulent heat fluxes and selected drought indices (SPEI-1, SPEI-3, SPI-3, SSI and EDDI). Drought events were identified as consecutive periods during which SPEI-3 was ≤ -1 and were used to analyse the behaviour of latent heat flux (LE), sensible heat flux (H), air temperature (TA), soil water content (SWC), incoming shortwave radiation (SW), precipitation (P) and evaporative fraction (EF). Years were selected based on drought occurrence, overlapping data availability among stations and a minimum data coverage of 80% during the identified drought periods. In addition, 2018 and 2019 were analysed as case-study years because of their exceptionally warm and dry conditions in Belgium. Time series were first inspected for each drought event, after which seasonal comparisons were performed for the selected years. All identified drought events are presented in Table 1.

	Station	Year	Drought period(s)	SPEI-3 min	SPI-3 min	CDI max	EDDI max	SSI min	Minimum coverage (%)	Coverage ≥80%	Included in analysis
0	BE-Bra	2015	21 Jun–01 Jul	-1.18	NaN	2.0	1.33	-1.02	90.5	Yes	Yes
1	BE-Bra	2016	21 Sep–21 Feb	-2.13	-1.74	4.0	1.47	-2.03	34.8	No	No
2	BE-Bra	2017	21 May–01 Jul	-1.68	-1.27	4.0	1.87	-1.12	86.5	Yes	Yes
3	BE-Bra	2018	01 Jul–11 Oct; 11 Nov–21 Nov	-2.57	-2.73	2.0	3.23	-1.27	14.3	No	No
4	BE-Bra	2019	11 Sep–11 Sep	-1.35	NaN	1.0	1.43	0.26	90.9	Yes	Additional case study
5	BE-Bra	2020	11 May–11 Aug; 11 Sep–11 Sep	-1.94	-1.69	5.0	2.16	-2.95	94.2	Yes	No
6	BE-Bra	2022	21 Mar–21 Mar; 01 May–21 May; 11 Aug–01 Oct	-1.77	-0.89	4.0	2.16	-2.95	85.5	Yes	Yes
7	BE-Bra	2025	01 Apr–11 Oct; 01 Nov–01 Nov	-2.72	-2.68	2.0	NaN	NaN	0.0	No	No
8	BE-Dor	2015	21 Jun–01 Jul; 21 Jul–01 Aug	-1.26	NaN	2.0	1.03	-0.81	95.2	Yes	Yes
9	BE-Dor	2016	21 Sep–21 Feb	-2.03	-1.89	2.0	0.94	-2.11	43.9	No	No
10	BE-Dor	2017	01 May–01 May; 21 May–11 Jul	-1.74	-1.24	3.0	1.63	-0.89	100.0	Yes	Yes
11	BE-Dor	2018	01 Jul–21 Nov	-2.38	-2.04	2.0	3.05	-3.05	61.0	No	No
20	BE-Lon	2019	01 Jul–01 Jul; 01 Aug–01 Aug; 21 Aug–21 Sep	-1.48	-1.10	2.0	1.34	-2.67	83.3	Yes	Additional case study
21	BE-Lon	2020	11 May–11 Sep	-1.96	-2.02	2.0	2.10	-3.17	89.6	Yes	No
22	BE-Lon	2021	01 May–01 May	-1.03	NaN	1.0	0.39	-0.56	90.9	Yes	No
23	BE-Lon	2022	01 May–21 May; 11 Jun–11 Jun; 01 Jul–01 Sep; 2...	-2.10	-1.70	2.0	3.17	-3.17	72.7	No	No
24	BE-Lon	2025	01 Apr–01 Apr; 21 Apr–11 Jul; 21 Aug–01 Sep; 0...	-2.53	-1.74	2.0	NaN	NaN	0.0	No	No
25	BE-Vie	2015	01 Jun–01 Jun; 21 Jun–21 Aug	-1.70	-2.41	5.0	1.50	-0.46	80.6	Yes	Yes
26	BE-Vie	2016	21 Sep–21 Feb	-1.92	-2.19	2.0	1.80	-2.41	28.7	No	No
27	BE-Vie	2017	01 Jun–21 Jun	-1.58	-0.99	2.0	1.81	-0.93	90.3	Yes	Yes
28	BE-Vie	2018	01 May–11 May; 11 Jul–21 Nov	-1.99	-2.11	2.0	3.26	-2.97	71.5	No	No
29	BE-Vie	2019	01 Jul–01 Jul; 01 Aug–21 Sep	-1.49	-1.07	2.0	1.84	-1.19	74.2	No	No
30	BE-Vie	2020	21 May–01 Oct	-1.96	-1.77	5.0	2.23	-2.60	84.0	Yes	No
31	BE-Vie	2022	01 May–21 May; 11 Jun–11 Jun; 01 Jul–01 Sep; 2...	-1.58	-1.45	3.0	2.93	-1.02	76.2	No	No
32	BE-Vie	2023	01 Jul–11 Jul	-2.02	-0.67	3.0	2.14	-1.64	90.5	Yes	No
33	BE-Vie	2025	01 Apr–21 Jun; 11 Jul–11 Jul; 21 Dec–21 Dec	-2.06	-1.93	5.0	NaN	NaN	0.0	No	No

Table 1. Identified events based on SPEI – 3 (data derived from https://drought.emergency.copernicus.eu/tumbo/edo/download/ https://cds.climate.copernicus.eu/)

After filtering out the data inconsitencies, following events were selected for further analysis. Years 2015, 2017, 2022 were selected because of data availability for every station and presence of drought periods . Each event was zoomed in for each year and each station in order to analyse the relationship between different variables. Year 2018 and 2019 were added for stations with available data because of exceptionally dry and hot conditions during this period.They were therefore considered as additional case study. These events are shown in Table 2.

	Station	Year	Drought period(s)	SPEI-3 min	SPI-3 min	CDI max	EDDI max	SSI min	Coverage ≥80%	Included in analysis
0	BE-Bra	2015	21 Jun–01 Jul	-1.18	NaN	2.0	1.33	-1.02	Yes	Yes
1	BE-Bra	2017	21 May–01 Jul	-1.68	-1.27	4.0	1.87	-1.12	Yes	Yes
2	BE-Bra	2018	01 Jul–11 Oct	-2.57	-2.73	2.0	3.23	-1.27	Yes	Additional case study
3	BE-Bra	2019	11 Sep–11 Sep	-1.35	NaN	1.0	1.43	0.26	Yes	Additional case study
4	BE-Bra	2022	21 Mar–21 Mar; 01 May–21 May; 11 Aug–01 Oct	-1.77	-0.89	4.0	2.16	-2.95	Yes	Yes
5	BE-Dor	2015	21 Jun–01 Jul; 21 Jul–01 Aug	-1.26	NaN	2.0	1.03	-0.81	Yes	Yes
6	BE-Dor	2017	01 May–01 May; 21 May–11 Jul	-1.74	-1.24	3.0	1.63	-0.89	Yes	Yes
7	BE-Dor	2022	01 May–11 Jun; 01 Jul–01 Sep; 21 Sep–21 Sep	-2.05	-1.62	6.0	1.77	-0.58	Yes	Yes
8	BE-Lon	2015	01 Aug–11 Aug	-1.15	-0.85	1.0	0.56	-0.45	Yes	Yes
9	BE-Lon	2017	21 May–11 Jul	-1.76	-1.18	5.0	1.69	-2.33	Yes	Yes
10	BE-Lon	2018	21 Jun–11 Oct	-2.55	-2.49	2.0	2.01	-1.68	Yes	Additional case study
11	BE-Lon	2019	01 Jul–01 Jul; 01 Aug–01 Aug; 21 Aug–21 Sep	-1.48	-1.10	2.0	1.34	-2.67	Yes	Additional case study
12	BE-Lon	2022	01 Jul–01 Sep	-1.68	-1.30	2.0	3.17	-3.17	Yes	Yes
13	BE-Vie	2015	01 Jun–01 Jun; 21 Jun–21 Aug	-1.70	-2.41	5.0	1.50	-0.46	Yes	Yes
14	BE-Vie	2017	01 Jun–21 Jun	-1.58	-0.99	2.0	1.81	-0.93	Yes	Yes
15	BE-Vie	2018	01 May–11 May	-1.17	0.05	2.0	1.91	-0.53	Yes	Additional case study
16	BE-Vie	2019	01 Jul–01 Jul	-1.28	NaN	2.0	1.84	-0.86	Yes	Additional case study
17	BE-Vie	2022	01 May–21 May; 11 Jun–11 Jun; 01 Jul–01 Sep	-1.58	-1.45	3.0	2.93	-1.02	Yes	Yes

Table 2 . Selected events per station (data derived from https://drought.emergency.copernicus.eu/tumbo/edo/download/ https://cds.climate.copernicus.eu/)

Calculated metrics

The datasets were merged on identical timestamps, missing values were removed, statistics were computed for each site, year and product. Metrics were not calculated for any combined values but for each product seperately. All metrics were calculated for daily values. Afterwards, there were averaged to create mean values for one representative figure per station per year and event. Additionally, the daily values were combined to create additional set of figures where each figure presented one station, with the daily measures accross all events combined to one value that described the mean between all the values accross all events for each station.

Error definition

$$ei = Pi - Oi$$

Pi - value from the evaluated product

Oi - the corresponding ICOS observation

Positive error means the product overestimated ICOS, while a negative error means the product underestimated ICOS.

Bias

$$Bias\ =\left(\frac{1}{n}\right)\Sigma_{i=1}^{n}(P_i-\ O_i)$$

Positive bias indicates systematic overestimation, while a negative bias indicates systematic underestimation ,
the absolute value of the overall bias was counted afterwards

|Bias|

It takes the absolute value only after averaging signed errors

RMSE

$$RMSE=\sqrt{\left(\frac{1}{n}\right)\sum_{i=1}^{n(P_i-O_i)^2}}$$

Pi - value from the evaluated product
Oi - corresponding ICOS observation
n - number of paired observations

Mean absolute error

$$MAE = \left(\frac{1}{n}\right) \Sigma_{i=1}^{n} |P_i - O_i|$$

Pearson correlation coefficient was calculated to quantify linear relationship between the prdocut estimates and the ICOS observation

$$r = \frac{\Sigma\_(i=1)\hat{}n\ (P\_i - \bar{P})(O\_i - \bar{O})}{\sqrt{(\Sigma\_(i=1)\hat{}n(P\_i - \bar{P})\hat{}2\ \Sigma\_(i=1)\hat{}n(O\_i - \bar{O})\hat{}2)}}$$

KGE Kling-Gupta Efficiency

Gupta, H. V., Kling, H., Yilmaz, K. K., & Martinez, G. F. (2009)

re = correlation

alpha = represents the ratio of product variability to observed variability

beta= represents the ratio of the product mean to the observed mean

$$KGE = 1 - \sqrt{(r-1)^2 + (\alpha - 1)^2 + (\beta - 1)^2}$$

$$\alpha = \frac{\sigma_P}{\sigma_O}$$

alpha p = standard deviation of the product

alpha O = standard deviation of the ICOS observations

$$\beta = \frac{\bar{P}}{\bar{O}}$$

P̄ = mean product value

Ō = mean ICOS value

GLEAM, GLDAS, FLUXCOM, and LSA SAF

LSA SAF Land Surface Analysis Satellite Application Facility) is an EUMETSAT intiative that provides operational land surface products derived primarily from Meteosat Second Generation (MSG) satellite observations. The products are generated using physically based retrieval algorithms that combine satellite observations with supporting meteorological and land surface information to estimate variables describing the surface energy and water balance. In this study, the latent heat flux (LE) and sensible heat flux (H) products were used. Together these variables describe how the available surface energy is partitioned between evaporation and atmospheric demand. These variables are directly comparable with eddy covariance observations from ICOS stations and therefore provide an appropriate basis for evaluating product performance during drought conditions. Spatial resolution over Europe is approximately 3 km and temporal resolution 30-minute (LSA SAF).

GLDAS (Global Land Data Assimilation System) is a framework that combines satellite and ground observations with meteorological forcing to drive physically based land surface models. The software drives multiple, offline land surface models. It is a large archive of modeled and observed global surface meteorological data, parameters and output that results in 1-degree and 0.25 degree resolution in 3-hourly steps. This study used data in 0.25 degree resolution. GLDAS uses vegetation-based tiling approach to simulate sub-grid scale variability, with a 1-km global vegetation dataset as its basis (GLDAS: Project Goals | LDAS).

GLEAM (Global Land Evaporation Amsterdam Model) is a satellite-driven model that estimates terrestrial evapotranspiration and its individual components, including transpiration, bare-soil evaporation, interception loss, open-water evaporation and snow sublimation. Potential evaporation is calculated using the Penman equation based on net radiation, air temperature, wind speed and vegetation characteristics. Actual evaporation is then estimated by applying an evaporative stress factor that accounts for water limitations using satellite observations and soil moisture information. Root-zone soil moisture is simulated using a multilayer water balance model, while satellite-derived surface soil moisture is assimilated to improve the estimates. In this study, the latent heat and sensible heat flux products from GLEAM were used, with a spatial resolution of 0.25° and a daily temporal resolution (www.gleam.eu).

FLUXCOM uses machine learning to merge carbon flux measurements from FLUXNET eddy covariance towers with remote sensing and meteorological data to estimate net ecosystem exchange, gross primary productivity and terrestrial ecosystem. It provides carbon fluxes from two complementary experimental setups with respect to the input covariates and resulting global gridded products. There is the remote sensing “RS” setup, where fluxes are estimated exclusively from Moderate Resolution Imaging Spectroradiometer (MODIS) satellite data. The second approach also exploits meteorological information. Data derived with this second approach, with 0.25 degree spatial, and daily temporal resolution, has been used for this research (fluxcom.org/Approach/).

Results

There are six terrestrial ICOS stations in Belgium. This study includes BE-Brasschaat (BE-Bra), BE-Dorinne (BE-Dor), BE-Lonzee (BE-Lon), and BE-Vielsalm (BE-Vie). Following the initial data-quality assessment, BE-Lochristi was excluded because no ICOS flux data were available, and BE-Maasmechelen was excluded due to data inconsistencies.

Station in Brasschaat (BE-Bra)

BE-Bra is an ICOS ecosystem station located in the experimental forest of Brasschaat, approximately 20 km northeast of Antwerp in the Belgian Campine region (51.30761° N, 4.51984° E) at an elevation of 16 m above sea level. The site experiences a temperate maritime climate with a mean annual temperature of 10.5 °C, mean annual precipitation of 920.7 mm, and mean annual incoming radiation of 112.5 W m^{-2}. The measurement site consists of a 2 ha even-aged Scots pine (Pinus sylvestris L.) stand embedded within a 150 ha mixed coniferous-deciduous forest dominated by Scots pine. The surrounding forest contains native broadleaf species, including silver birch (Betula pendula), rowan (Sorbus aucuparia) and pedunculate oak (Quercus robur), as well as introduced species such as northern red oak (Quercus rubra) and sweet chestnut (Castanea sativa). (meta.icos-cp.eu). As a mature coniferous forest with predominantly sandy soils, BE-Bra provides an opportunity to investigate the response of a forest ecosystem to drought conditions and to evaluate the performance of different evapotranspiration products. (icos-belgium.be)

Figure 1 presents the complete multi-year evolution of the measured turbulent fluxes and meteorological variables at BE-Bra, illustrating the seasonal variability and the timing of the selected drought events. It was created based on meteorological data and computed drought indices. Overview figures for the remaining stations (BE-Lon, BE-Vie and BE-Dor) are provided in Appendix A (Figures A1–A3).

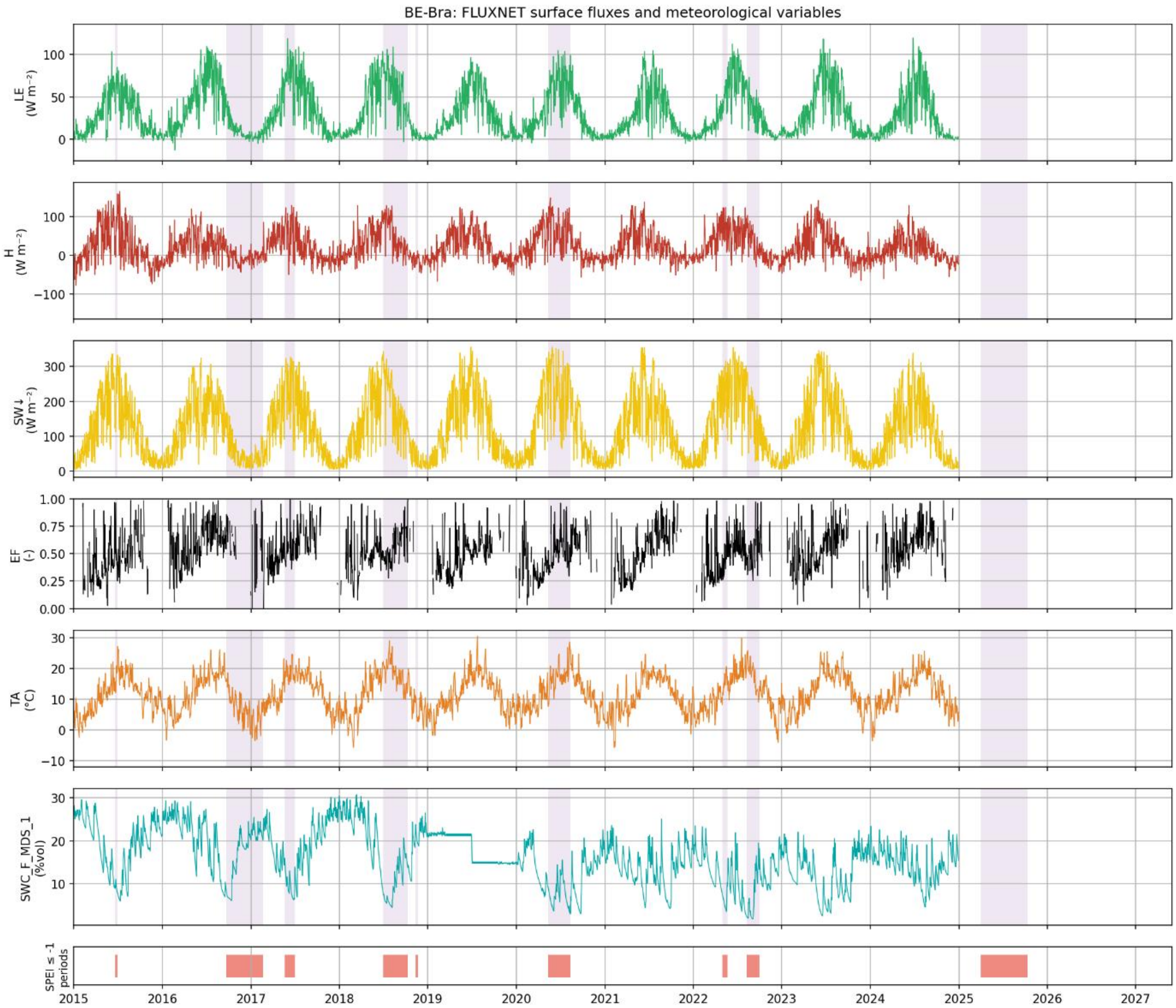

Figure 1. *Overview of measured flluxes and meteorological variables (ICOS Carbon Portal; figure created gy the author))*

	Station	Year	Event	Drought period	SPEI-3 min	SPEI-3 mean	SPEI-1 min	SPEI-1 mean	SPI-3 min	SPI-3 mean	CDI max	CDI mean	EDDI max	EDDI mean	SSI min	SSI mean
0	BE-Bra	2015	1	21 Jun–01 Jul	-1.18	-1.14	-1.00	-0.77	NaN	NaN	2.0	1.50	1.33	0.89	-1.02	-0.62
1	BE-Bra	2017	3	21 May–01 Jul	-1.68	-1.33	-2.26	-1.21	-1.27	-1.27	4.0	2.00	1.87	1.21	-1.12	-0.51
2	BE-Bra	2018	4	01 Jul–11 Oct	-2.57	-1.87	-2.04	-1.02	-2.73	-1.59	2.0	2.00	3.23	1.23	-1.27	-0.25
3	BE-Bra	2019	6	11 Sep–11 Sep	-1.35	-1.35	-1.61	-1.61	NaN	NaN	1.0	1.00	1.43	1.28	0.26	0.40
4	BE-Bra	2022	9	21 Mar–21 Mar	-1.04	-1.04	-1.77	-1.77	NaN	NaN	2.0	2.00	2.16	1.93	-2.28	-1.98
5	BE-Bra	2022	10	01 May–21 May	-1.59	-1.28	-1.51	-0.98	-0.89	-0.89	4.0	2.67	1.35	0.96	-2.95	-1.36
6	BE-Bra	2022	11	11 Aug–01 Oct	-1.77	-1.36	-1.34	-0.22	-0.89	-0.89	4.0	2.67	2.00	1.12	-2.95	-0.88

Table 3. *Values of drought indices for selected drought events (data derived from https://drought.emergency.copernicus.eu/tumbo/edo/download/ https://cds.climate.copernicus.eu/)*

BE Bra 2015 and 2017

The first drought event at BE-Bra occurred between the end of June and the beginning of July 2015 and was relatively moderate according to the drought indices. Meteorological drought occurred simultaneously with increased atmospheric evaporative demand and declining soil moisture conditions. During the event, LE remained relatively high but showed considerable day-to-day variability, while H also fluctuated strongly. Although soil water content continued to decrease throughout the drought, EF did not show a persistent decline. The absence of a strong decline in LE or EF suggests that evapotranspiration was not strongly constrained by the decreased soil moisture. The 2017 drought event at BE-Bra occurred between the end of May and the beginning of July and was more severe and persistent than the event observed in 2015. All drought indices consistently indicated severe meteorological drought, increased atmospheric evaporative demand and declining soil moisture conditions. Similar to 2015, LE remained relatively high at the beginning of the drought period and generally continued to increase into early summer despite the decline in soil moisture, suggesting that evapotranspiration was initially maintained even as water availability in the measured soil layer decreased. High incoming shortwave radiation and elevated air temperatures during the first part of the event provided favourable conditions for evapotranspiration. However, as the drought progressed and soil moisture reached its lowest values towards the end of June and the beginning of July, LE became increasingly variable, with several declines, while H showed strong fluctuations. Although EF also became more variable during the latter part of the event, it did not show a sustained decrease.Following the drought period, soil moisture increased and LE generally remained high during July and August. Similar to 2015, the 2017 event shows that the forest ecosystem was able to maintain substantial latent heat flux throughout much of the prolonged drought period despite declining soil moisture. Considering relatively moderate warm and dry conditions during 2015 and 2017 throughout all examined years, figures will be provided in the Appendix B (B1-B8) and only mentioned briefly throughout this report, unless especially relevant for a particular case.

Be BRA 2022 event 3

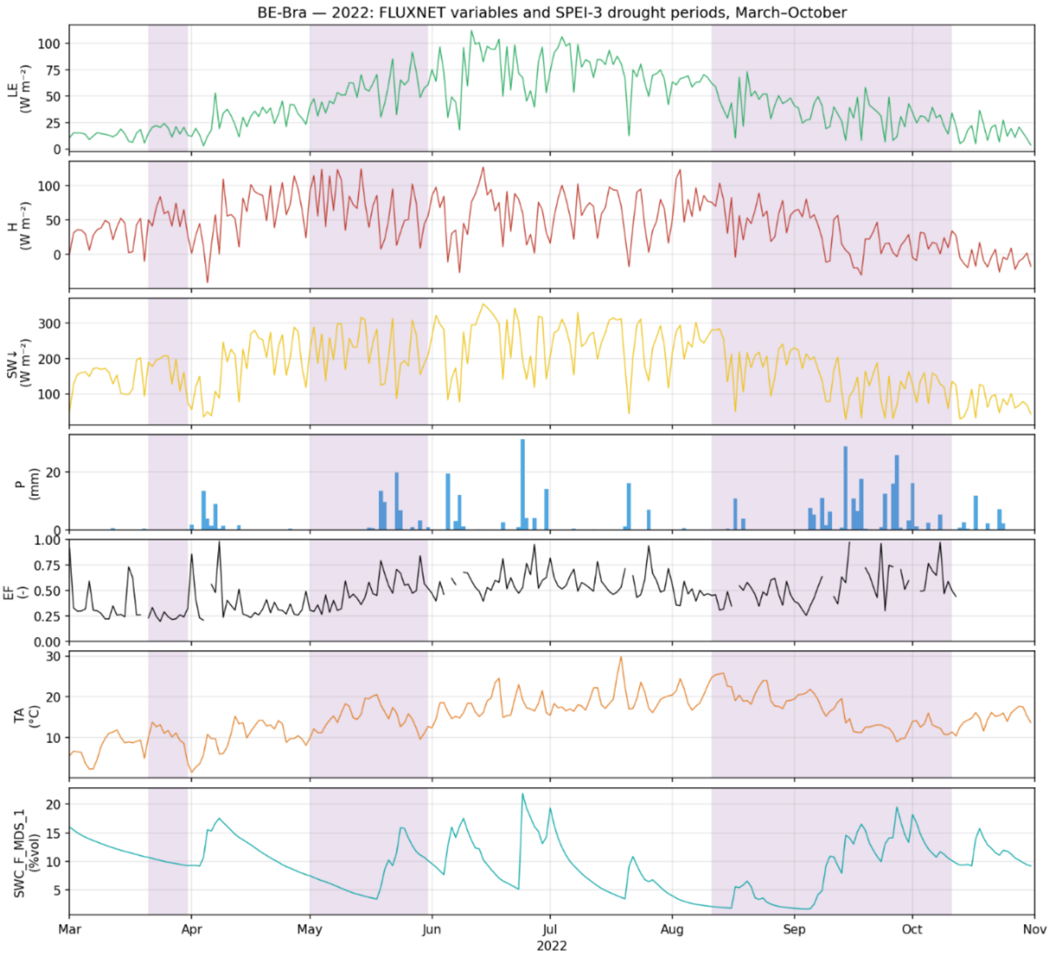

Figure 2*. Fluxnet variables BE Bra 2022 (ICOS Carbon Portal; figure created by the author)*

The 2022 drought conditions at BE-Bra differed from those observed in 2015 and 2017 because several drought periods occurred throughout the observed season. The first event occurred at the end of March and was relatively moderate according to the drought indices. However, the combination of short-term water-balance deficits, increased atmospheric evaporative demand and dry soil conditions suggests that this event could represent a flash drought.

During this early-season event, LE remained relatively low, while H was generally higher and EF remained below approximately 0.4. When interpreting this energy partitioning, the seasonal development of the forest should be considered. Incoming shortwave radiation and air temperature were still relatively low compared to summer conditions. Although the forest is evergreen, seasonal differences in canopy development, together with the relatively low radiation and air temperatures, likely limited transpiration. During May, increasing solar radiation enhanced evapotranspiration, resulting in increasing LE and EF despite the continued decline in soil moisture. Similar to the 2015 and 2017 events, this does not yet suggest clear water limitation. This may explain the absence of drought conditions between June and August and the relatively high LE during this period, as the forest canopy could still access sufficient available soil water.

The situation changed in August. Lower LE and EF together with low soil moisture suggest increasing water limitation, particularly under the combination of high incoming shortwave radiation and elevated air temperature.

Summary

BE-Bra is a coniferous forest site located at approximately 16 m elevation. Across the analysed drought events, latent heat flux remained relatively high even after meteorological drought developed and the measured soil water content continued to decrease. One possible explanation is the rooting characteristics of the forest vegetation. Trees may access water stored in deeper soil layers that are not represented by the relatively shallow soil moisture measurements. Declining soil water content in the observed soil layer does not necessarily imply an immediate reduction in the total amount of water available for transpiration. This could explain why LE remained comparatively high during several drought periods and why a persistent decrease in EF was generally absent. The delayed response of LE to declining soil moisture suggests that the forest ecosystem may be able to buffer short- to medium-duration meteorological drought conditions, although the increasing variability of LE during the prolonged 2017 drought and the lower LE and EF observed during the late-summer drought in 2022 may indicate the onset of water limitation. Atmospheric conditions also contributed to the observed flux behaviour. High incoming shortwave radiation increases the energy available for evapotranspiration, while elevated air temperatures increase atmospheric evaporative demand. When sufficient water remained accessible to the vegetation, these conditions could sustain or even enhance LE despite declining soil moisture. However, if water availability became increasingly limited, the same high evaporative demand could intensify vegetation water stress, resulting in stomatal regulation, reduced transpiration and a shift in energy partitioning from LE towards H. Such a clear and persistent transition was not observed at BE-Bra, suggesting that water availability remained sufficient to maintain substantial evapotranspiration during most of the analysed drought periods.

Additional analysis 2018 / 2019

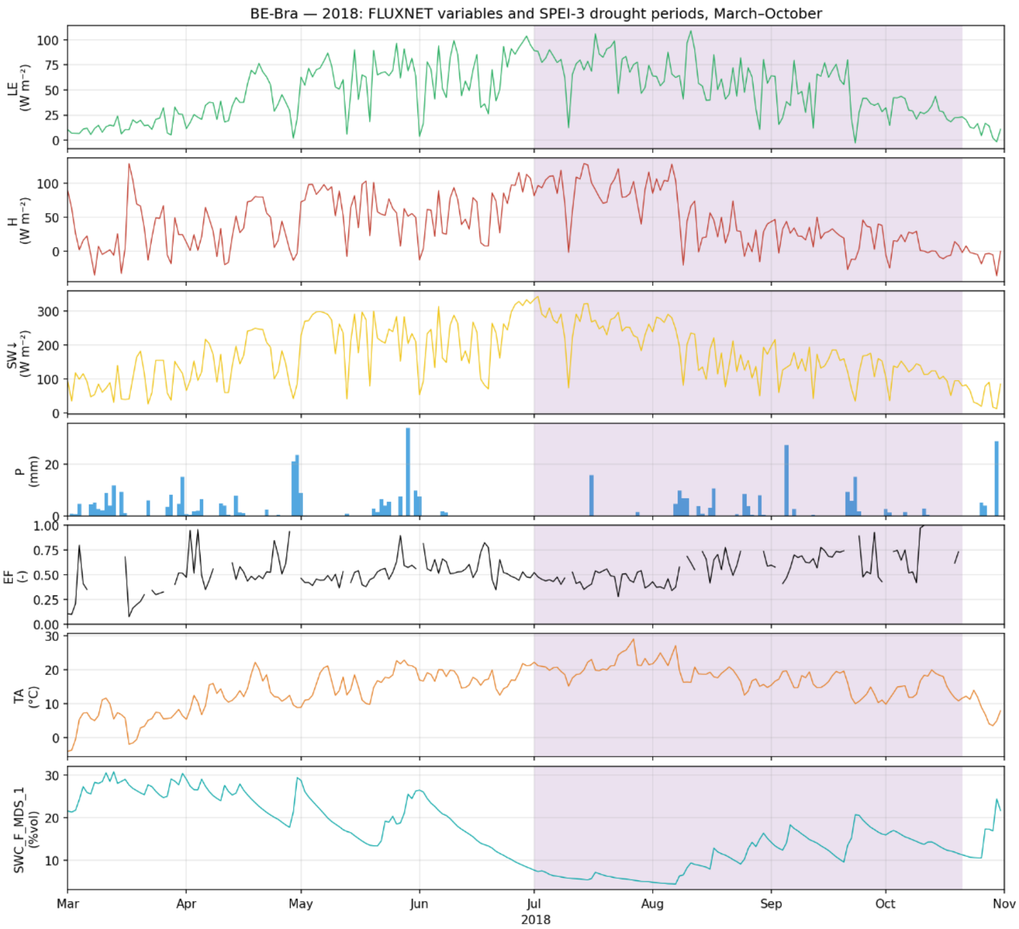

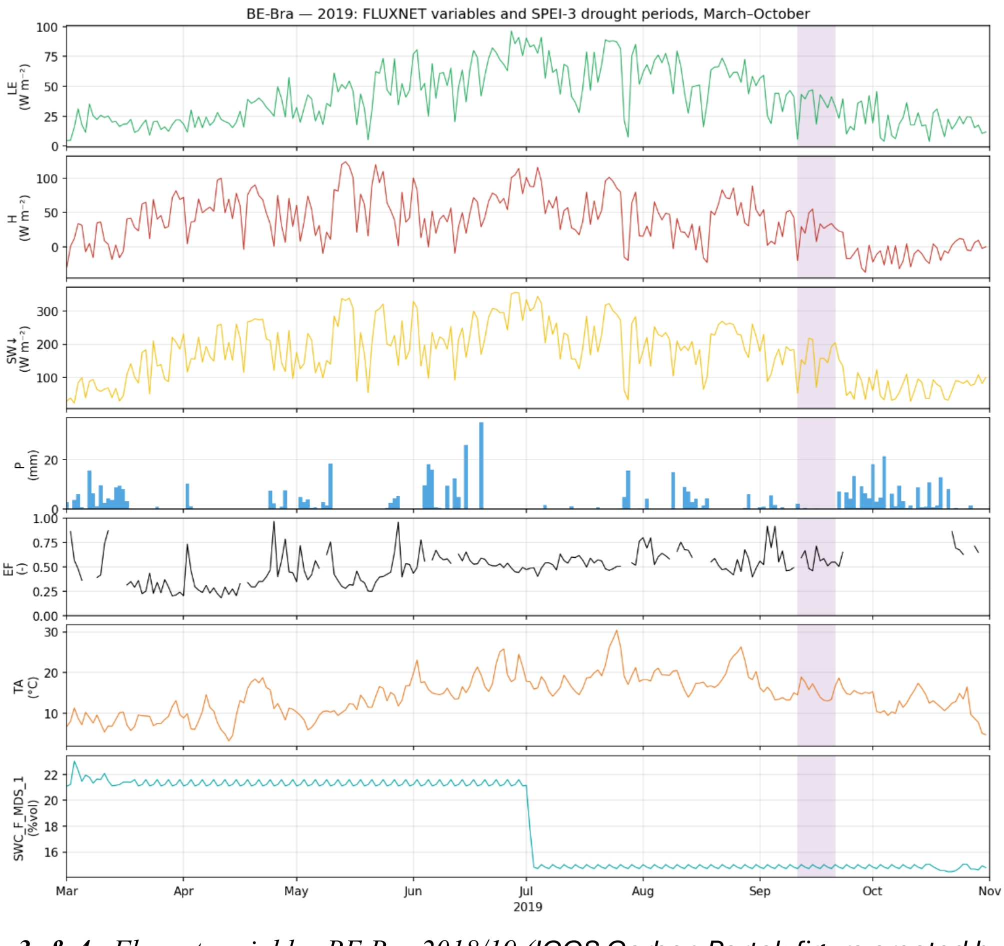

Figure 3. & 4.. *Fluxnet variables BE Bra 2018/19 (ICOS Carbon Portal; figure created by the author)*

The additional analysis of 2018 and 2019 provides further insight into the response of the coniferous forest at BE-Bra during warm and dry conditions. In 2018, a prolonged drought period developed from July onwards and happened simultaneously with elevated air temperatures and high incoming solar radiation. During the first part of the drought, LE remained relatively high despite the decline in soil moisture, while EF remained relatively stable and H reached high values. This suggests that evapotranspiration was initially maintained despite increasing meteorological drought and depletion of moisture in the measured soil layer. Later in summer, LE gradually declined, but EF did not show a corresponding persistent decrease and even increased during parts of August and September. The reduction in LE therefore appears to be partly related to decreasing available energy and seasonal progression rather than a clear transition towards a water-limited system.

The interpretation of 2019 is more uncertain because the soil moisture record shows an abrupt decrease around the beginning of July, followed by nearly constant values for the remaining season. This behaviour is unlikely to represent natural soil moisture variability and suggests a possible measurement issue. Therefore, the soil moisture measurements were not used as strong evidence of soil water limitation during this period. The drought event identified in September was relatively short, and LE had already begun to decline before its onset. H also decreased during and after the event, while EF remained relatively stable. Together with declining incoming solar radiation and moderate temperatures, this suggests that the late-season reduction in turbulent fluxes was more strongly influenced by seasonal changes in available energy than by a drought-induced shift from LE towards H.

The additional 2018 and 2019 case studies support the response observed during the main analysis years at BE-Bra. Even during prolonged warm and dry conditions, the coniferous forest generally maintained substantial LE and showed no consistent decline in EF. These additional years therefore reinforce the interpretation of a relatively buffered ecosystem response to meteorological drought, with no clear transition towards a water-limited system.

Evaporative fraction

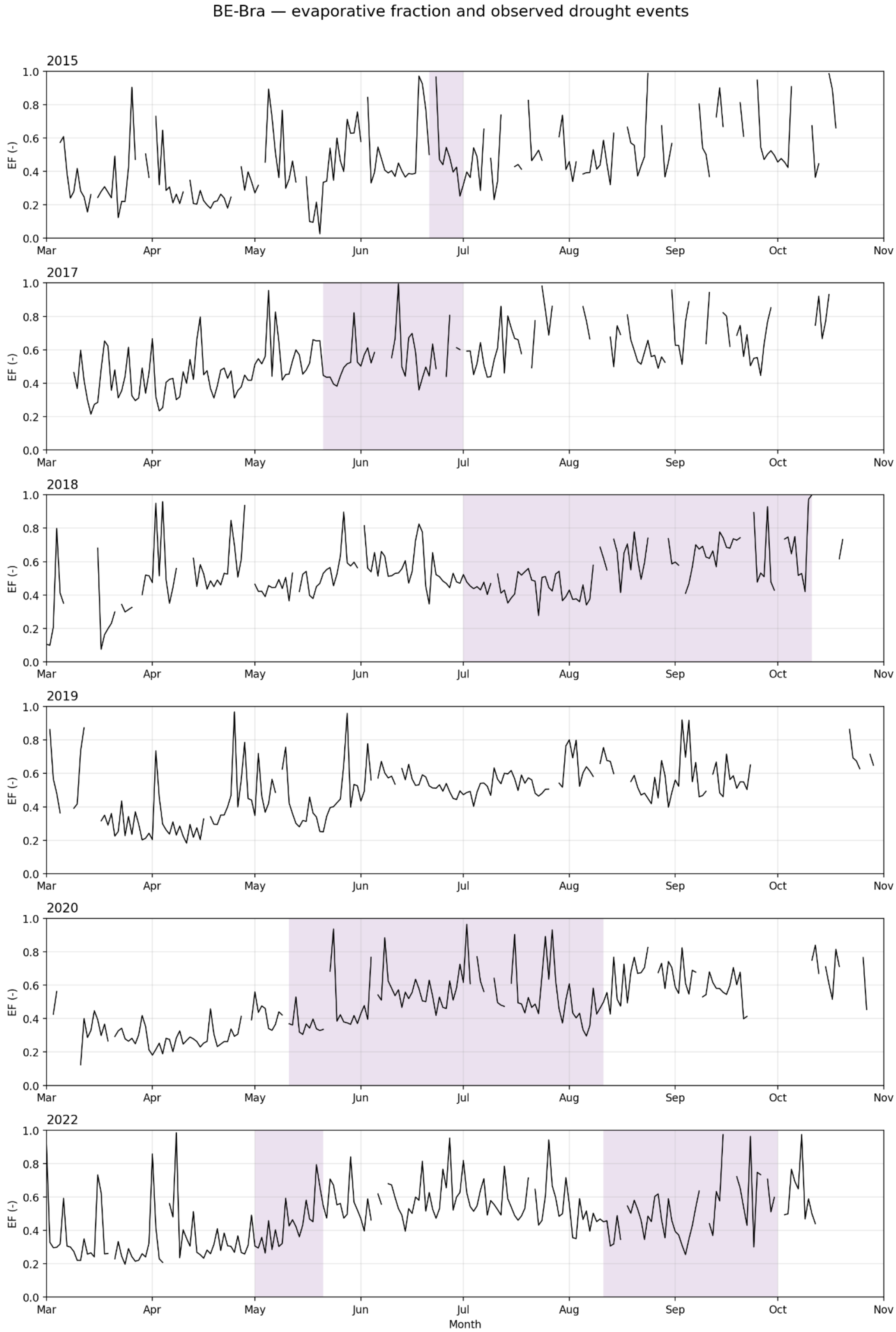

Figure 5. *Evaporative fraction BE Bra (computed using LE H ICOS (ICOS Carbon Portal; figure prepared by the author)*

Figure shows the temporal evolution of the evaporative fraction during the analysed drought events at BE-Bra. Although short-term fluctuations are evident, no systematic decrease in EF was observed during the drought periods. Instead, EF remained relatively stable throughout the events, suggesting that the partitioning between latent and sensible heat fluxes remained largely unchanged despite the drought conditions.

Comparison between FLUXNET and GLEAM; GLDAS and LSA SAF at BE Bra

The comparison between the different products was based on the computed EF for each station and each year. Figures for year 2015 and 28017 will be provided in Appendix (C-C4) unles particularly relevant for the analysis. Similar figures were also generated separately for LE and H. These figures will be included in the Appendix (C4 -C24) unless they are required for additional analysis.

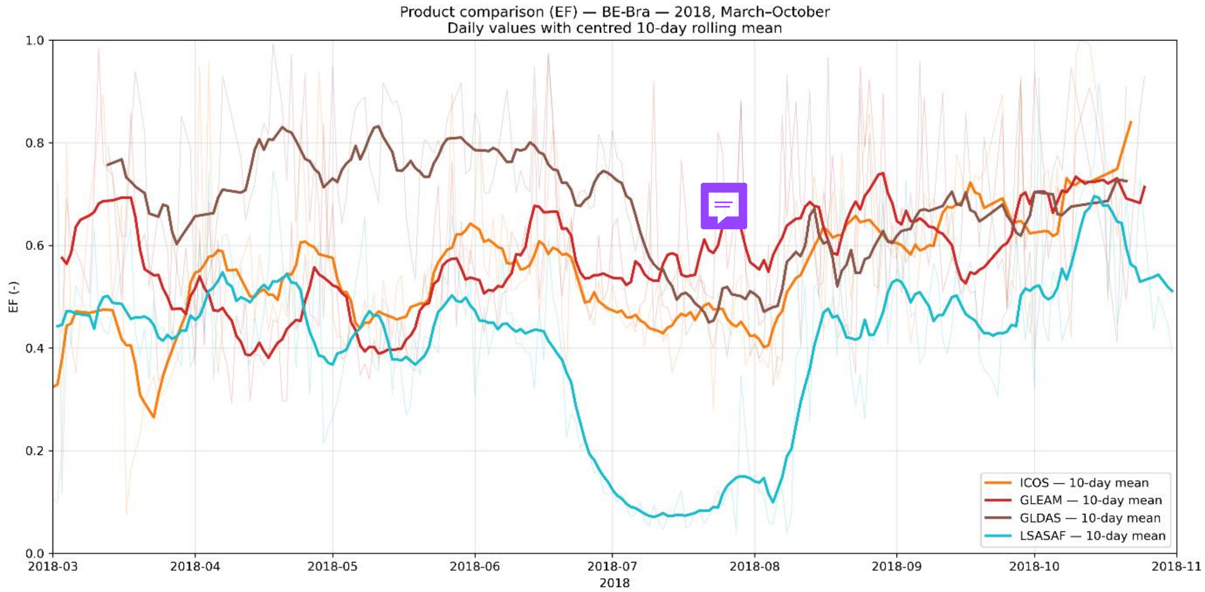

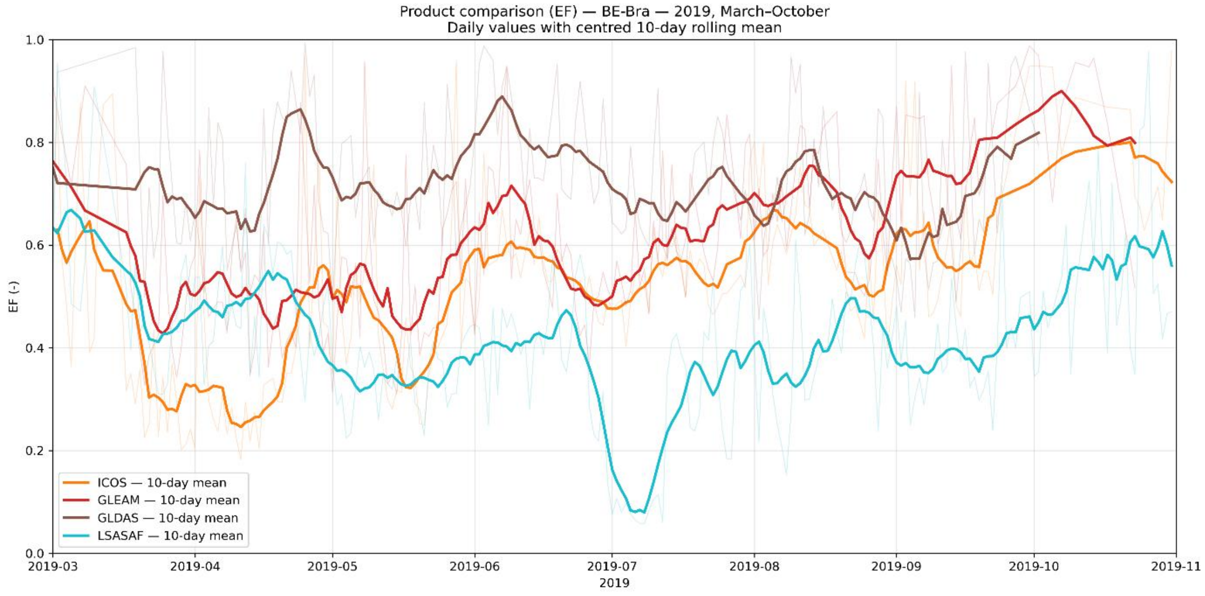

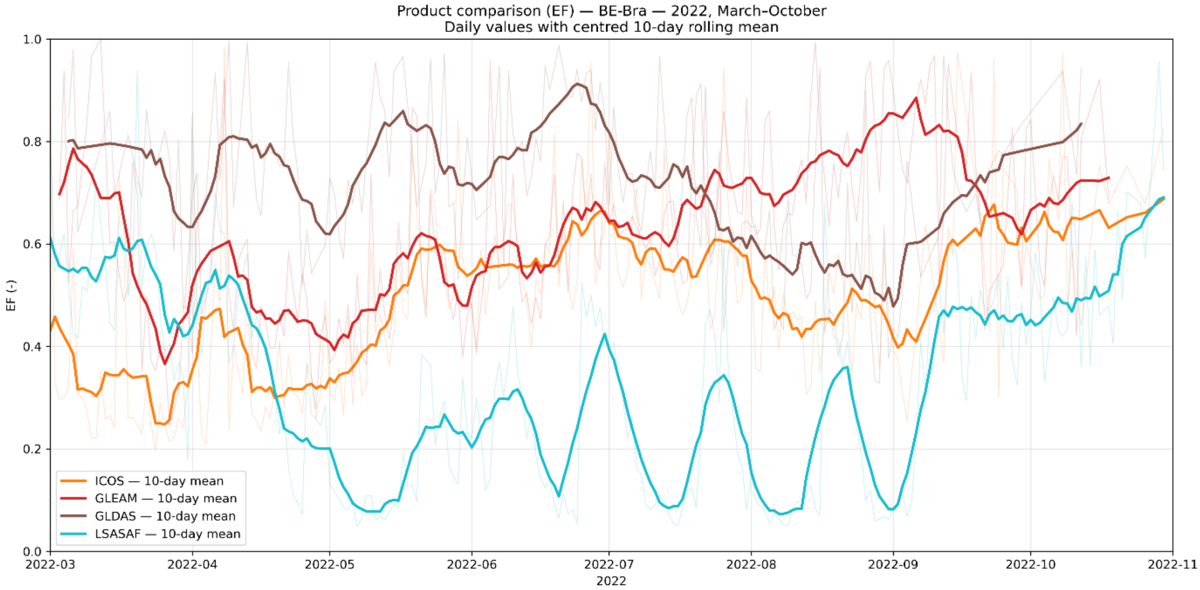

Figure 6.,7 & 8. *Comparison BE Bra GLEAM GLDAS LSASAF (ICOS Carbon Portal, GLEAM, GLDAS, and LSA-SAF; figure created by the author)*

Figures present the evaporative fraction (EF) at BE-Bra for 2018, 2019 and 2022. Differences in the magnitude and seasonal evolution of EF are observed between the products. ICOS observations and GLEAM generally exhibit the highest EF values throughout the observed periods, whereas LSA SAF consistently produces lower estimates. GLDAS also remains below the ICOS observations during most periods. The largest discrepancies between the products occur during the summer months. Overall, GLEAM shows the closest agreement with the ICOS observations at the coniferous forest site, whereas LSA SAF exhibits the largest deviations, particularly during the summer drought periods.

Diurnal cycles

To simplify the comparison between the evaluated products, event-averaged daytime diurnal LE and H cycles were created for consecutive two-month periods, three times per year. Each cycle represents the average daytime diurnal variation over a two-month period. These figures are intended to compare the overall shape of the diurnal cycle, as well as the timing and magnitude of the daytime LE and H peaks, across the different products.

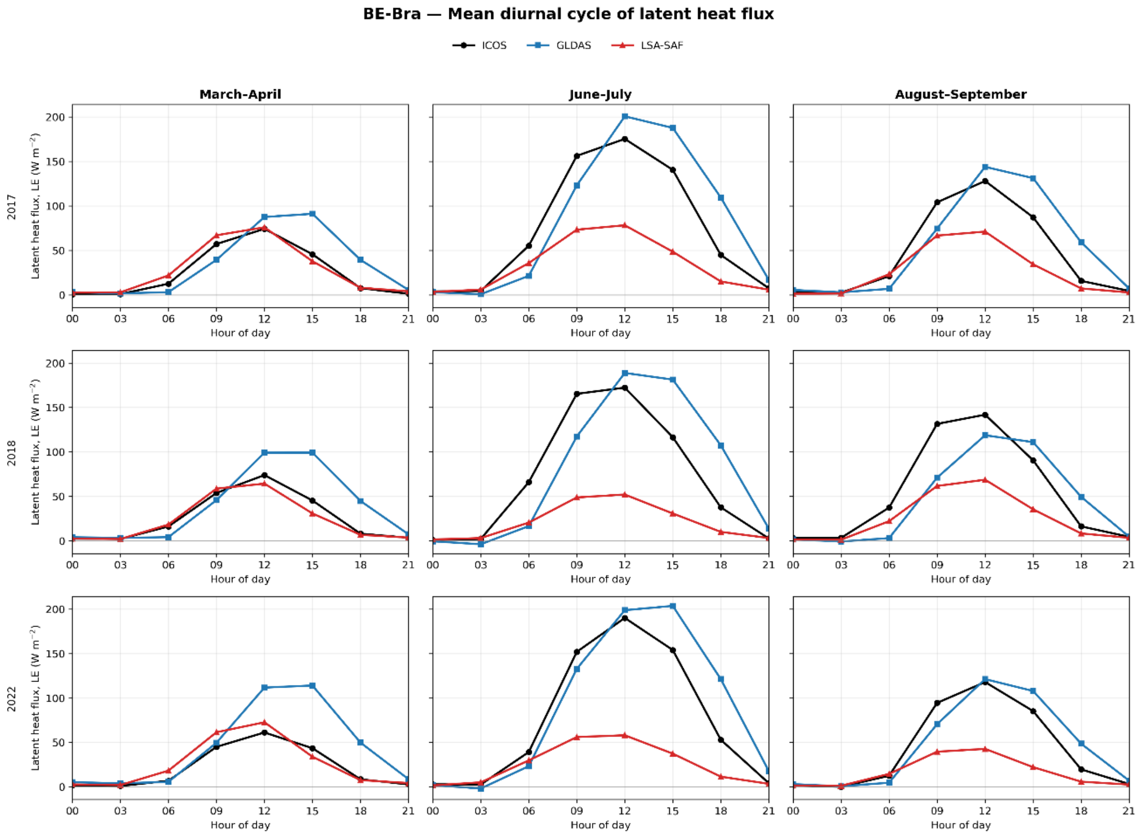

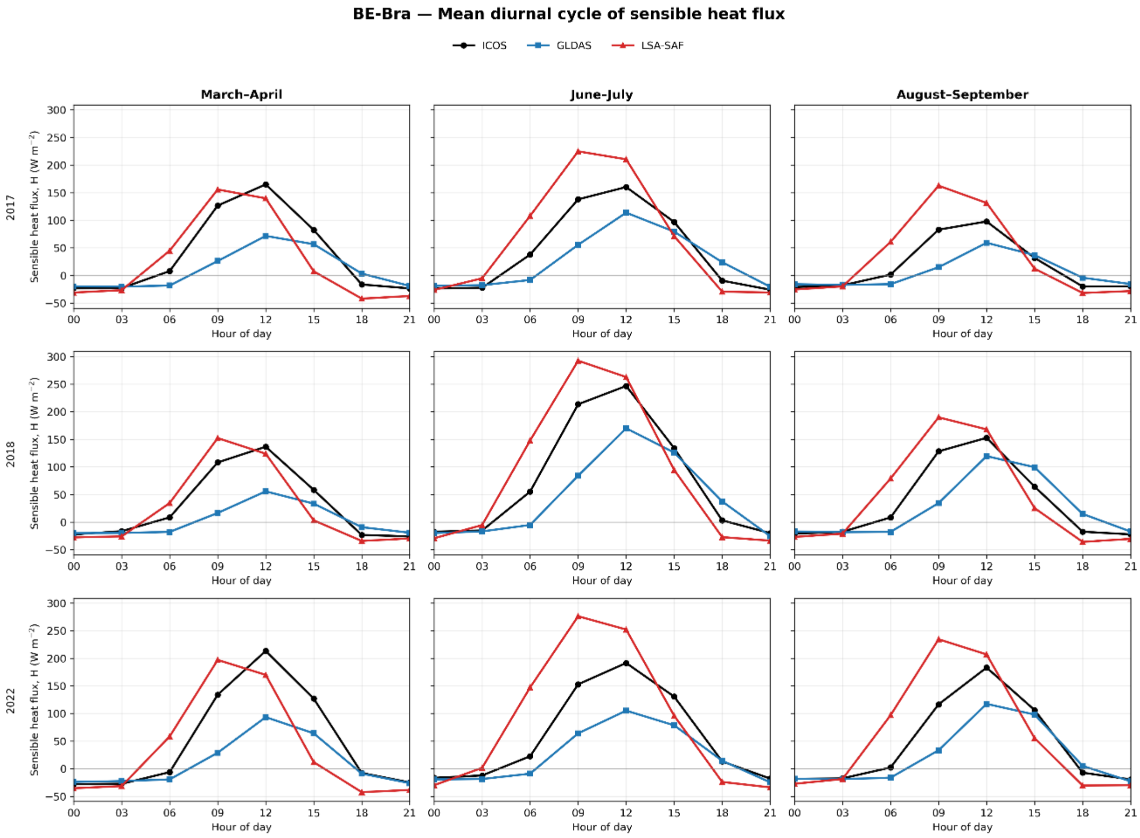

Figure 9 & 10. *Averaged daytime LE and H cycles (ICOS Carbon Portal, GLEAM, GLDAS, and LSA-SAF; figure created by the author)*

Overall performance metrics

For each station and event, performance metrics were computed from the daily average values, including KGE, RMSE, MAE, bias, absolute bias, Pearson correlation, α, and β. Across the evaluated stations, GLEAM generally showed the strongest agreement with the ICOS observations, reflected by higher KGE values and lower RMSE and MAE than the other products. However, performance varied between ecosystems and years, indicating that no single product consistently outperformed the others under all conditions. The resulting tables are presented in the Appendix E1-E4. For each station, the event-specific metrics were averaged across all events to obtain a single performance value for EF, LE, and H, which is presented in a separate set of figures.Across the evaluated stations, GLEAM generally showed the strongest agreement with the ICOS observations, reflected by higher KGE values and lower RMSE and MAE than the other products. However, performance varied between ecosystems and years, indicating that no single product consistently outperformed the others under all conditions.

BE-Bra

	site	variable	product	KGE	RMSE	MAE	bias	absolute_bias	pearson_r	alpha	beta	n
0	BE-Bra	EF	GLDAS	-0.01	0.30	0.26	0.22	0.22	0.11	0.87	1.45	782
1	BE-Bra	EF	GLEAM	0.48	0.17	0.13	0.06	0.06	0.50	0.93	1.13	782
2	BE-Bra	EF	LSASAF	0.00	0.26	0.22	-0.14	0.14	0.04	0.96	0.72	782
3	BE-Bra	LE	GLDAS	0.52	22.76	16.94	12.30	12.30	0.81	1.19	1.39	1825
4	BE-Bra	LE	GLEAM	0.68	17.85	13.28	8.57	8.57	0.84	1.03	1.27	1825
5	BE-Bra	LE	LSASAF	0.32	24.24	15.70	-12.18	12.18	0.66	0.56	0.61	1825
6	BE-Bra	H	GLDAS	-0.01	36.54	27.93	-21.97	21.97	0.72	0.68	0.08	1825
7	BE-Bra	H	GLEAM	0.67	23.80	17.47	-5.74	5.74	0.84	0.85	0.76	1825
8	BE-Bra	H	LSASAF	0.73	24.51	18.50	4.39	4.39	0.82	0.90	1.18	1825

Table 4. Metrics BE Bra (ICOS Carbon Portal, GLEAM, GLDAS, and LSA-SAF; figure created by the author)

BE Lon

BE-Lon is a cropland site located in the Hesbaye region of southern Belgium at an elevation of approximately 167 m. The site has an area of 11.8 ha and is managed using a four-year crop rotation consisting of sugar beet (Beta vulgaris L.), winter wheat (Triticum aestivum L.), potato (Solanum tuberosum L.) and winter wheat. (meta.icos-cp.eu) Compared with the forest and grassland sites, the annual crop rotation results in substantial seasonal changes in vegetation cover, rooting depth and canopy development, which may influence the ecosystem response to drought. (icos.belgium.be)

	Station	Year	Event	Drought period	SPEI-3 min	SPEI-3 mean	SPEI-1 min	SPEI-1 mean	SPI-3 min	SPI-3 mean	CDI max	CDI mean	EDDI max	EDDI mean	SSI min	SSI mean
0	BE-Lon	2015	1	21 Jun–01 Jul	-1.13	-1.12	-1.30	-1.04	NaN	NaN	4.0	2.5	1.36	0.75	-2.27	-1.28
1	BE-Lon	2015	2	01 Aug–11 Aug	-1.15	-1.12	-0.45	-0.42	-0.85	-0.85	1.0	1.0	0.56	0.17	-0.45	0.06
2	BE-Lon	2017	4	21 May–11 Jul	-1.76	-1.36	-1.97	-0.92	-1.18	-0.73	5.0	3.0	1.69	0.81	-2.33	-0.94
3	BE-Lon	2018	5	21 Jun–11 Oct	-2.55	-1.72	-2.16	-0.94	-2.49	-1.45	2.0	2.0	2.01	0.81	-1.68	-0.50
4	BE-Lon	2019	7	01 Jul–01 Jul	-1.21	-1.21	-1.37	-1.37	NaN	NaN	1.0	1.0	1.34	1.00	-2.67	-1.81
5	BE-Lon	2019	8	01 Aug–01 Aug	-1.28	-1.28	-0.55	-0.55	NaN	NaN	1.0	1.0	0.72	0.61	-0.42	-0.17
6	BE-Lon	2019	9	21 Aug–21 Sep	-1.48	-1.25	-1.43	-0.55	-1.10	-1.10	2.0	1.0	1.07	0.68	-2.27	-1.18
7	BE-Lon	2022	12	01 May–21 May	-2.10	-1.82	-1.98	-1.67	-1.70	-1.70	2.0	2.0	1.05	0.82	-3.17	-1.85
8	BE-Lon	2022	13	11 Jun–11 Jun	-1.27	-1.27	-0.15	-0.15	NaN	NaN	2.0	2.0	0.53	0.42	-1.69	-1.10
9	BE-Lon	2022	14	01 Jul–01 Sep	-1.68	-1.53	-1.97	-1.24	-1.30	-1.21	2.0	2.0	3.17	1.50	-3.17	-1.70
10	BE-Lon	2022	15	21 Sep–01 Oct	-1.17	-1.09	0.94	1.17	NaN	NaN	2.0	2.0	1.03	0.10	-0.94	-0.18

Table 5 . *Values of drought indices for selected event at BE Lon*

BE Lon 2015 and 2017 Event

The first drought event at BE-Lon occurred between the end of June and the beginning of July 2015. The drought was characterised by stronger short-term than accumulated water-balance deficits, elevated atmospheric evaporative demand, and pronounced soil moisture depletion.

Soil moisture had been declining progressively for several weeks before the onset of the event and reached its minimum around late June, consistent with the strongly negative SSI values. Despite these dry soil conditions, LE remained relatively high and exhibited several pronounced peaks throughout the drought period. Similarly, EF generally remained high, while H stayed comparatively low and variable. This indicates that a substantial proportion of the available turbulent energy continued to be partitioned into latent rather than sensible heat flux despite the preceding soil drying. The drought event 2017 at BE-Lon occurred between the end of May and the end of July and was the longest and most severe event observed at this station among the selected common analysis years. It was characterised by persistent precipitation deficits, elevated atmospheric evaporative demand, and pronounced soil moisture depletion. It was characterised by persistent precipitation deficits, elevated atmospheric evaporative demand, and pronounced soil moisture depletion. Overall, the 2017 drought at BE-Lon provides clearer evidence of drought-induced limitation of evapotranspiration than the shorter 2015 event. While the 2015 drought occurred during the peak growing season, when the cropland was still able to sustain relatively high latent heat flux despite declining soil moisture, the prolonged 2017 drought appears to have progressively reduced this capacity. The persistent soil moisture deficit, combined with continued high atmospheric evaporative demand, resulted in increased sensible heating and a lower evaporative fraction. Unlike BE-Bra, BE-Lon showed a possible shift from energy-limited to moisture-limited system.

BE-Lon 2022 Events

The 2022 observed season at BE-Lon was characterised by several drought periods, including a prolonged event from the beginning of May to the end of May, a short event in June, an extended summer drought from the beginning of July to September, and a final event between the end of September and the beginning of October. The season was characterised by repeated drought events occurring against a background of progressively declining low soil moisture.

During the May event, LE remained relatively high and variable despite the decline in soil moisture, while EF generally remained high. Incoming shortwave radiation and air temperature increased during this period, providing favourable conditions for evapotranspiration. As observed during the previous drought events at BE-Lon, the persistence of high LE and EF suggests that evapotranspiration was initially maintained despite the dry conditions, likely reflecting water availability within the actively rooted soil layer together with the seasonal development of the crop. The short June event occurred after a temporary increase in soil moisture. LE remained high and EF showed no persistent decline, suggesting that this event did not result in clear water limitation of evapotranspiration. However, soil moisture subsequently decreased again and remained low throughout July and August. During the prolonged summer drought, a much clearer change in surface-energy partitioning became visible. LE progressively declined from its high early-summer values and remained relatively low during August, while H increased substantially and EF decreased for an extended period. This response happened together with persistently low soil moisture, elevated air temperatures and continued atmospheric evaporative demand. The simultaneous decrease in LE and EF and increase in H provides strong evidence that evapotranspiration became increasingly constrained by water availability during the prolonged summer drought.

A sharp increase in soil moisture occurred at the beginning of September, followed by a rapid increase in LE and EF and a decline in H. This response further supports the interpretation that the low LE and EF observed during the previous drought period were associated with water limitation rather than only seasonal changes in radiation or vegetation activity. During the final September–October event, soil moisture remained considerably higher than during the summer drought, while EF remained high and H relatively low. Despite the recurrence of meteorological drought conditions, the ecosystem response was weaker than during the prolonged summer drought.

The 2022 season overall demonstrates that individual drought events do not necessarily produce comparable responses in surface fluxes. The strongest response occurred when meteorological drought happened together with the persistent soil moisture depletion, resulting in reduced LE and EF and increased H. The rapid recovery of the turbulent fluxes following soil moisture replenishment further supports the interpretation that water availability became the dominant limitation during the later stages of the prolonged summer drought.

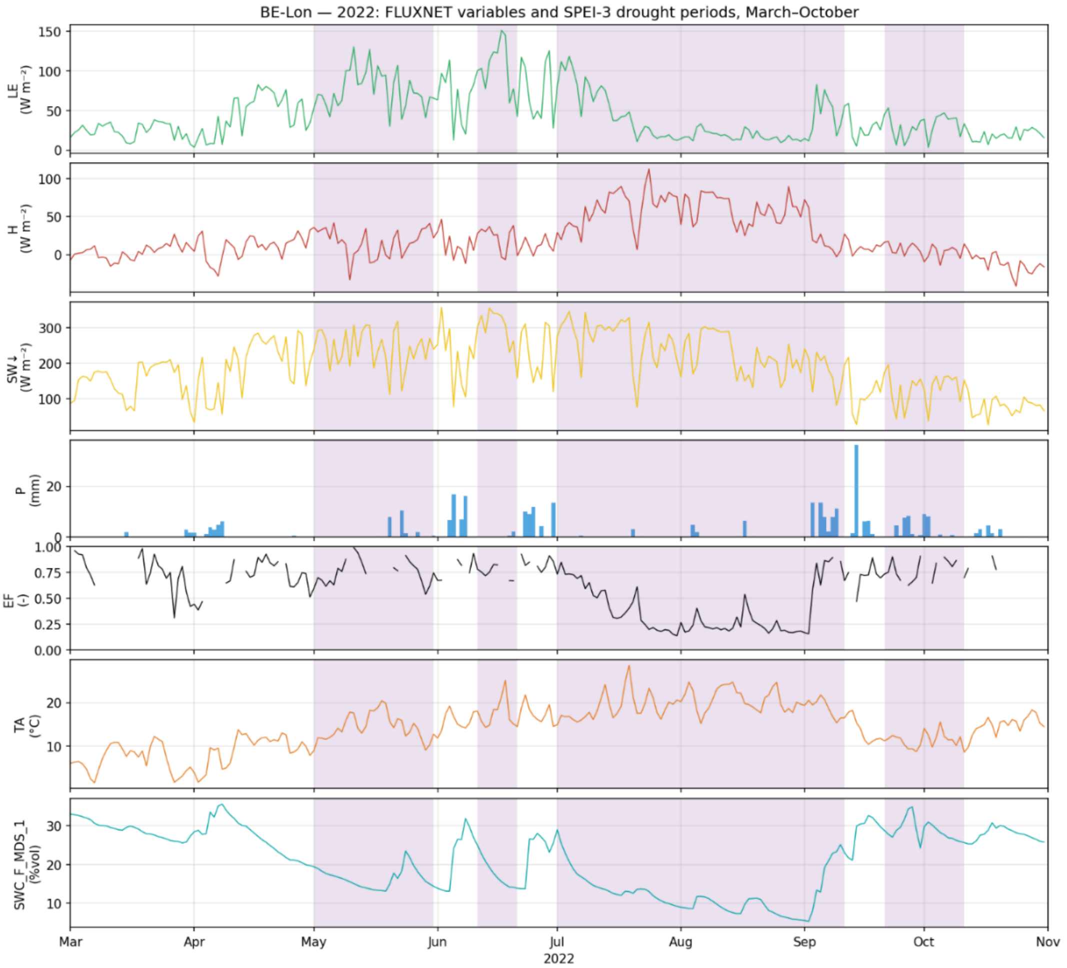

Figure 11. *Fluxnet variables BE Lon 2022(ICOS Carbon Portal; figure created by the author)*

Summary

BE-Lon is a cropland site located at approximately 170 m elevation, where the seasonal development and management of vegetation strongly influence the observed surface fluxes. During periods of active crop growth, transpiration contributes to high LE and EF, whereas after crop senescence or harvest, reduced vegetation cover and increased exposure of bare soil may decrease LE and shift a larger proportion of the available energy towards H. Consequently, changes in LE, H and EF cannot automatically be attributed to drought stress, as they may also reflect crop phenology and land-management practices.

Compared with a forest ecosystem, the rooting depth and water-storage capacity accessible to annual crops may be more limited, potentially making evapotranspiration more sensitive to declining soil moisture. This is particularly visible during the prolonged drought periods in 2017 and 2022, when persistently low SWC coincided with decreasing LE and EF and increasing H. The rapid recovery of LE and EF following soil moisture replenishment in 2022 further supports the interpretation that water limitation contributed to the observed changes in energy partitioning.

However, separating drought effects from seasonal vegetation dynamics remains challenging. A decline in LE and EF during late summer could result from soil moisture limitation, crop harvest, or a combination of these processes.

Aditional case 2018 2019

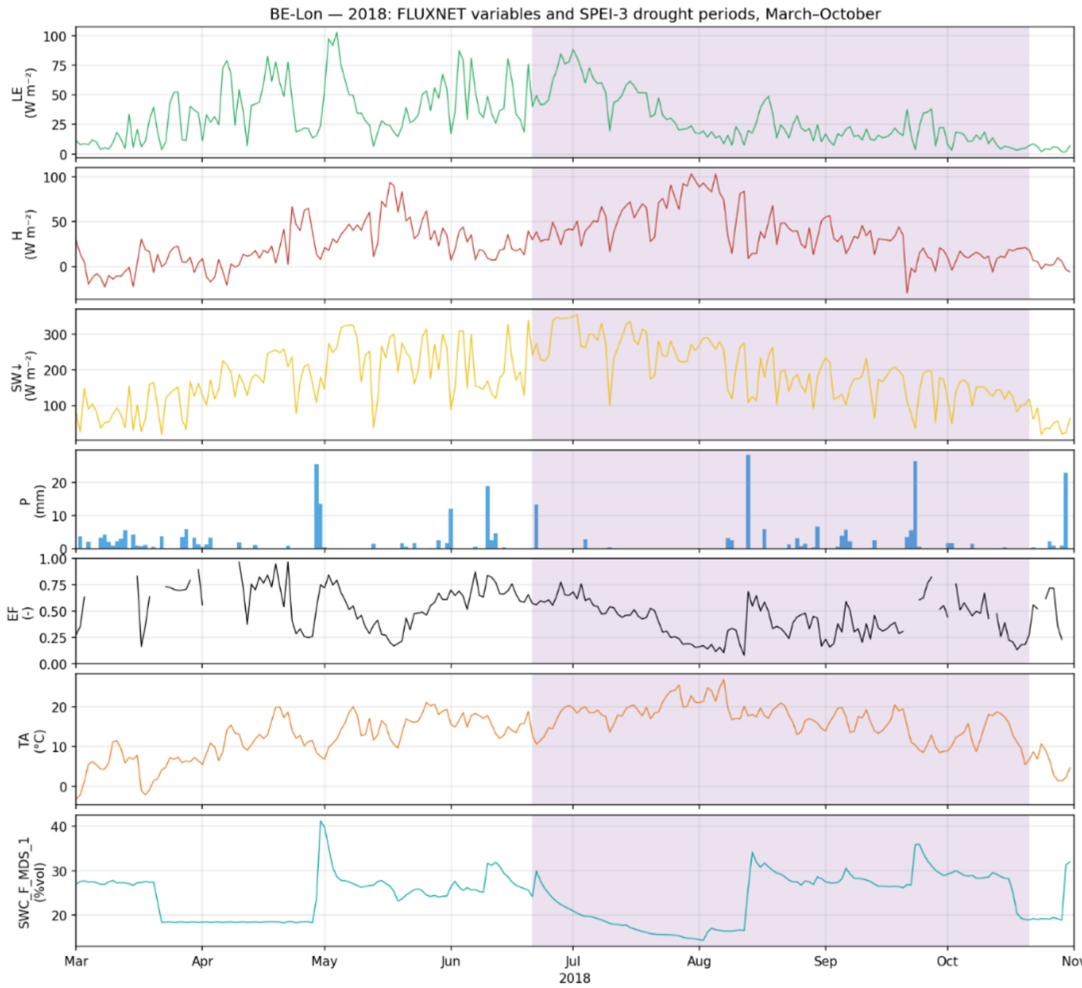

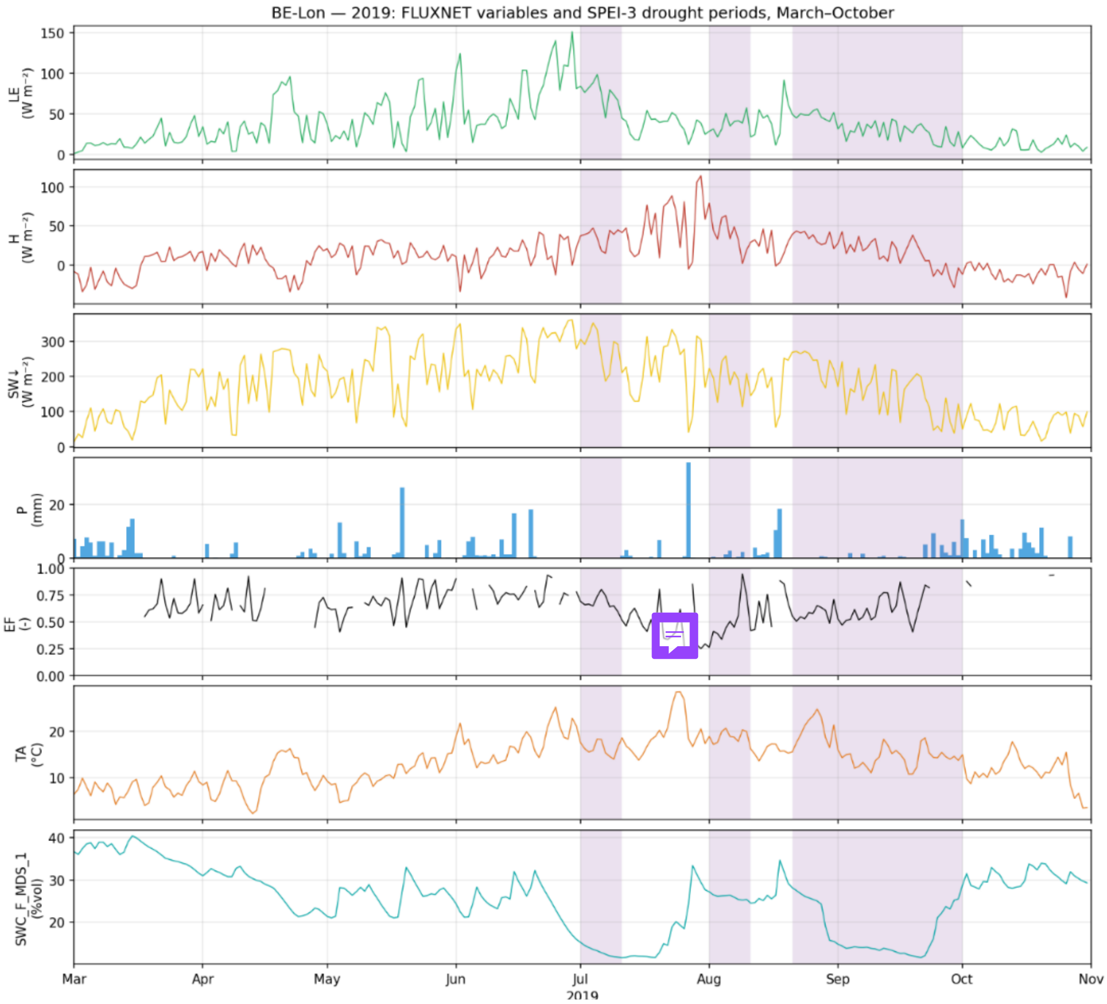

***Figure 12 & 13.**. Fluxnet variables BE Lon 2018/19 (ICOS Carbon Portal;figure created by author)*

The additional analysis of 2018 and 2019 shows a more pronounced change in surface-energy partitioning at the cropland site BE-Lon than at the forest site BE-Bra. In 2018, LE progressively decreased from July onwards as SWC declined, while H remained relatively high and EF decreased, indicating increasing water limitation and a shift from latent towards sensible heat flux. Because BE-Lon is a cropland site, crop phenology may also have contributed to the observed reduction in LE and EF.

A similar response was observed during the prolonged summer drought in 2019. Declining SWC was accompanied by lower LE and EF and higher H, while the recovery of LE and EF following soil moisture replenishment suggests a strong coupling between soil water availability and turbulent fluxes. However, the gradual late-season decline in LE may also partly reflect seasonal vegetation development.

The additional case-study years support the interpretation that BE-Lon responds more directly to declining soil water availability than the forest sites.

Evaporative fraction

In contrast to BE-Bra, BE-Lon showed a clearer response of the evaporative fraction during several drought events. During the prolonged droughts of 2018 and 2022, EF declined systematically and remained low for extended periods, indicating a stronger sensitivity to prolonged soil moisture depletion than observed at BE-Bra.

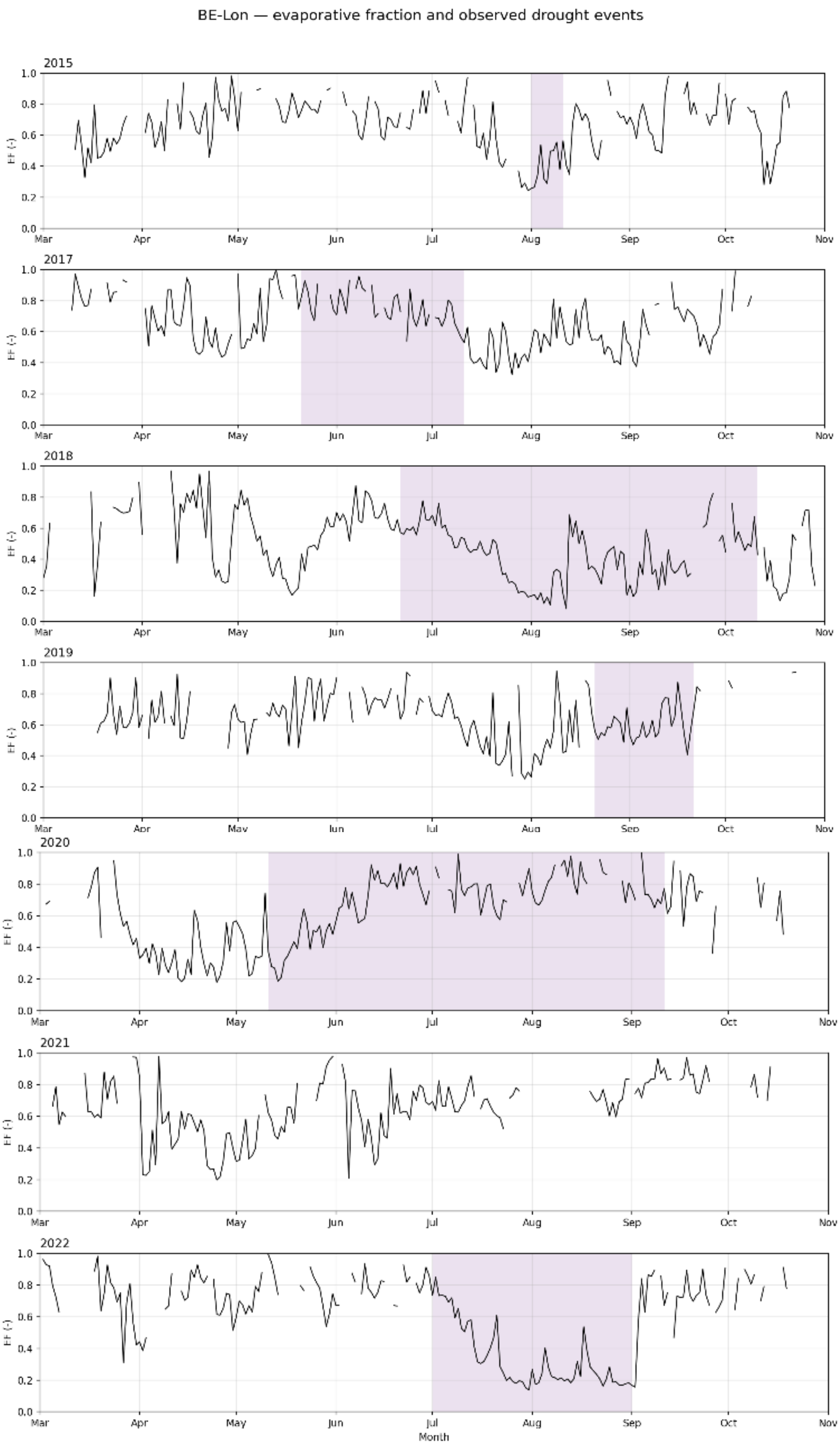

Figure 13.. *Evaporative fraction BE Lon (ICOS Carbon Portal;figure created by author)*

Comparison between GLEAM, GLDAS, LSA SAF against ICOS flux towers

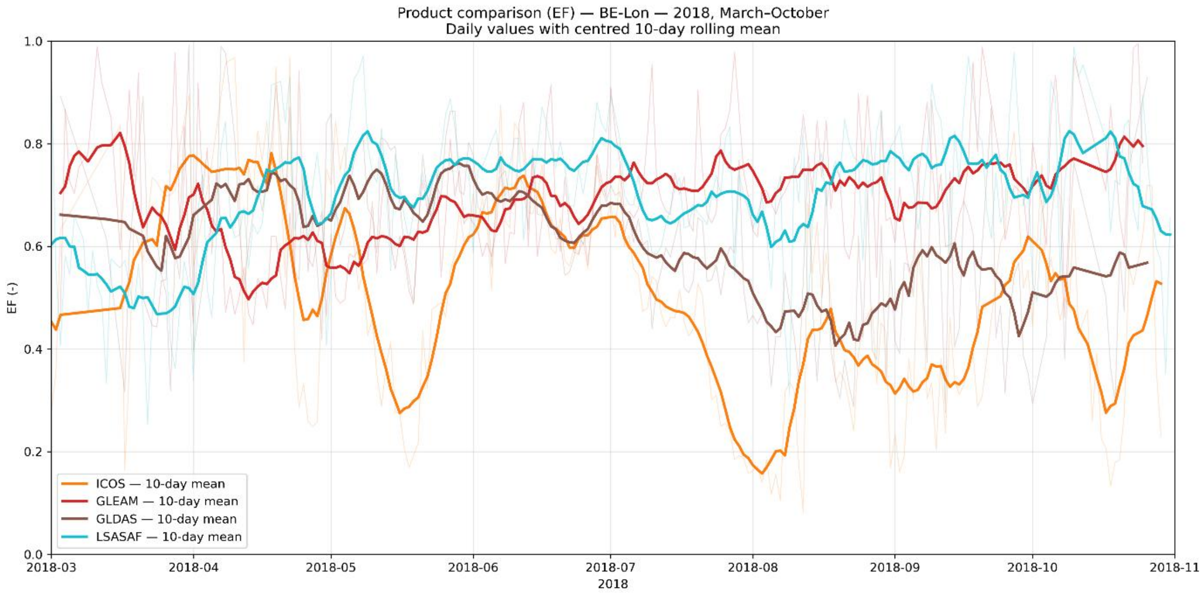

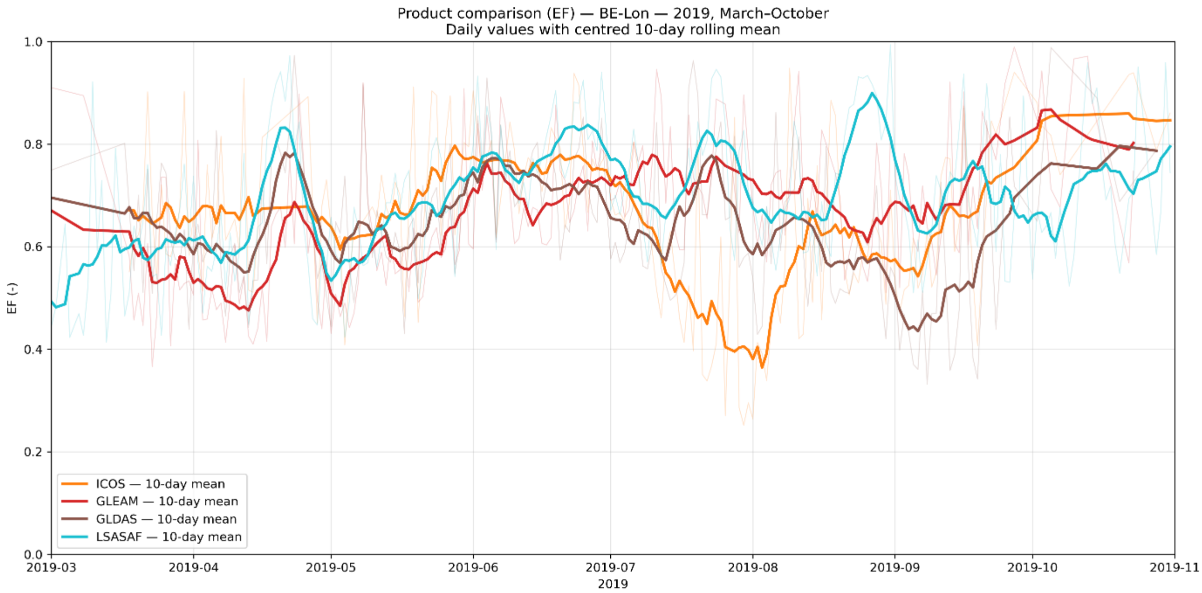

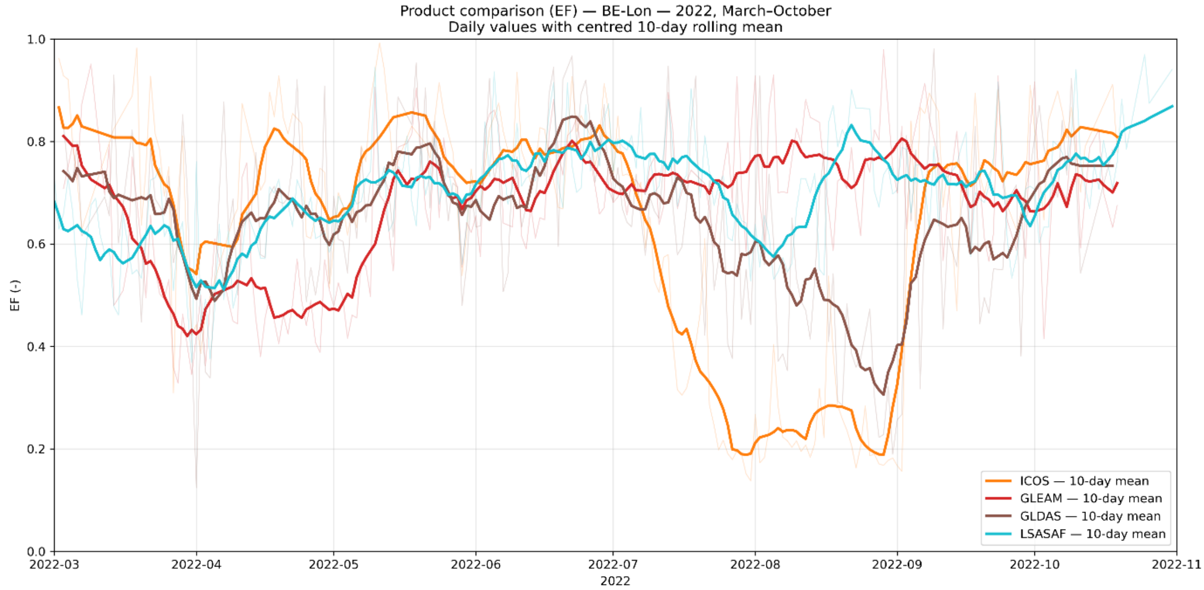

Figure 14.,15 & 16. *Comparison BE Lon GLEAM GLDAS LSASAF (ICOS Carbon Portal, GLEAM, GLDAS, and LSA-SAF; figure created by the author)*

ICOS shows the largest decline in EF during the summer of 2022, reaching values around 0.2. GLEAM also decreases during this period but less strongly than ICOS. GLDAS remains relatively high and does not reproduce the pronounced decline observed at ICOS. LSA-SAF generally shows the highest EF values throughout much of the drought period and likewise fails to capture the ICOS minimum. Overall, all three products underestimate the magnitude of the EF decline observed at the ICOS site.

Because EF represents the ratio between latent and total turbulent heat flux, separate LE and H figures were analysed to identify the processes responsible for the observed changes.

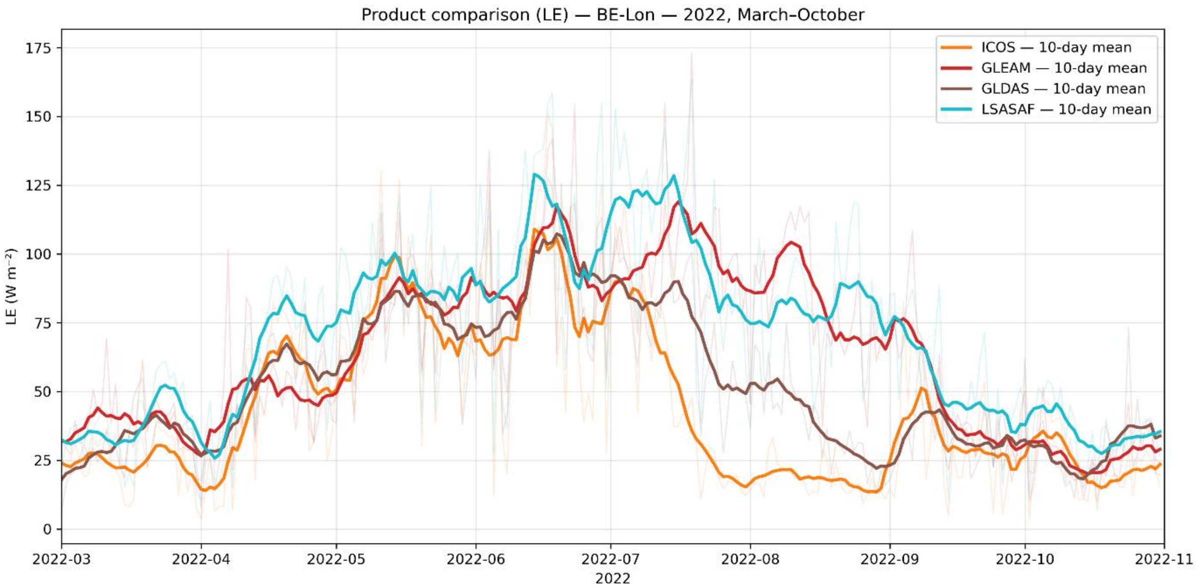

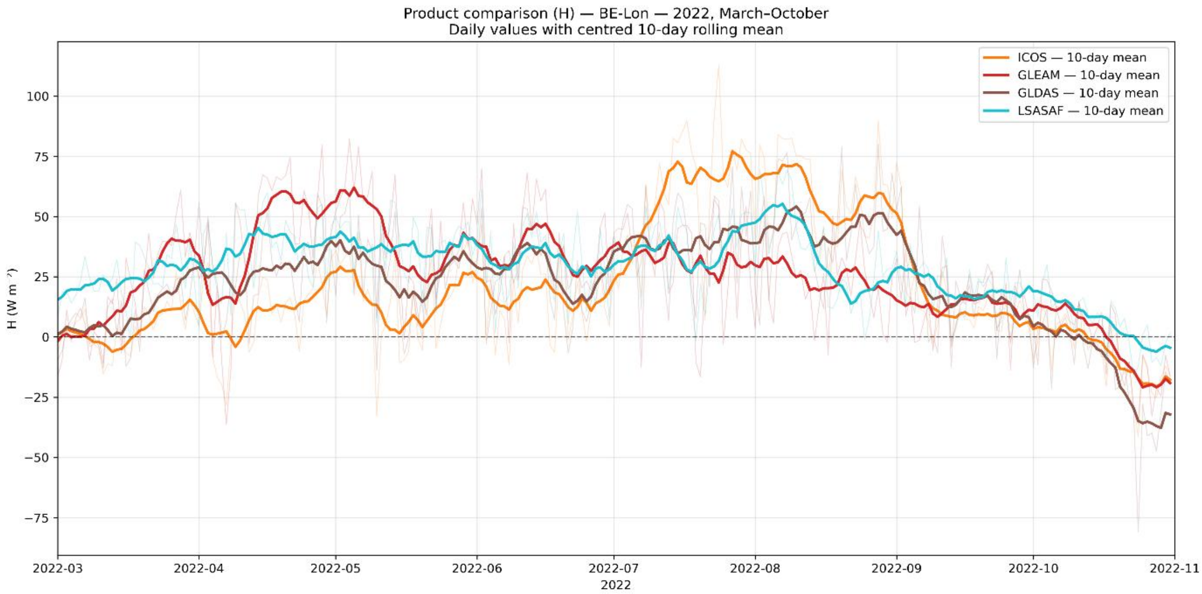

__Figure 17.& 18.__ Comparison BE Lon GLEAM GLDAS LSASAF (ICOS Carbon Portal, GLEAM, GLDAS, and LSA-SAF; figure created by the author)

These figures show that the pronounced decline in EF at ICOS was associated with a sharp reduction in latent heat flux accompanied by an increase in sensible heat flux, whereas all products underestimated the magnitude of these changes. The corresponding LE and H figures are provided in Appendix C4-C24.

Diurnal cycles

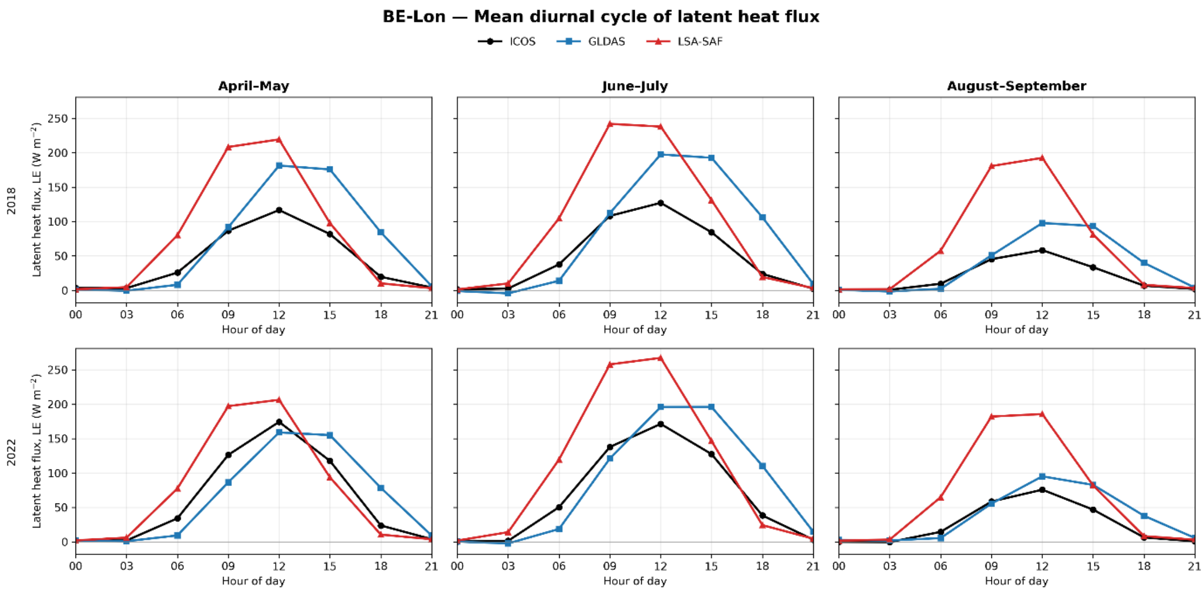

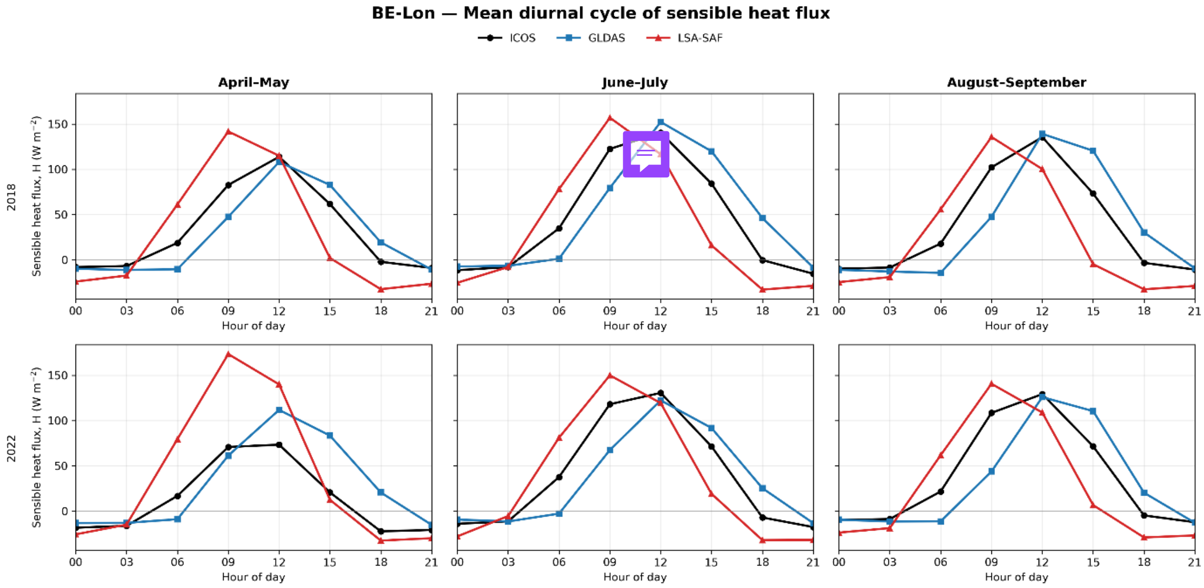

Figure 19. & 20. *Averaged daytime LE and H cycles (ICOS Carbon Portal, GLEAM, GLDAS, and LSA-SAF; figure created by the author)*

At BE-Lon, the event-averaged daytime EF cycles show similar temporal across the three periods. Before and during drought, ICOS and GLDAS generally follow comparable diurnal flow, while LSA-SAF tends to show higher EF values during the afternoon. After drought, the differences between the products become smaller, although LSA-SAF still indicates a stronger afternoon increase.

Overall performance metrics

	site	variable	product	KGE	RMSE	MAE	bias	absolute_bias	pearson_r	alpha	beta	n
0	BE-Lon	EF	GLDAS	0.38	0.19	0.15	0.01	0.01	0.45	0.70	1.01	862
1	BE-Lon	EF	GLEAM	-0.16	0.26	0.21	0.03	0.03	-0.11	0.68	1.04	862
2	BE-Lon	EF	LSASAF	-0.09	0.25	0.19	0.08	0.08	0.02	0.56	1.14	862
3	BE-Lon	LE	GLDAS	0.54	20.11	14.94	11.43	11.43	0.84	1.09	1.42	1825
4	BE-Lon	LE	GLEAM	0.25	28.35	20.41	18.35	18.35	0.78	1.25	1.67	1825
5	BE-Lon	LE	LSASAF	0.12	29.13	20.08	19.52	19.52	0.88	1.50	1.72	1825
6	BE-Lon	H	GLDAS	0.73	17.65	13.40	1.31	1.31	0.82	1.12	1.15	1825
7	BE-Lon	H	GLEAM	0.33	22.67	16.37	5.01	5.01	0.69	1.08	1.59	1825
8	BE-Lon	H	LSASAF	0.08	20.98	16.80	6.97	6.97	0.68	0.72	1.82	1825

Table 6. Metrics BE Lon (*ICOS Carbon Portal, GLEAM, GLDAS, and LSA-SAF; figure created by the author ICOS Carbon Portal, GLEAM, GLDAS, and LSA-SAF; figure created by the author*)

Performance varied across the evaluated variables and products at BE-Lon.For LE and H, GLDAS generally achieved the highest KGE values, the strongest correlations and the lowest error metrics, while differences between the products were smaller for EF. LSA-SAF showed intermediate response while GLEAM generally exhibited lower KGE values and higher errors. Correlation coefficients were highest for LE and H across all products, indicating a better representation of these fluxes than of EF.

BE Vie

BE-Vie is a mature mixed forest located in the Ardennes region of southern Belgium at an elevation of approximately 490 m. The site has a temperate maritime climate, with a mean annual temperature of 8.2 °C and a mean annual precipitation of 915.6 mm. The forest is dominated by European beech (Fagus sylvatica L.) and Douglas fir (Pseudotsuga menziesii (Mirb.) Franco), together with several other coniferous and deciduous tree species (meta.icos-cp.eu/). The approximately 35 m tall forest canopy and mature vegetation distinguish BE-Vie from the grassland and cropland sites and may influence its response to drought. (https://www.icos-cp.eu/)

	Station	Year	Event	Drought period	SPEI-3 min	SPEI-3 mean	SPEI-1 min	SPEI-1 mean	SPI-3 min	SPI-3 mean	CDI max	CDI mean	EDDI max	EDDI mean	SSI min	SSI mean
0	BE-Vie	2015	1	01 Jun–01 Jun	-1.02	-1.02	-1.73	-1.73	NaN	NaN	0.0	0.00	0.59	0.41	-0.46	-0.28
1	BE-Vie	2015	2	21 Jun–21 Aug	-1.70	-1.46	-1.21	-0.44	-2.41	-1.77	5.0	2.86	1.50	0.78	-0.38	-0.05
2	BE-Vie	2017	4	01 Jun–21 Jun	-1.58	-1.32	-1.54	-0.82	-0.99	-0.99	2.0	2.00	1.81	1.48	-0.93	-0.71
3	BE-Vie	2018	5	01 May–11 May	-1.17	-1.15	-1.31	-1.26	0.05	0.05	2.0	1.50	1.91	1.48	-0.53	-0.19
4	BE-Vie	2018	6	11 Jul–21 Nov	-1.99	-1.67	-2.19	-1.23	-2.11	-1.79	2.0	2.00	3.26	1.23	-2.97	-1.35
5	BE-Vie	2019	7	01 Jul–01 Jul	-1.28	-1.28	-1.55	-1.55	NaN	NaN	2.0	2.00	1.84	1.69	-0.86	-0.55
6	BE-Vie	2019	8	01 Aug–21 Sep	-1.49	-1.26	-1.29	-0.43	-1.07	-1.03	2.0	2.00	1.23	0.59	-1.19	-0.55
7	BE-Vie	2022	10	01 May–21 May	-1.58	-1.40	-1.72	-1.50	-1.45	-1.45	3.0	2.33	1.47	1.09	-1.02	-0.53
8	BE-Vie	2022	11	11 Jun–11 Jun	-1.11	-1.11	-0.41	-0.41	NaN	NaN	2.0	2.00	0.93	0.73	-0.46	-0.34
9	BE-Vie	2022	12	01 Jul–01 Sep	-1.52	-1.35	-2.02	-1.11	-1.31	-1.02	2.0	2.00	2.93	1.47	-0.82	-0.50
10	BE-Vie	2022	13	21 Sep–01 Oct	-1.39	-1.32	0.81	1.00	NaN	NaN	2.0	2.00	0.56	-0.04	-0.43	-0.08

Table 7 *Values of drought indices at BE Vie*

BE Lon Event 2015 and 2017

The 2015 season at BE-Vie included two drought events that differed in duration and severity . During both events, SWC progressively declined, while LE remained relatively high and EF showed no persistent decrease despite increasing atmospheric evaporative demand. H exhibited variability rather than sustained increase. Results suggest relatively weak response to declining measured soil moisture. The 2017 drought event was characterised by declining SWC, elevated atmospheric evaporative demand, and relatively high radiation and air temperature. Despite continued soil moisture depletion, LE remained high, EF showed no sustained decrease and H did not exhibit a persistent increase. The ecosystem displayed a similarly weak response to drought as observed in 2015 , suggesting that evapotranspiration was maintained despite declining measured soil moisture.

BE Vie 2022 Event

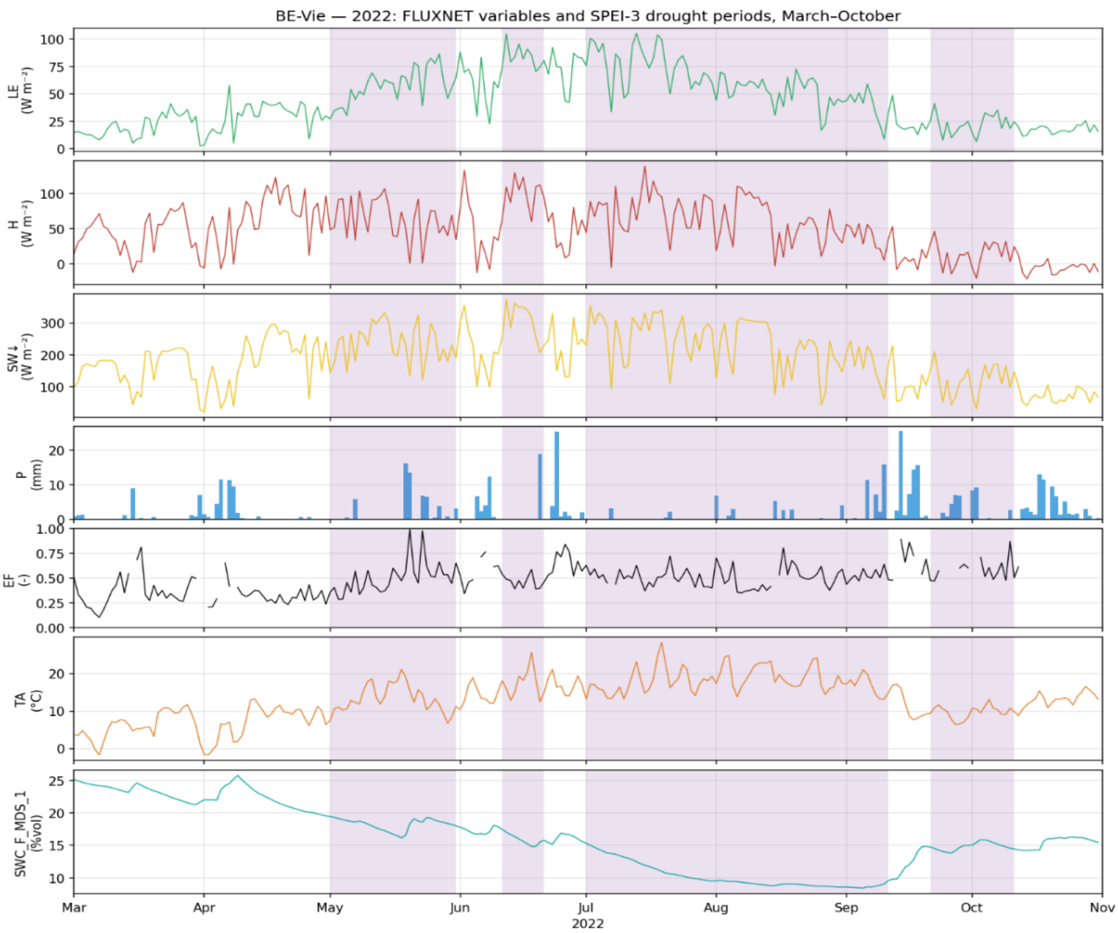

Figure 21. *FLUXNET variables BE Vie 2022 (ICOS Carbon Portal, GLEAM, GLDAS, and LSA-SAF; figure created by the author)*

The 2022 season at BE-Vie was characterised by several drought events and a prolonged period of declining soil moisture. During the May event, LE increased while EF remained relatively stable despite increasingly dry soil conditions. Together with high incoming shortwave radiation and air temperature, this suggests that water availability had not yet become sufficiently limiting to reduce evapotranspiration.

The most persistent drought developed between July and September. Throughout this period, SWC progressively declined and reached its seasonal minimum during August. Despite the prolonged meteorological drought, high atmospheric evaporative demand and declining SWC, LE remained relatively high for much of the event. Similarly, EF remained relatively stable, while H showed substantial variability but no persistent increase. These observations indicate that the mixed forest maintained considerable evapotranspiration despite the progressive depletion of moisture in the measured soil layer.

Towards the end of the summer drought, LE gradually declined, but this coincided with decreasing incoming shortwave radiation, lower air temperatures and the end of the drought period. Consequently, the reduction in LE cannot be attributed solely to soil moisture limitation. In contrast to BE-Lon, no pronounced shift from LE towards H was observed despite the prolonged period of low SWC.

Overall, the 2022 season provides further evidence that evapotranspiration at BE-Vie was relatively resistant to declining moisture in the measured soil layer. Similar to the previous years, LE and EF were maintained throughout much of the prolonged summer drought, suggesting that the ecosystem was buffered against short- to medium-term soil drying. The underlying mechanisms are discussed in the summary section.

Summary

BE-Vie is a mixed forest site located at approximately 493 m elevation, making it the highest-elevation site included in the analysis. Compared with the lower-elevation stations, the climatic conditions at BE-Vie may be cooler and potentially wetter, reducing atmospheric evaporative demand and contributing to slower depletion of available water resources. However, elevation alone cannot explain the observed flux response, as local precipitation, soil properties and vegetation characteristics also influence ecosystem water availability.

Similar to BE-Bra, the forest vegetation at BE-Vie may have access to water stored below the depth represented by the SWC measurements. Consequently, the progressive decline in measured SWC did not immediately correspond to reductions in LE or EF. During several prolonged drought events, substantial evapotranspiration was maintained despite declining soil moisture and elevated atmospheric evaporative demand, suggesting that the mixed forest was able to buffer meteorological drought, potentially through access to deeper soil water and the greater water-storage capacity of the rooting zone.

The behaviour of H should also be interpreted with caution. A prolonged drought does not necessarily result in an immediate increase in H, as vegetation that continues to transpire can maintain a substantial proportion of the available energy as latent heat flux. During some periods, H even decreased towards the later stages of the drought, but this coincided with declining radiation and seasonal cooling, which likely reduced the total amount of available energy. The relatively stable EF therefore provides stronger evidence that no clear and persistent shift from latent towards sensible heat flux occurred.

BE-Vie showed a relatively buffered response to meteorological drought. Even during prolonged periods of declining soil moisture and elevated atmospheric evaporative demand, LE and EF were generally maintained, while no consistent increase in H was observed. Compared with the cropland site BE-Lon, the mixed forest appears less sensitive to short- to medium-term soil moisture depletion, although the underlying mechanisms cannot be confirmed from the available measurements alone.

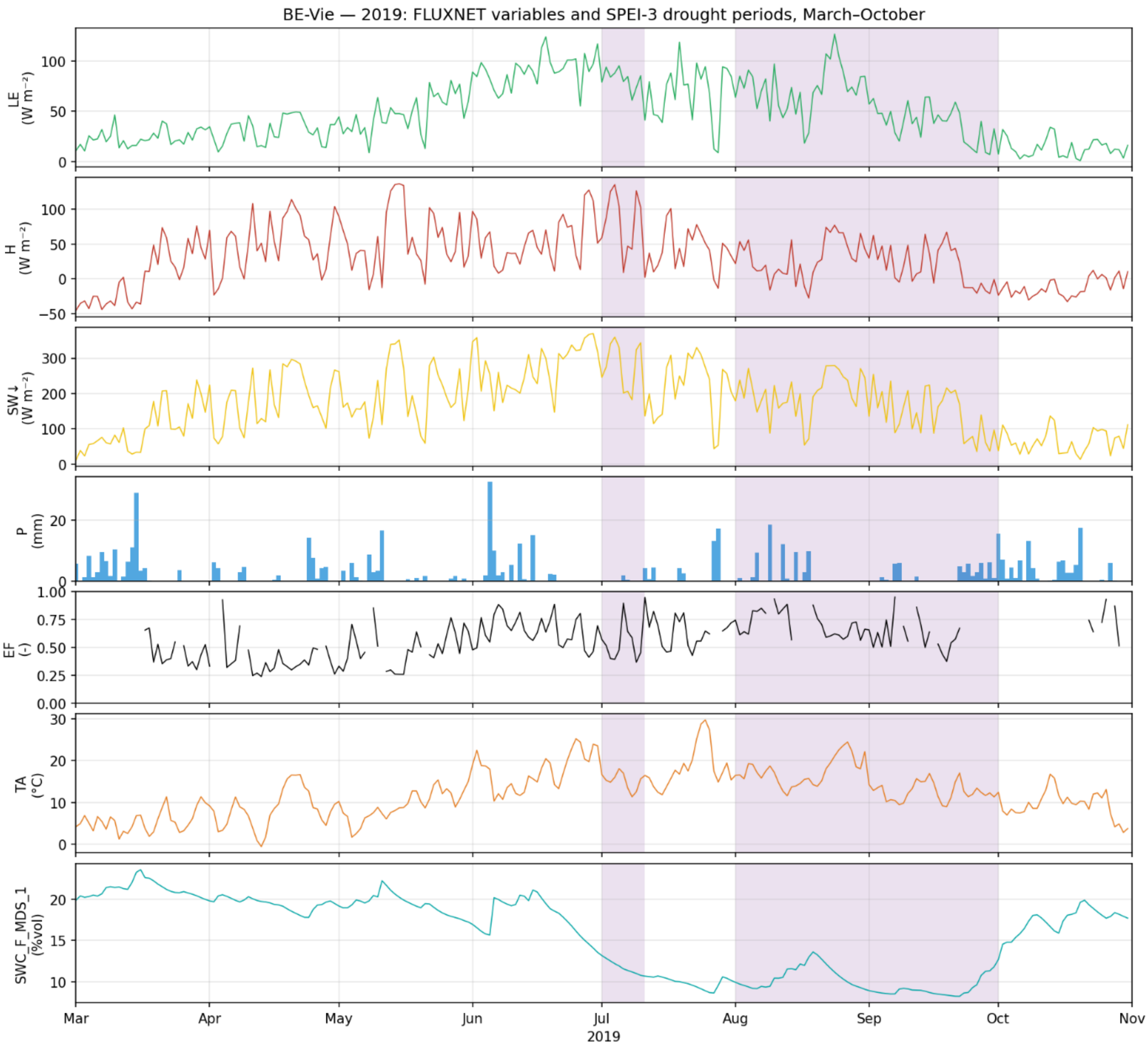

Figure 22. & 23. *Fluxnet variables BE Vie 2018/19 (ICOS Carbon Portal; figure created by the author)*

The additional analysis of 2018 and 2019 further illustrates the response of the mixed forest at BE-Vie to prolonged warm and dry conditions. In 2018, SWC progressively declined throughout the summer and reached very low values from August onwards. Nevertheless, LE remained relatively high during much of the drought period, while EF remained generally stable and H showed no persistent increase. This absence of a clear shift from LE towards H is consistent with the buffered response observed during the main analysis years.

A similar response was observed in 2019. Prolonged drought conditions were accompanied by progressively declining SWC, yet LE remained relatively high during much of the summer, while EF showed only limited variation and H remained strongly variable. Although LE gradually declined towards late summer, this coincided with decreasing incoming shortwave radiation and lower air temperatures, making it difficult to attribute the reduction exclusively to soil moisture limitation.

The additional case-study years reinforce the response observed during 2015, 2017 and 2022. Even under prolonged drought conditions and progressive drying of the measured soil layer, the mixed forest maintained substantial LE and relatively stable EF, with no consistent shift towards higher H. These findings further support the interpretation that BE-Vie exhibited a relatively buffered response to drought, while also highlighting the difficulty of separating drought effects from seasonal reductions in available energy and vegetation activity.

Evaporative fraction

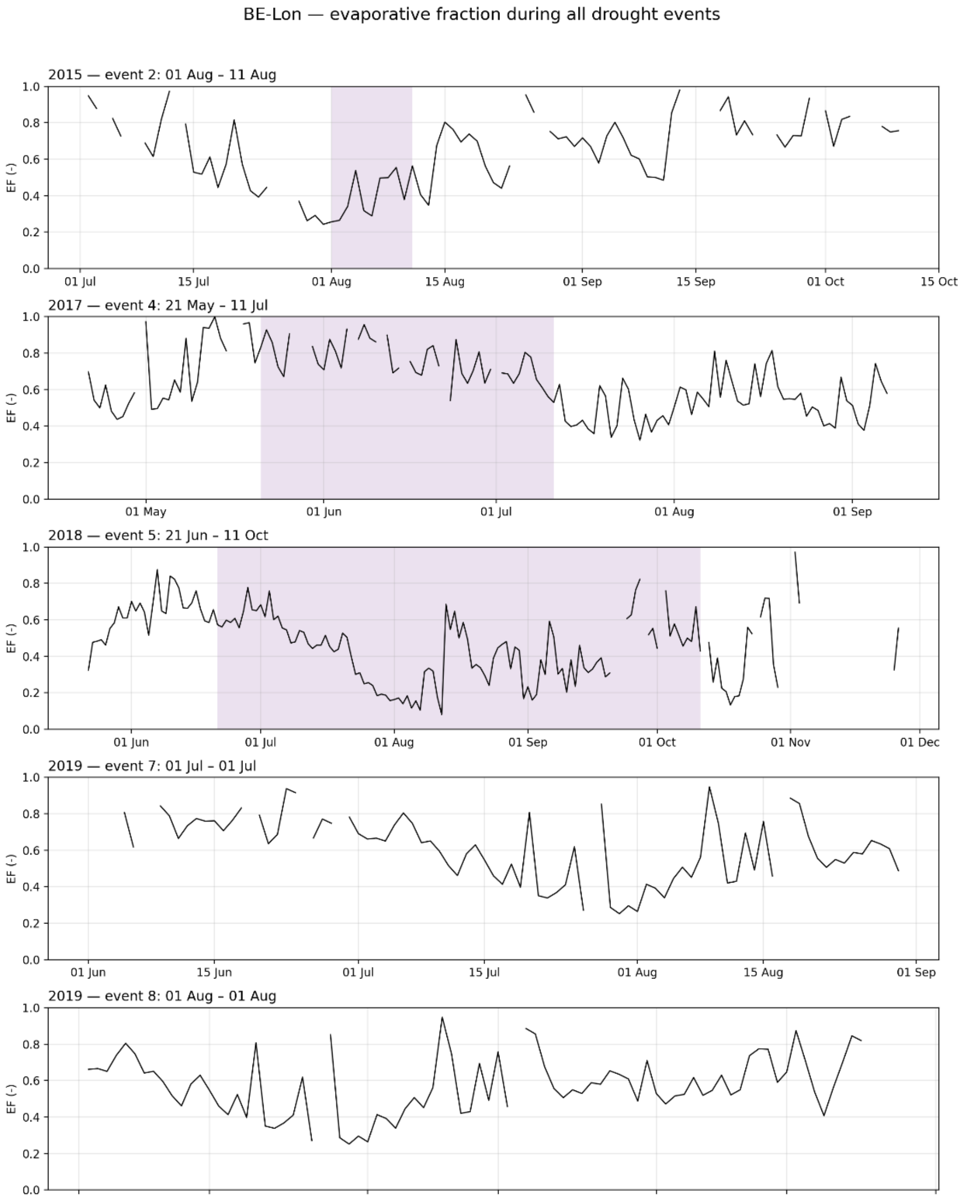

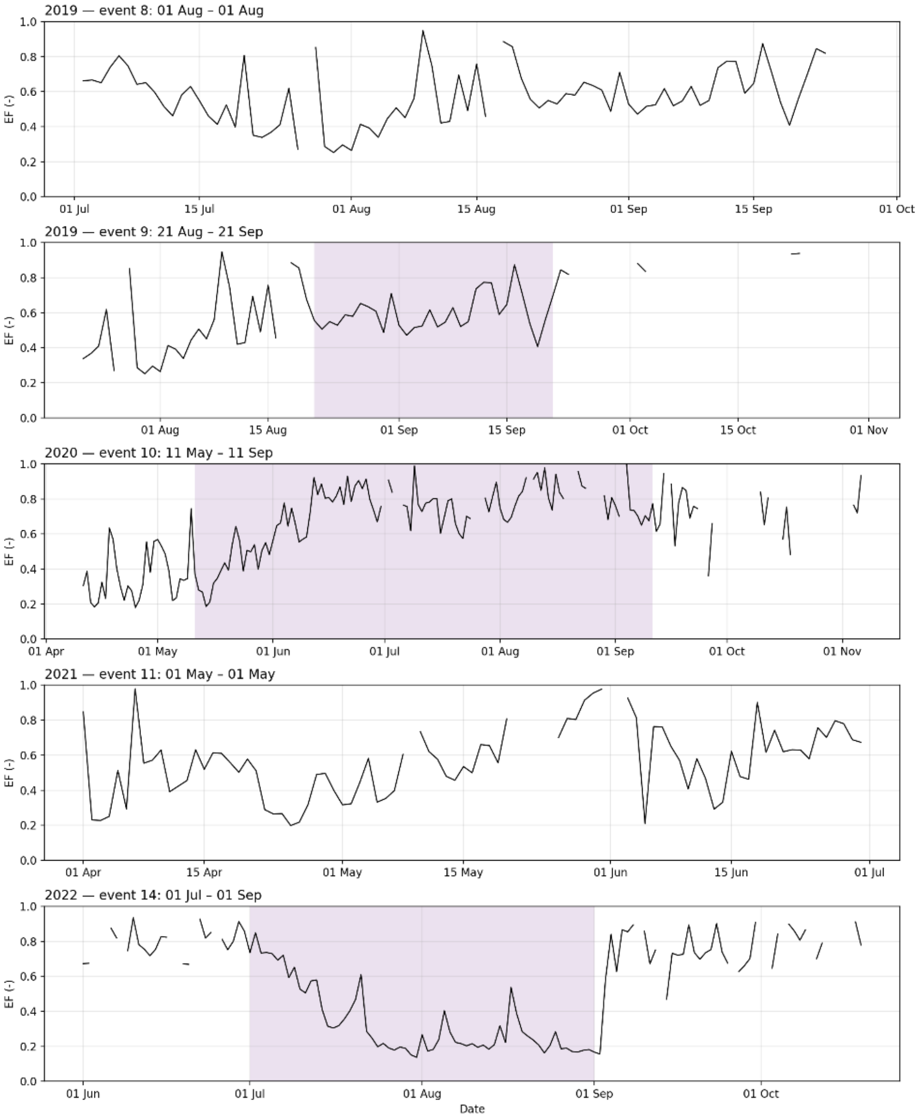

Figure 24.*. Evaporative fraction BE Vie (computed using LE H ICOS data)*

The evaporative fraction at BE-Vie showed systematic variability but no consistent decrease during the identified drought events. During the prolonged drought of 2022, EF generally remained within a moderate range, with only minor temporary decreases. Similar to BE-Dor and BE-Bra, BE-Vie exhibited a relatively stable evaporative fraction throughout the drought periods, indicating no clear shift in surface-energy partitioning.

Comparison between GLEAM, GLDAS, LSA SAF against ICOS flux tower

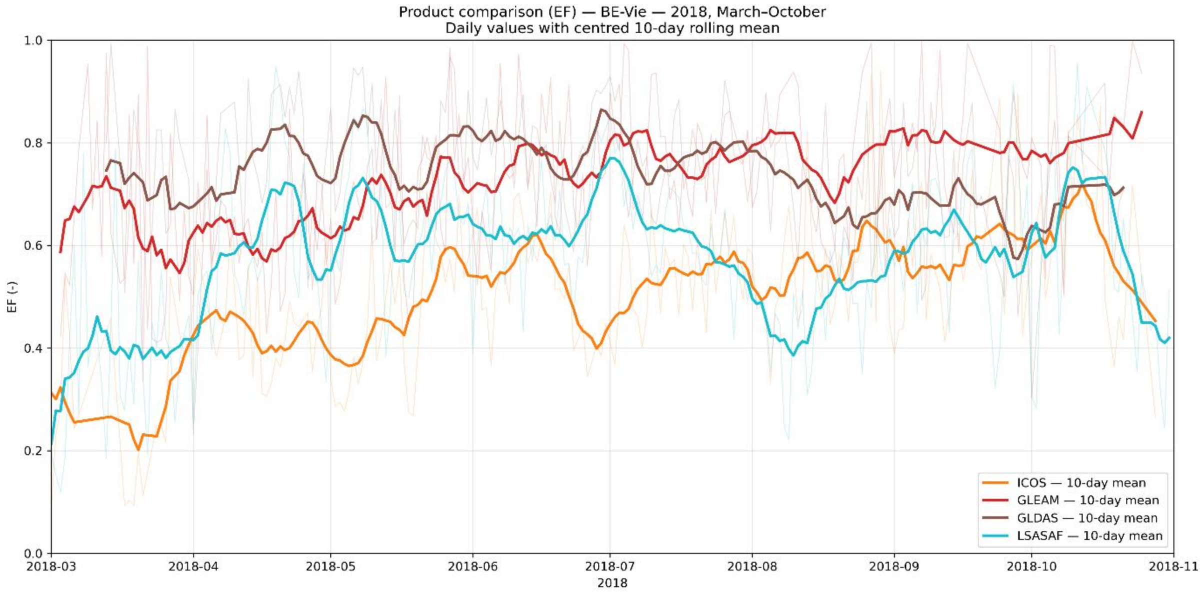

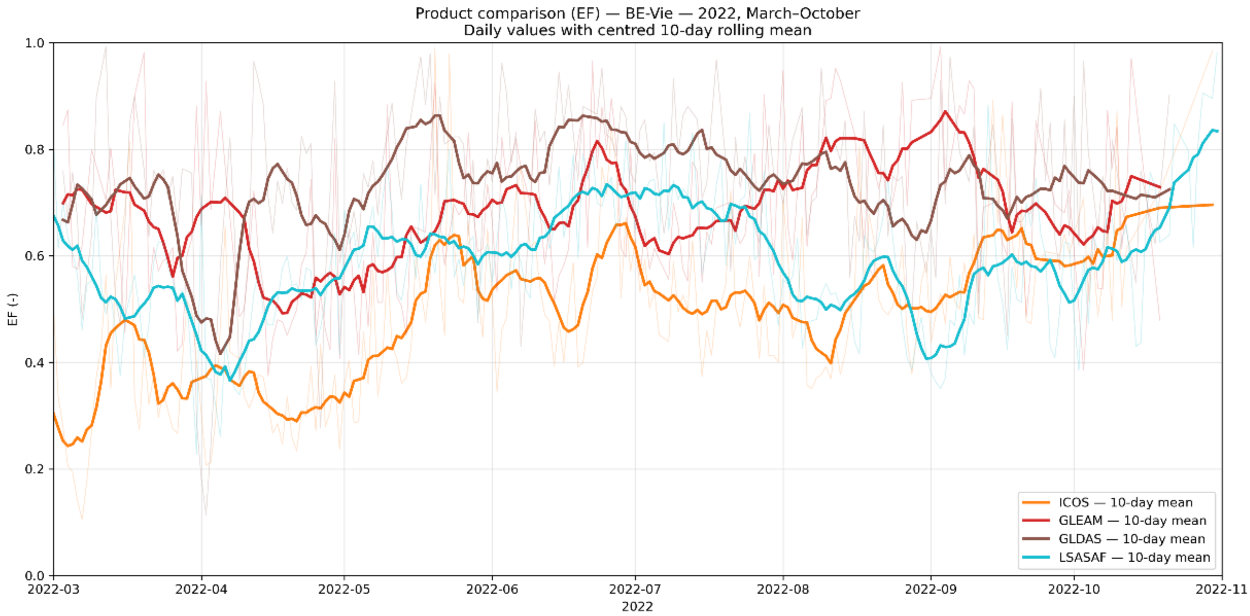

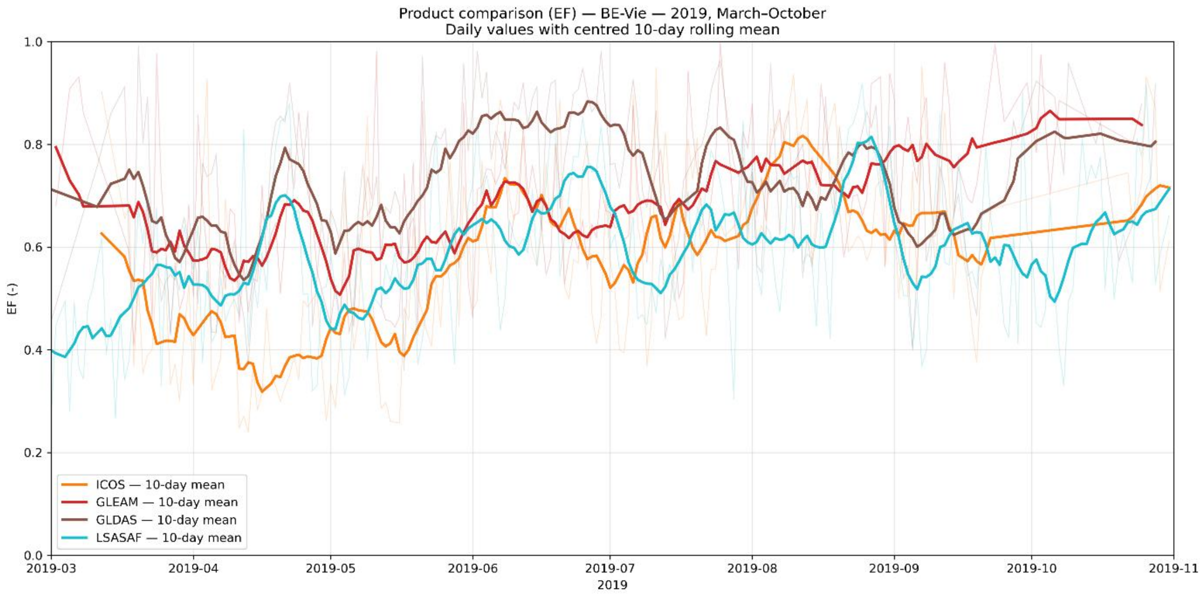

Figure 25.,26. & 27. *Comparison BE Lon GLEAM GLDAS LSASAF* (*ICOS Carbon Portal, GLEAM, GLDAS, and LSA-SAF; figure created by the author)*

BE-Vie shows a different behaviour from BE-Lon, with less pronounced deviations between the products. All products generally follow the seasonal evolution of EF, although they differ in magnitude. ICOS consistently reports lower EF than the other products throughout much of the growing season. GLEAM maintains relatively high EF during summer, while GLDAS also remains consistently above ICOS. LSA-SAF exhibits greater short-term variability but likewise does not reproduce the persistently lower EF observed at ICOS. Overall, all products tend to overestimate EF relative to the ICOS observations during much of the observed season.

Diurnal cycles

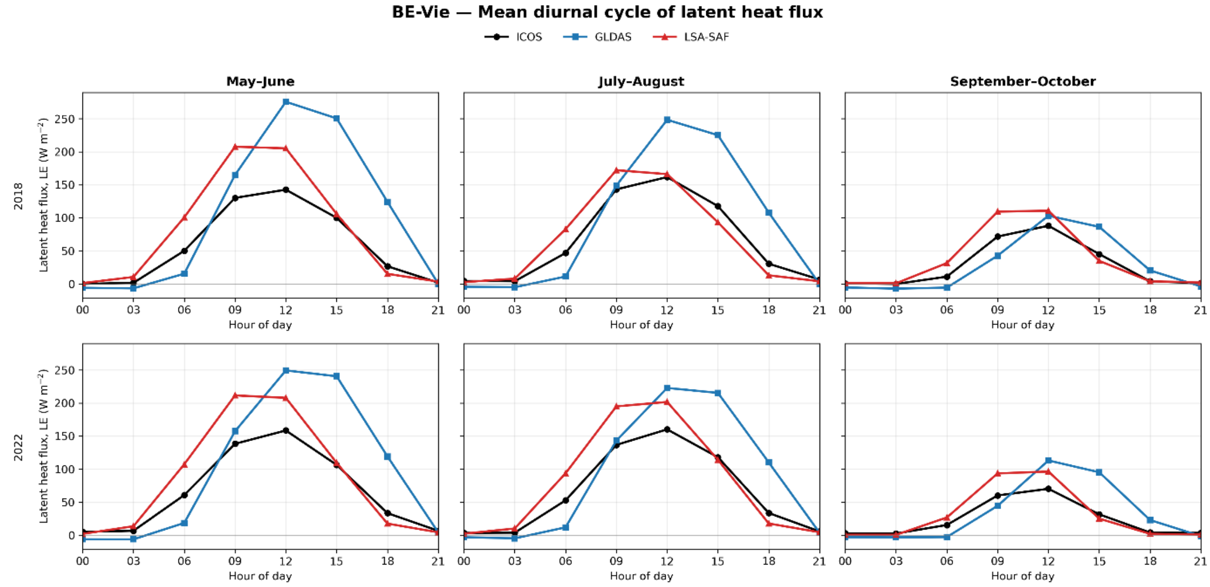

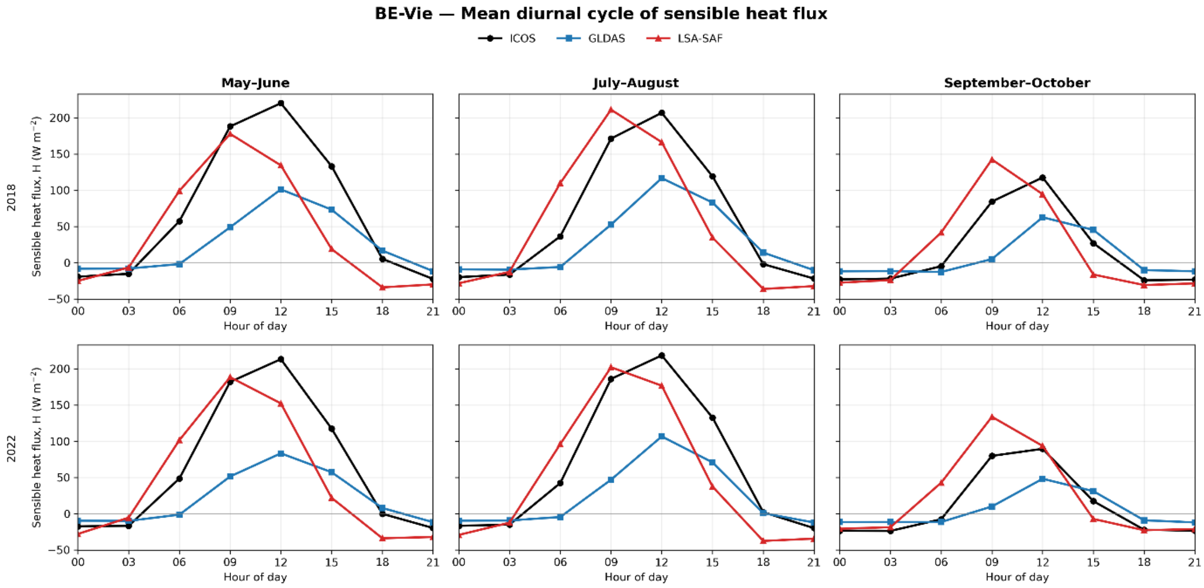

Figure 28. & 29. *Averaged daytime LE and EF cycles (ICOS Carbon Portal, GLEAM, GLDAS, and LSA-SAF; figure created by the author)*

At BE-Vie, shape of the diurnal EF cycle is similar before, during, and after drought. GLDAS generally produces higher EF values during the morning and midday, whereas LSA-SAF shows the strongest increase during the late afternoon. ICOS follows a similar temporal pattern but generally remains lower than both products until the late afternoon.

Overall performance metrics

	site	variable	product	KGE	RMSE	MAE	bias	absolute_bias	pearson_r	alpha	beta	n
0	BE-Vie	EF	GLDAS	0.07	0.29	0.25	0.21	0.21	0.18	0.86	1.40	813
1	BE-Vie	EF	GLEAM	0.41	0.22	0.19	0.16	0.16	0.51	0.89	1.31	813
2	BE-Vie	EF	LSASAF	0.10	0.22	0.18	0.10	0.10	0.15	0.76	1.20	813
3	BE-Vie	LE	GLDAS	0.42	23.40	16.85	14.07	14.07	0.90	1.37	1.44	1825
4	BE-Vie	LE	GLEAM	0.38	24.67	19.47	18.04	18.04	0.88	1.22	1.56	1825
5	BE-Vie	LE	LSASAF	0.61	17.66	11.60	7.55	7.55	0.92	1.30	1.24	1825
6	BE-Vie	H	GLDAS	0.16	34.33	25.29	-13.30	13.30	0.70	0.55	0.36	1825
7	BE-Vie	H	GLEAM	0.38	27.46	20.62	-10.32	10.32	0.82	0.68	0.51	1825
8	BE-Vie	H	LSASAF	0.52	29.48	22.92	-0.60	0.60	0.75	0.59	0.97	1825

Table 8. *Metrics BE Vie (ICOS Carbon Portal, GLEAM, GLDAS, and LSA-SAF; figure created by the author)*

At BE-Vie, GLEAM generally showed the highest KGE values, while the performance of GLDAS and LSA-SAF varied more between years. The results indicate that product performance differed from year to year.

Be Dor

BE-Dor is a permanent grazed grassland located in the Condroz region of southern Belgium at an elevation of approximately 248 m. The site has remained permanent grassland for more than a century and is intensively managed through cattle grazing and mineral and organic fertilisation. The temperate maritime climate (Cfb) is characterised by a mean annual temperature of 10.3 °C and a mean annual precipitation of approximately 828 mm. (meta.icos-cp.eu/)

Compared with the forest sites, the grassland vegetation is expected to have a shallower rooting system and may therefore respond more directly to changes in water availability in the upper soil layers.

	Station	Year	Event	Drought period	SPEI-3 min	SPEI-3 mean	SPEI-1 min	SPEI-1 mean	SPI-3 min	SPI-3 mean	CDI max	CDI mean	EDDI max	EDDI mean	SSI min	SSI mean
0	BE-Dor	2015	1	21 Jun–01 Jul	-1.26	-1.24	-1.31	-0.98	NaN	NaN	2.0	2.00	1.03	0.47	-0.81	-0.27
1	BE-Dor	2015	2	21 Jul–01 Aug	-1.10	-1.06	-0.22	-0.21	NaN	NaN	2.0	2.00	0.69	0.13	-0.24	-0.04
2	BE-Dor	2017	4	01 May–01 May	-1.00	-1.00	-0.66	-0.66	NaN	NaN	2.0	2.00	-0.39	-0.69	-0.56	-0.33
3	BE-Dor	2017	5	21 May–11 Jul	-1.74	-1.30	-1.78	-0.74	-1.24	-0.63	3.0	2.17	1.63	0.81	-0.89	-0.65
4	BE-Dor	2018	6	01 Jul–21 Nov	-2.38	-1.64	-2.24	-1.01	-2.04	-1.62	2.0	2.00	3.05	0.80	-3.05	-0.96
5	BE-Dor	2019	7	01 Jul–01 Jul	-1.22	-1.22	-1.54	-1.54	NaN	NaN	2.0	2.00	1.67	1.27	-2.02	-1.82
6	BE-Dor	2019	8	01 Aug–01 Aug	-1.18	-1.18	-0.45	-0.45	NaN	NaN	2.0	2.00	0.66	0.56	-1.83	-1.60
7	BE-Dor	2019	9	21 Aug–21 Sep	-1.42	-1.25	-1.29	-0.54	-1.13	-1.13	2.0	2.00	0.86	0.47	-1.49	-1.19
8	BE-Dor	2022	11	01 May–11 Jun	-2.05	-1.55	-2.14	-1.09	-1.62	-0.86	3.0	2.60	1.35	0.86	-0.58	-0.39
9	BE-Dor	2022	12	01 Jul–01 Sep	-1.73	-1.46	-1.97	-1.06	-0.92	-0.76	6.0	2.71	1.77	1.19	0.62	0.89
10	BE-Dor	2022	13	21 Sep–21 Sep	-1.12	-1.12	1.25	1.25	NaN	NaN	2.0	2.00	0.90	0.54	0.57	0.75

Table 9. Values of drought indices at BE Dor

BE Dor 2015 and 2017

The 2015 drought event at BE-Dor was characterised by moderate meteorological drought, elevated atmospheric evaporative demand, and declining soil moisture. Despite decreasing SWC, LE remained relatively high, EF showed no persistent decline, and H remained variable without a sustained increase. Following soil mositure replenishment, LE remained elevated, indicating that the short, moderate drought did not result in a clear shift from latent to sensible heat flux. The 2017 drought event was longer and characterised by persistently low SWC and enhanced atmospheric evaporative demand. LE and H remained relatively high throughout most of the event, while H stayed low and stable. No clear shift from latet to sensible heat fluxwas observed, suggesting tgat evapotranspiration was largely maintained despite prolonged soil moisture depletion. The gradual decline in LE later in the season likely reflected decreasing available energy and vegetation phenology rather than drought alone.

BE Dor 2022 Event 3

The 2022 season at BE-Dor was characterised by several drought periods, with the main events extending from the beginning of May to the beginning of June and from July to September, followed by a shorter event in September. The first event was associated with severe meteorological drought and enhanced atmospheric evaporative demand, while the soil moisture anomaly remained relatively moderate.

During the May–June event, LE remained relatively high and variable, while EF also remained high. H increased gradually but stayed substantially lower than LE, indicating that latent heat flux continued to dominate the surface-energy partitioning. SWC remained relatively stable throughout this period, suggesting that the severe meteorological drought had not yet translated into strong soil moisture limitation at the site.

The prolonged July–September drought showed a different pattern. Although meteorological drought and atmospheric evaporative demand remained pronounced, measured SWC stayed relatively high throughout the event. LE gradually declined, while H remained elevated and EF decreased moderately towards late summer. Because these changes occurred without a corresponding decline in measured soil moisture, the reduction in LE cannot be attributed only to soil water limitation. Seasonal vegetation development, decreasing available energy or management effects may also have contributed to the observed flux response.

An abrupt increase in measured SWC occurred around late June, from approximately 20 to nearly 40% water content, after which values remained persistently elevated. This sudden and sustained discontinuity differs from the gradual variations observed during previous years and should therefore be interpreted with caution. It may indicate mistake in the data record rather than an increase in soil moisture. The discontinuity also likely explains why SSI remained positive during the prolonged summer drought despite the severe meteorological drought indicated by SPEI, CDI and EDDI.

Summary

BE-Dor is a grassland site located at approximately 248 m elevation. Compared with the forest sites, the vegetation is likely to have a shallower effective rooting zone and may therefore depend more directly on water availability in the upper soil layers. Across the analysed events, however, LE generally remained high as long as sufficient soil moisture was available, even under elevated atmospheric evaporative demand. This indicates that high EDDI values alone did not necessarily result in reduced evapotranspiration.

The analysed events also demonstrate that the ecosystem response depended on the interaction between atmospheric demand and soil water availability. During periods when SWC remained relatively high, elevated EDDI happened simultaneously with stable LE and relatively stable EF. In contrast, reductions in LE and EF were more visible when declining soil moisture occurred together with continued drought conditions, indicating a shift towards increasingly water-limited conditions. However, this response was not consistent across all analysed years.

The interpretation of BE-Dor is complicated by the apparent discontinuity in the SWC record during 2022.

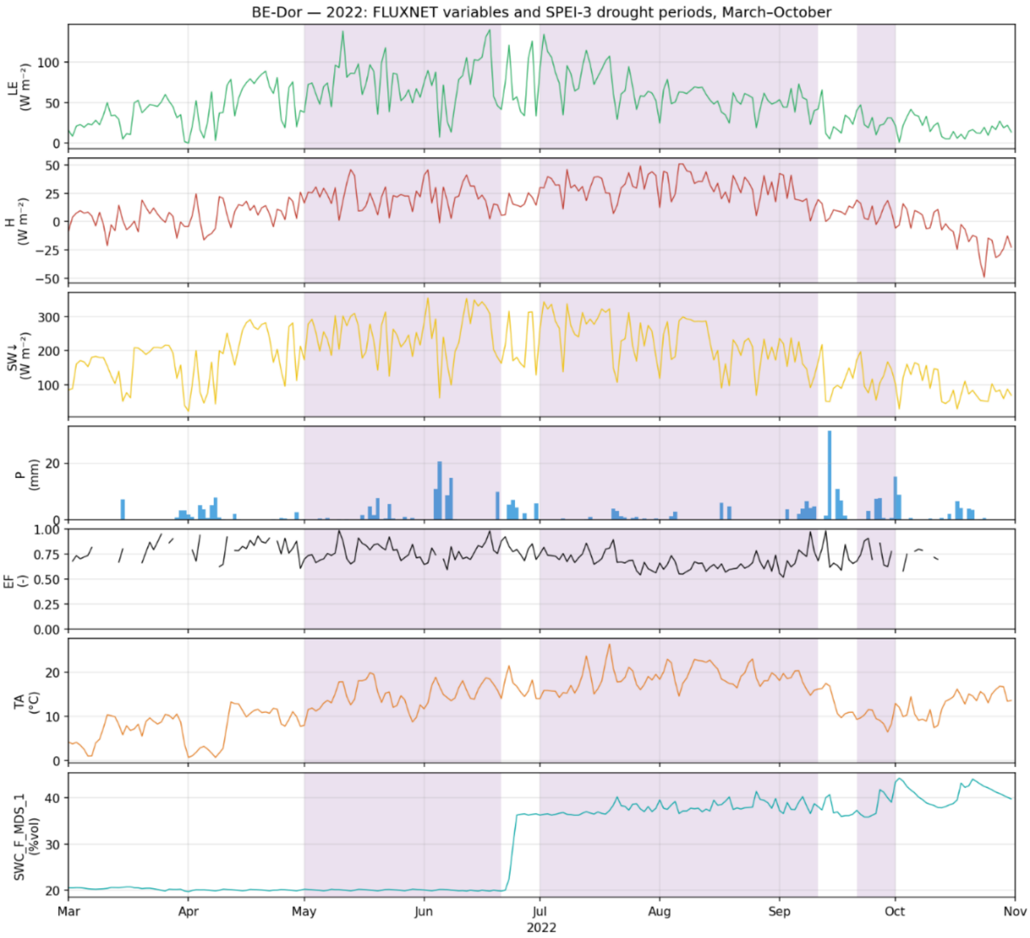

Figure 30. *Fluxnet variables BE Dor 2017 (ICOS Carbon Portal; figure created by the author)*

Evaporative fraction

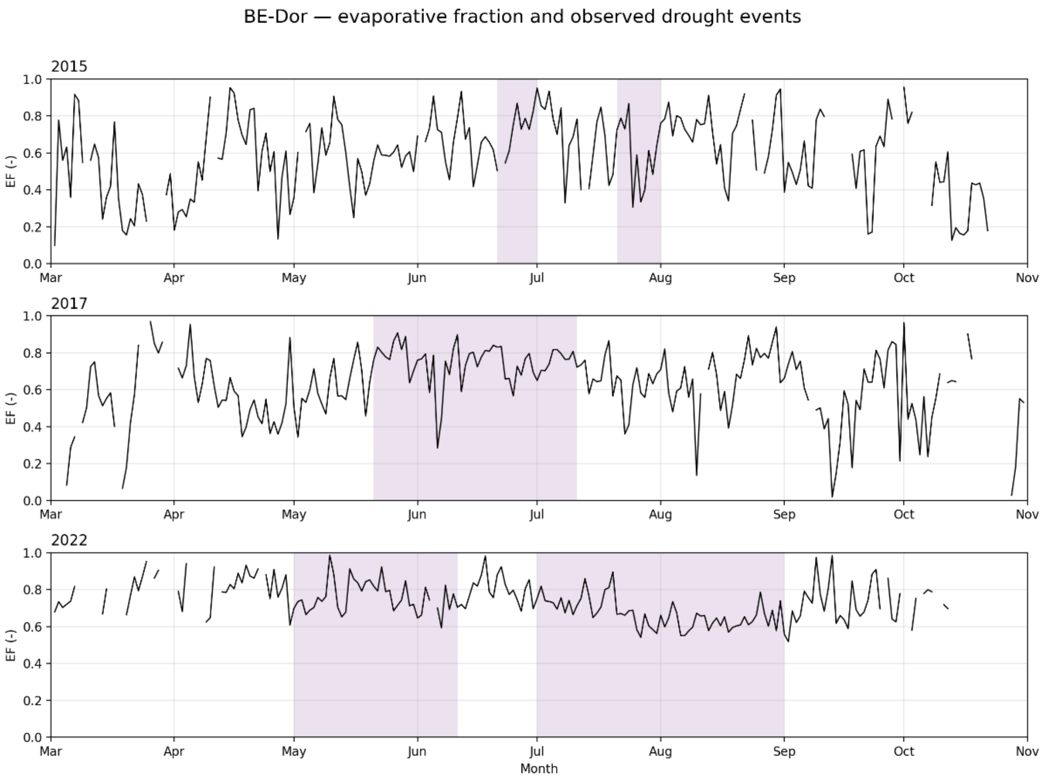

Figure 25.. *Evaporative fraction BE Dor (ICOS Carbon Portal)*

Figure presents the seasonal evolution of the evaporative fraction (EF) at BE-Dor during the analysed years. EF remained generally high throughout the observed seasons, indicating that a large proportion of the available energy was partitioned into latent heat flux. Although the response of EF varied between drought events and years, most values remained between approximately 0.5 and 0.9, with only modest decreases during prolonged dry periods.

Overall, BE-Dor exhibited limited reductions in evaporative fraction during the identified drought events, suggesting that evapotranspiration was largely maintained throughout the growing seasons. Similar to the forest sites, this behaviour may indicate that vegetation was able to access water below the depth represented by the SWC measurements, although this cannot be confirmed from the available observations.

Comparison between LSA GLEAM and GLDAS against ICOS observations

BE-Dor exhibited a different pattern from both BE-Lon and BE-Vie. Although all products reproduced the general seasonal evolution of EF, their relative performance varied throughout the season and between years. No single product consistently reproduced the ICOS observations more accurately than the others. Instead, the agreement with ICOS changed over time, with different products providing the closest match during different periods. The remaining figures can be found in Appendix C1-C4.

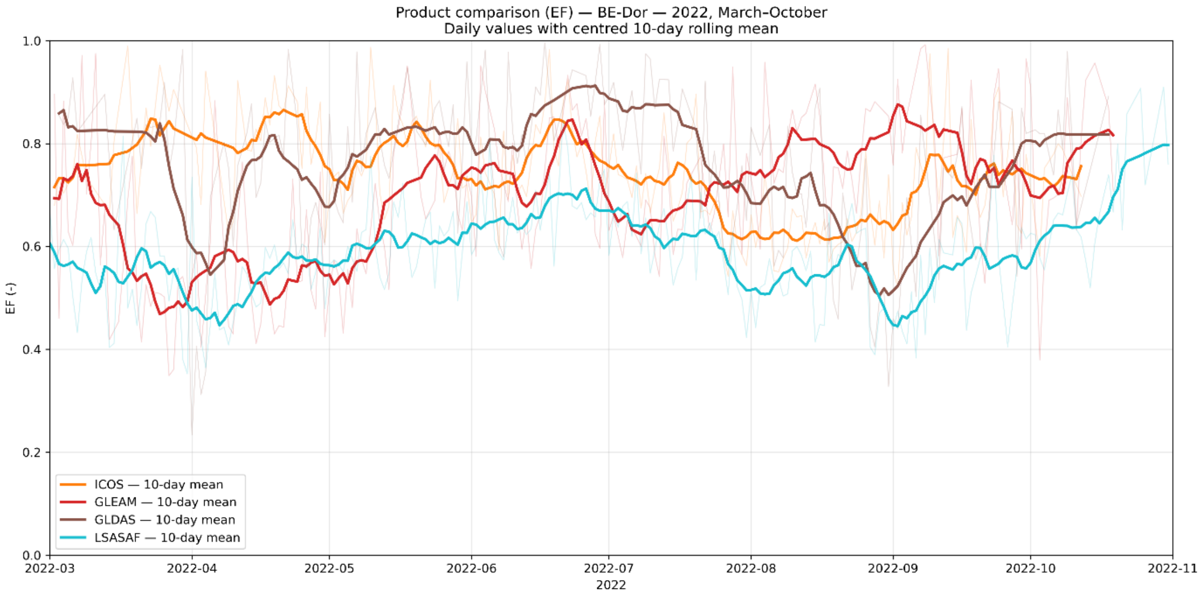

Figure 26. *Comparison BE Lon GLEAM GLDAS LSASAF (ICOS Carbon Portal, GLEAM, GLDAS, and LSA-SAF; figure created by the author)*

Diurnal cycles

At BE-Dor, the overall shape of the diurnal cycle remained similar across the three periods for LE. LSA-SAF overestimated sensible heat flux.

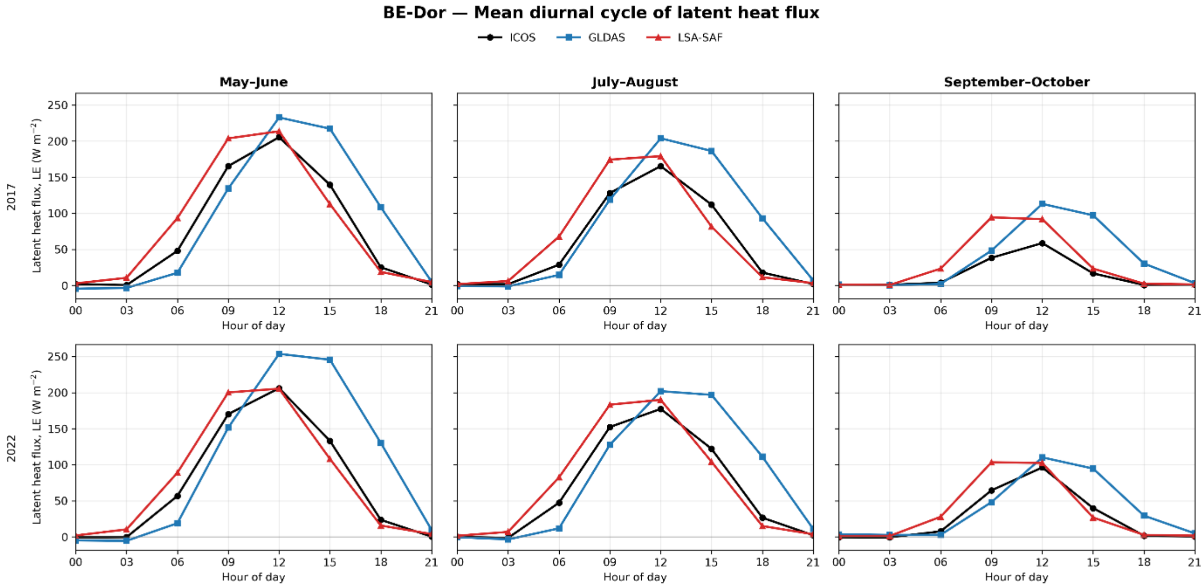

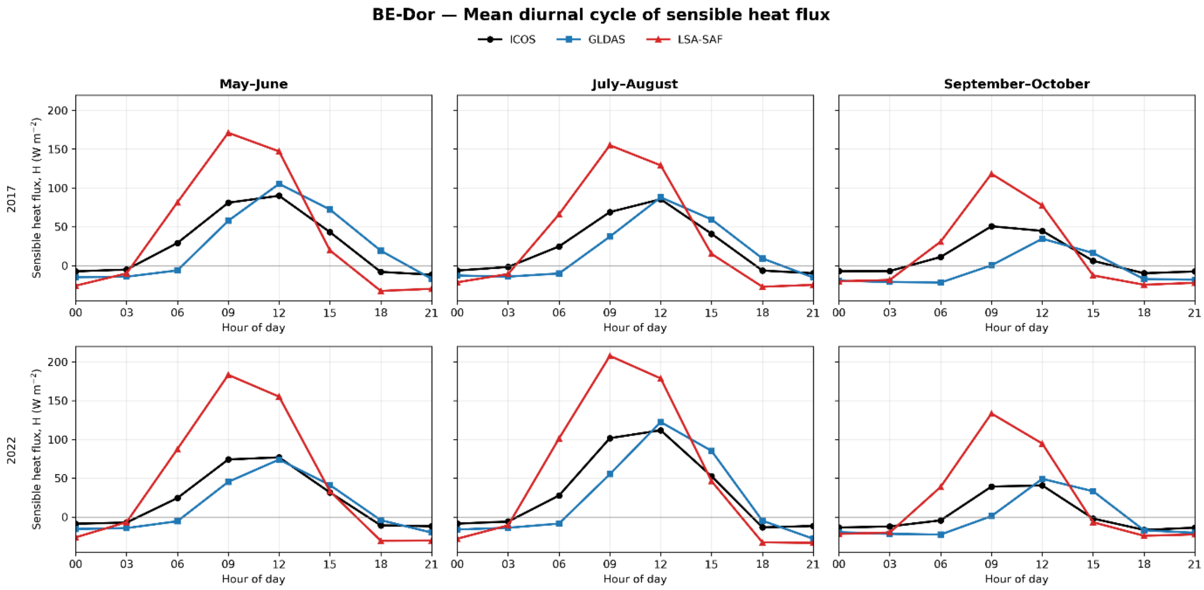

Figure 31 & 32. *Averaged LE and H diurnal cycles (Comparison BE Lon GLEAM GLDAS LSASAF (ICOS Carbon Portal, GLEAM, GLDAS, and LSA-SAF; figure created by the author)*

Overall performance metrics

	site	variable	product	KGE	RMSE	MAE	bias	absolute_bias	pearson_r	alpha	beta	n
0	BE-Dor	EF	GLDAS	0.33	0.19	0.14	0.09	0.09	0.36	0.85	1.13	470
1	BE-Dor	EF	GLEAM	0.07	0.21	0.16	-0.01	0.01	0.07	0.98	0.99	470
2	BE-Dor	EF	LSASAF	0.43	0.14	0.11	-0.06	0.06	0.58	0.64	0.90	470
3	BE-Dor	LE	GLDAS	0.28	28.46	21.82	20.22	20.22	0.85	1.11	1.69	1095
4	BE-Dor	LE	GLEAM	0.38	25.97	20.21	17.54	17.54	0.85	1.03	1.60	1095
5	BE-Dor	LE	LSASAF	0.66	16.19	12.36	9.81	9.81	0.93	1.03	1.34	1095
6	BE-Dor	H	GLDAS	-0.02	27.06	16.14	-9.77	9.77	0.49	1.11	0.12	1095
7	BE-Dor	H	GLEAM	0.40	27.70	17.85	-0.55	0.55	0.43	1.18	0.95	1095
8	BE-Dor	H	LSASAF	-0.06	26.54	18.31	10.37	10.37	0.48	1.03	1.93	1095

Table 10. Values of drought indices at BE Dor

Discussion

Product-related differences

No product had the best overall performance across all stations. The results suggest that difference in product methodology and spatial resolution on one side, and ecosystem differences on the other side, influenced general performance of the models. Possible explanations are noted below.

LSA SAF did not exhibit consistent behaviour across all stations. Its performance depended strongly on ecosystem type. At the evergreen forest site, LSA SAF underestimated latent heat while it overestimated sensible heat flux. This behaviour was clearly visible in the mean diurnal cycles, where the observed daytime peak in latent heat was drastically lower than the ICOS measurements. Such behaviour suggests that the product partitioned a larger fraction of the available surface energy into atmospheric heating rather than evapotranspiration. This behaviour however was not observed at every station. At BE Vie, LSA SAF achieved the highest KGE for latent heat among the evaluated products, as it did for grassland site at BE Dor. LSA SAF derives latent and sensible heat fluxes primarily from satellite observations using a physically based surface energy balance approach. That is why its estimates are strongly influenced by remotely sensed surface characteristics, such as land surface temperature and vegetation conditions, as well as the assumptions made within the algorithm.

GLEAM works in a different way. Rather than directly retrieving surface fluxes, it estimates evapotranspiration using the Penman equation combined with soil moisture constraints, vegetation stress and a multilayer water balance model. Root-zone soil moisture is further constrained through the assimilation of satellite observations, allowing the model to better represent water availability for vegetation. GLEAM generally showed stable performance across the analysed stations and achieved the highest agreement for latent heat and evaporative fraction at the evergreen forest site (BE-Bra). Unlike GLDAS, GLEAM is specifically designed to estimate terrestrial evaporation and takes vegetation stress into account, root-zone soil moisture and interception processes. These features may enable the product to better represent forest ecosystems, where transpiration can be maintained during drought through continued access to deeper soil water. GLEAM performed less successfully at the cropland site (BE-Lon), particularly for evaporative fraction. This may reflect the greater influence of crop phenology, agricultural management and rapidly changing surface conditions, which are difficult to represent using a globally parameterised evaporation model. This could potentially explain continuous GLDAS low performance metrics value at observed forest sites.

GLDAS differs again from other products. It is a land surface modelling system that simulates soil moisture, vegetation processes and energy exchanges through physically based process representations. Its performance depends strongly on how well the model represents local vegetation and soil conditions. GLDAS exhibited the strongest ecosystem dependence among the evaluated products. It consistently provided the highest agreement with the ICOS observations at the cropland site (BE-Lon), where it achieved the best performance for evaporative fraction, latent heat and sensible heat. In contrast, its performance was weaker at the forest sites, particularly for evaporative fraction. As a land surface model, GLDAS explicitly simulates soil moisture, vegetation processes and surface energy exchange through physically based equations. This modelling approach may be particularly well suited for cropland ecosystems, where evapotranspiration is closely linked to shallow soil moisture dynamics and seasonal vegetation development. When applied to forest ecosystems, it might be difficult to represent the processes correctly as they are characterised by more complex processes such as canopy interception, heterogeneous vegetation structure and deep rooting systems.

The observed differences suggest that the strengths and limitations of each product are closely linked to their underlying modelling approach and become evident under different environmental conditions.

Overall ecosystem response to drought.

Across the analysed drought events, the four ICOS sites showed contrasting responses to meteorological drought depending on ecosystem type, vegetation characteristics and soil water availability.

Forest buffered against drought

The two forest ecosystems, BE-Bra and BE-Vie, showed a similar response to the analysed drought events. Despite several prolonged drought periods, latent heat flux generally remained high and the evaporative fraction showed no persistent decrease, indicating that evapotranspiration was maintained throughout much of the observed season. At both sites, this response occurred despite a progressive decline in the measured soil water content during prolonged droughts. This suggests that the reduction in measured SWC did not necessarily correspond to the total amount of water available for vegetation. One possible explanation is that the forest vegetation was able to access water stored below the depth represented by the initial soil moisture measurements. To further investigate the relationship between measured soil moisture and vegetation water availability, additional soil moisture observations from multiple depths were analysed for the observed sites (Figure 41) These profiles provide additional information on the temporal evolution of soil moisture throughout the rooting zone and help to investigate whether water remained available below the depth represented by the SWC measurements from the shallow top layer used in the initial results.

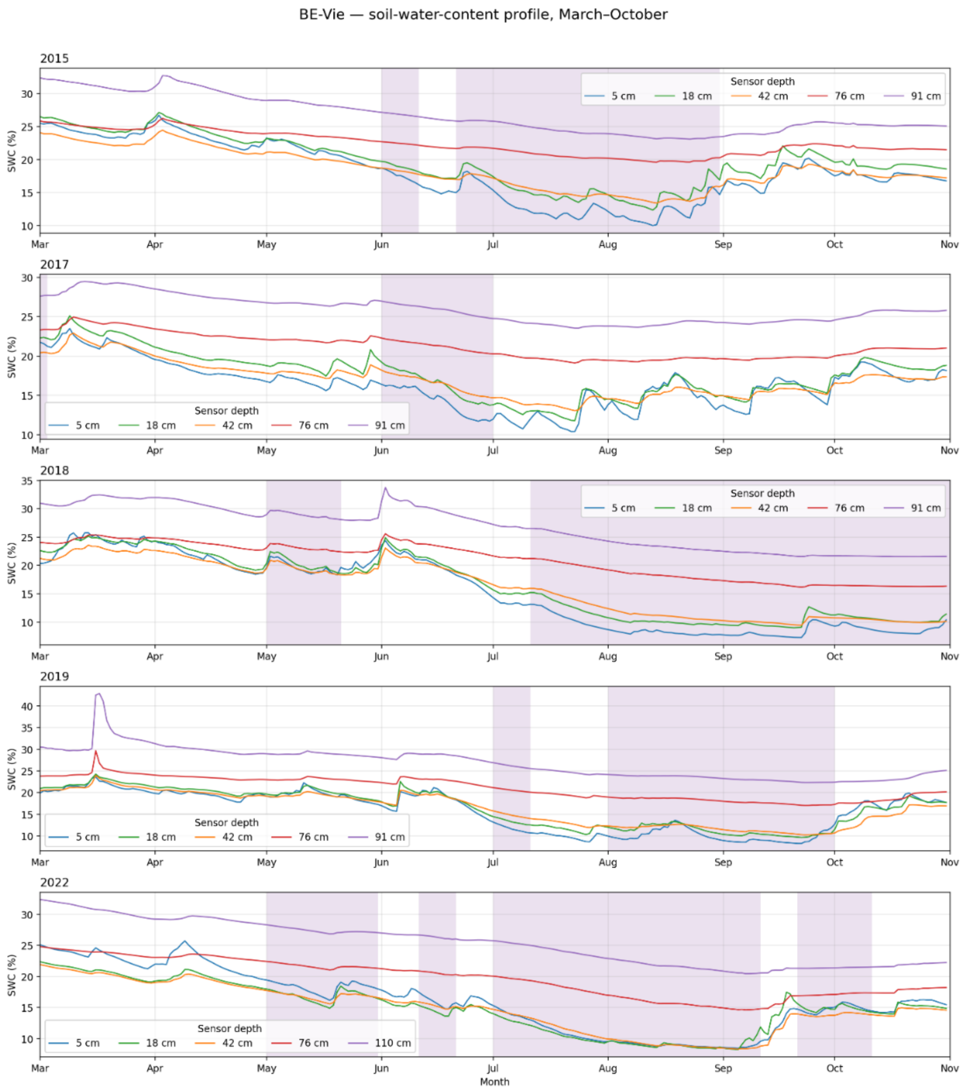

Figure 33. *soil water content profile (ICOS Carbon Portal; figure created by the author)*

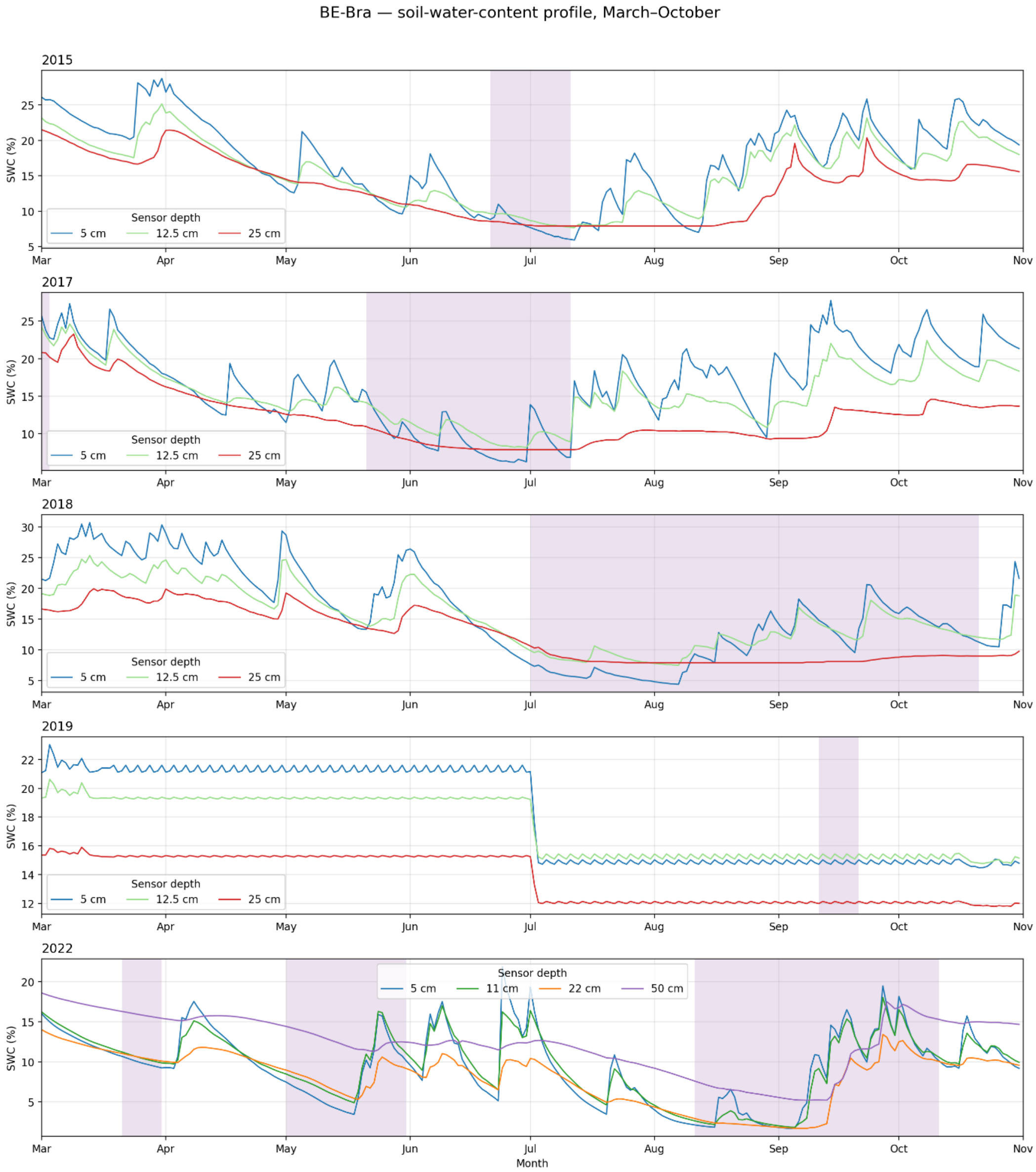

Figure 34. *soil water content profile (ICOS Carbon Portal; figure created by the author)*

At both forest sites, the upper soil layers showed a clear decline in soil moisture during the prolonged drought periods, while the deeper layers exhibited a more gradual decrease and generally maintained higher soil moisture values. The deeper soil layers at BE-Vie showed a particularly gradual decline throughout most analysed years, while a similar pattern was observed at BE-Bra, although the available measurements extended to shallower depths. Despite these differences, both sites exhibited evidence of larger water availability at depth than suggested by the initial results.

In contrast, the cropland site showed stronger response to declining soil moisture, further supporting that ecosystem characteristics played an important role in the energy partitioning. The stronger decline in LE and EF at BE-Lon suggests that vegetation characteristics, rooting depth and seasonal crop development influenced the ecosystem response differently than at the forest sites. These factors are discussed in the following section.

Different ecosystem response at grassland and cropland

BE-Lon is an intensively managed cropland with a four-year crop rotation. Unlike the forest sites, the vegetation changes completely from year to year as different crops are cultivated. That means that canopy structure, phenology and water use vary between the seasons. During the growing season, crops establish, rapidly increase their leaf area and transpiration, and later undergo harvest, after which transpiration declines significantly. In addition, the major crops cultivated at BE-Lon are capable of developing relatively deep root systems under favourable conditions, although rooting depth varies substantially among species, soil characteristics and environmental conditions. Because information on the crop grown during each analysed year was unavailable, the actual rooting characteristics during the study period could not be assessed. The crop species cultivated during each analysed year could not be identified from the available ICOS documentation. Future studies could potentially benefit from retreiving annual crop management information from site operators to better relate evapotranspiration dynamics to crop phenology and rooting characteristics. To provide additional context, soil moisture observations from multiple depths were examined for BE-Lon (Figure 34)

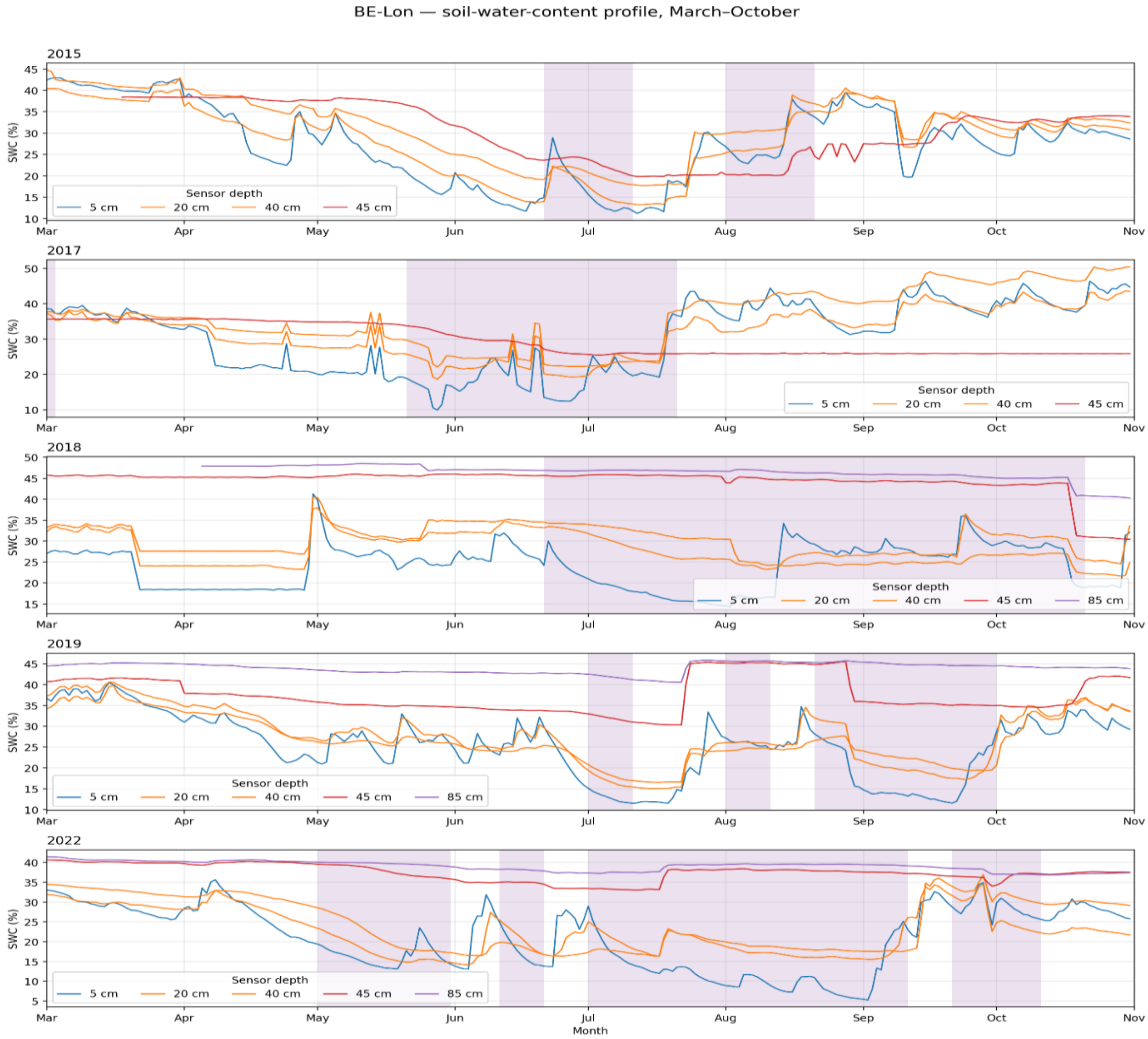

Figure 35. *soil water content profile (ICOS Carbon Portal)*

The profiles indicate that, although the upper soil layers generally dried notably during drought periods, soil moisture at 85 cm remained comparatively stable during most of the analysed years. This suggests that water remained available at greater depth despite pronounced drying near the surface. Considering that the crop species typically cultivated at BE-Lon are capable of developing relatively deep root systems, this may indicate that deeper soil water was potentially accessible during at least part of the growing season. However, because information on the crop species cultivated during each analysed year and their developmental stages was unavailable, it cannot be determined whether the crops had already established deep root systems during the drought periods to effectively utilize this water. For example, if drought occurred during the early stages of crop development, the root systems may not yet have reached the deeper soil layers where water remained available. The timing of drought relative to crop development could therefore have influenced the extent to which deeper soil water was accessible. It is important to note that this could not be supported by evidence because information on the crop species and growth stages during the analysed years was unavailable.

BE-Dor exhibited a different response to drought than both the forest and cropland sites. As a managed grassland, the ecosystem remained capable of sustaining relatively high LE while sufficient soil moisture was available, despite elevated atmospheric evaporative demand. This suggests that, similar to the other ecosystems, atmospheric demand alone did not determine the drought response. Unlike the forest and cropland sites, the additional multi-depth soil moisture observations did not allow a similarly detailed interpretation because the available measurement depths differed considerably between years and the 2022 observations contained substantial inconsistencies.

Land cover

Spatial representativeness should be considered when comparing the ICOS observations with gridded evapotranspiration products. Unlike the ICOS measurements, which originate from the eddy covariance surrounding the tower, each product represents a fixed grid cell. As a result, the land surface represented by the products does not necessarily correspond exactly to the area contributing to the measured turbulent fluxes. To explore these spatial differences, the ICOS station locations were compared with the corresponding grid cells of each evapotranspiration product using ECOCLIMAP land-cover datasets. (Figure 44).

The footprint size varied significantly among datasets, with LSA-SAF representing the smallest spatial extent and GLDAS the largest. In addition, the ICOS stations were not always located near the centre of the corresponding product grid cells. This means that the represented product area in reality is much larger squared area, but the tower could physically be much closer to another type of landscape.

In addition, the land-cover classes composition within each product footprint was quantified and represented in percentages. This allowed the represented landscape to be compared not only visually, but also in terms of the proportion of the different land-cover classes.

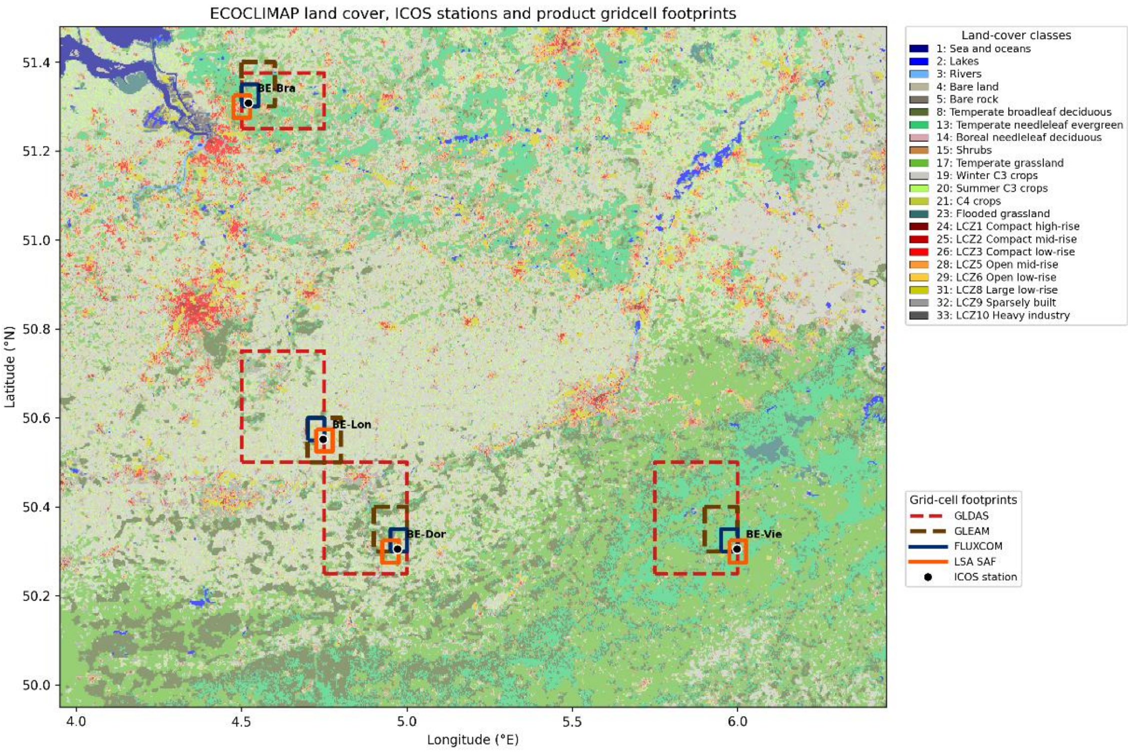

Figure 36. *land cover; product footprints ECOCLIMAP ((ECOCLIMAP-SG; ICOS Carbon Portal; GLDAS; GLEAM;LSA-SAF;FLUXCOM))*

In addition, the land-cover classes composition within each product footprint were quantified and represented in percentages.

0	BE-Bra	FLUXCOM	Temperate needleleaf evergreen	39.81	Temperate broadleaf deciduous	13.27	Temperate grassland	13.27	Shrubs	10.18	23.46
1	BE-Bra	GLDAS	Temperate needleleaf evergreen	26.10	Winter C3 crops	23.33	Temperate grassland	19.01	Shrubs	7.66	23.90
2	BE-Bra	GLEAM	Temperate needleleaf evergreen	33.96	Winter C3 crops	22.44	Temperate grassland	13.42	Shrubs	7.02	23.15
3	BE-Bra	LSA SAF	Temperate needleleaf evergreen	30.25	LCZ9 Sparsely built	12.65	Temperate grassland	10.49	Shrubs	10.18	36.42
4	BE-Dor	FLUXCOM	Winter C3 crops	39.82	Temperate grassland	20.68	Temperate broadleaf deciduous	20.37	C4 crops	7.72	11.42
5	BE-Dor	GLDAS	Winter C3 crops	39.98	Temperate broadleaf deciduous	17.67	Temperate grassland	11.49	LCZ9 Sparsely built	7.60	23.27
6	BE-Dor	GLEAM	Winter C3 crops	37.66	Temperate broadleaf deciduous	26.08	Temperate grassland	14.89	Temperate needleleaf evergreen	5.79	15.59
7	BE-Dor	LSA SAF	Winter C3 crops	45.68	Temperate grassland	19.76	Temperate broadleaf deciduous	16.66	C4 crops	7.41	10.49
8	BE-Lon	FLUXCOM	Winter C3 crops	68.83	Summer C3 crops	12.96	C4 crops	10.19	LCZ9 Sparsely built	3.40	4.63
9	BE-Lon	GLDAS	Winter C3 crops	57.48	Summer C3 crops	10.44	C4 crops	7.80	LCZ9 Sparsely built	6.44	17.84
10	BE-Lon	GLEAM	Winter C3 crops	69.14	Summer C3 crops	13.19	C4 crops	8.18	LCZ9 Sparsely built	3.86	5.63
11	BE-Lon	LSA SAF	Winter C3 crops	73.46	Summer C3 crops	14.81	C4 crops	8.33	LCZ9 Sparsely built	1.54	1.85
12	BE-Vie	FLUXCOM	Temperate needleleaf evergreen	63.58	Temperate grassland	21.91	Temperate broadleaf deciduous	8.64	Shrubs	5.56	0.31
13	BE-Vie	GLDAS	Temperate needleleaf evergreen	41.72	Temperate grassland	35.42	Temperate broadleaf deciduous	13.59	Shrubs	5.69	3.58
14	BE-Vie	GLEAM	Temperate needleleaf evergreen	46.69	Temperate grassland	35.26	Temperate broadleaf deciduous	9.49	Shrubs	5.79	2.78
15	BE-Vie	LSA SAF	Temperate needleleaf evergreen	70.37	Temperate broadleaf deciduous	14.20	Temperate grassland	8.64	Shrubs	6.79	0.00

Table 11 *Percentages classes within footprints (ECOCLIMAP-SG; ICOS Carbon Portal; GLDAS; GLEAM;LSA-SAF;FLUXCOM)*

Despite the differences in spatial resolution, all products consistently represented the dominant ecosystem surrounding each ICOS station. BE-Bra and BE-Vie remained mostly forested across all evaluated products, while BE-Lon was consistently dominated by cropland and BE-Dor represented a mixed grassland landscape. This suggests that all products captured the primary land-cover characteristics of the study sites despite representing different spatial extents. Although the dominant ecosystem remained consistent, the proportion of the surrounding land-cover classes differed considerably among products. These differences generally became stronger as footprint size increased. Larger grid cells incorporated a greater proportion of neighbouring land-cover types, resulting in a more heterogeneous representation of the landscape than the higher-resolution products. This was evident at BE-Vie, where the proportion of temperate needleleaf evergreen forest ranged from approximately 42% in GLDAS to over 70% in LSA-SAF. The larger GLDAS footprint included substantially more surrounding grassland, while the smaller LSA-SAF footprint represented a considerably more homogeneous forest landscape. In contrast, BE-Lon showed consistency among products. All footprints were strongly dominated by winter C3 crops, with relatively small differences in the contribution of the remaining land-cover classes. This indicates that, despite differences in footprint size, all products represented a broadly similar agricultural landscape. These findings indicate that spatial representativeness should be considered when interpreting match between gridded evapotranspiration products and point-based eddy covariance observations.

Soil texture

In addition to vegetation characteristics and land cover, soil properties influence the storage and availability of water for evapotranspiration. The dominant topsoil texture within product footprints was therefore examined to assess whether broad differences in soil texture could contribute to the observed ecosystem responses.

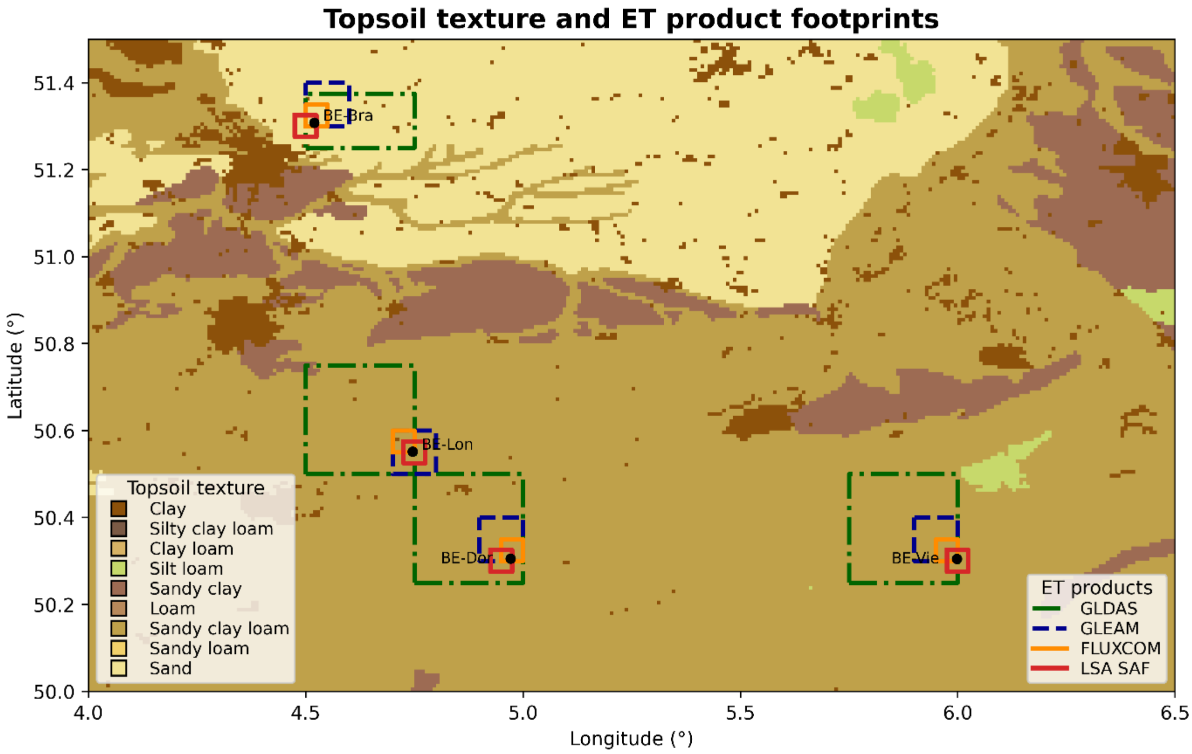

Figure 37. *Soil texture (Harmonized World Soil Database; ICOS Portal; figure created by author)*

The analysed sites were predominantly characterized by loamy soil textures, although local variations were observed. BE-Lon, BE-Dor and BE-Vie were largely situated on loamy soils, whereas BE-Bra was located close to a transition towards sandier textures. Despite these local differences, the overall variation in topsoil texture among the evaluated product footprints was smaller than the variation observed for land cover. Because loamy soils generally provide a balance between water retention and drainage, the broadly similar texture patterns suggest that large differences in topsoil texture alone are unlikely to explain the different ecosystem responses observed among the study sites. Important to mention is that this analysis represents only the upper soil layer and does not investigate differences in soil depth and hydraulic properties.

The broad soil characteristics were further supported by the dominant WRB soil groups identified at each ICOS site (Figure Appendix) with BE-Bra classified as Gleyic Podzols, BE-Lon and BE-Dor as Haplic Luvisols, and BE-Vie as Dystric Cambisols. These classifications provide additional information on soil development and properties but do not directly reflect differences in topsoil texture or plant-available water. (base on HWSD data- map computed but maybe irrelevant for the analysis) The complete percentage distribution of the topsoil texture classes and WRB soil groups within each product footprint is provided in Appendix .

Limitations

Spatial representation

A major source of uncertainty in this study arises from differences in the spatial representation of the evaluated datasets. The products differ significantly in spatial resolution, ranging from approximately 3 km for LSA-SAF to 0.25° for GLDAS and GLEAM. Consequently, each product represents a different spatial extent around the ICOS tower. Although a nearest-neighbour approach was applied to spatially match the products with the station locations, the selected grid cell did not always place the station near its centre. In some cases, neighbouring grid cells represented notably different land-cover compositions, which may have contributed to the observed differences in product performance.

Temporal representation

The evaluated products also differ in their native temporal resolution. To enable direct comparison, all datasets were aggregated to common daily and sub-daily time steps. While this harmonisation was necessary, temporal aggregation inevitably smooths short-term variability and reduces the magnitude of extreme fluxes. This could have caused differences in peak evapotranspiration or energy partitioning may have been underestimated.

Product methodology

The three evaluated products are based on fundamentally different methodologies, ranging from satellite retrievals to land surface modelling and evaporation modelling. In addition, they rely on different forcing datasets, parameterisations and assumptions. As a result, it is difficult to attribute the observed differences in performance to a single factor, since multiple methodological differences influence the final flux estimates simultaneously.

Environmental information

Several environmental variables that could have improved the interpretation of the results were not available within the scope of this study. Information on rooting depth, annual crop type, vegetation dynamics (e.g. LAI), groundwater availability and local management practices was not included. These factors can influence evapotranspiration during drought and may partly explain the observed differences between products and ecosystems.

Reference observations

The ICOS eddy covariance observations used as reference data are themselves subject to uncertainty. Measurement errors, gap-filling procedures and the issue of imperfect energy balance closure may influence the observed latent and sensible heat fluxes. Part of the disagreement between products and observations may also originate from uncertainties in the reference measurements.

Recommendations

Expanded spatial and temporal coverage

Future research should extend the analysis to a larger number of ICOS stations representing a wider range of climate zones and ecosystem types. Including additional drought events and longer time series would allow assessment of product performance under a broader range of environmental conditions.

Improved spatial matching

The comparison could be further improved by applying more advanced footprint modelling instead of nearest-neighbour matching. Accounting for the dynamic ICOS flux footprint and weighting the contribution of surrounding grid cells may provide a more representative comparison between tower observations and gridded products.

Additional environmental variables

Future studies should incorporate complementary environmental information, such as rooting depth, groundwater availability, vegetation characteristics (e.g. LAI), crop type and management practices. Each site provides a contact of an ICOS station-specific operator that could potentially be contacted for additional data not stated in the available manual.

Product-specific evaluation

Given the strong ecosystem dependence observed in this study, future evaluations should assess product performance separately for different ecosystem types rather than relying solely on overall performance statistics. Such an approach would help identify the environmental conditions under which individual products perform best and support more informed product selection for drought monitoring and modelling applications.

Conclusion

The comparison demonstrated that the evaluated products reproduced drought responses with varying success depending on the ecosystem. Forest ecosystems generally maintained higher evaporative fractions and latent heat fluxes during drought, indicating that they remained relatively energy-limited despite declining soil moisture. In contrast, cropland exhibited a stronger transition towards water limitation, reflected by reduced latent heat flux and evaporative fraction together with increased sensible heat flux. These contrasting ecosystem responses influenced product performance, highlighting that the suitability of individual products depends not only on their modelling approach but also on whether the dominant controls on evapotranspiration are primarily energy- or water-limited. This study demonstrates that evaluating evapotranspiration products requires consideration of both product methodology and ecosystem functioning. Differences in the transition between energy-limited and water-limited conditions strongly influenced product performance, emphasizing that no single product is universally applicable across all ecosystems or drought conditions. Rather than identifying a universally "best" product, the results highlight the importance of understanding the strengths, limitations, and underlying assumptions of each product. Such knowledge could potentially enable researchers to make more informed decisions when selecting evapotranspiration products for specific ecosystems, applications, and research questions.

References

Canadell, J. G., Jackson, R. B., Ehleringer, J. R., Mooney, H. A., Sala, O. E., & Schulze, E.-D. (1996). *Maximum rooting depth of vegetation types at the global scale*. *Oecologia, 108*(4), 583–595. https://doi.org/10.1007/BF00329030

Copernicus Climate Change Service (C3S). (2025). *Climate Data Store (CDS): ERA5 reanalysis data*. https://cds.climate.copernicus.eu/

European Commission, Joint Research Centre. (2018). *European Drought Observatory (EDO): Combined Drought Indicator methodology*. https://www.sciencedirect.com/science/article/pii/S2214581818303136

European Commission, Joint Research Centre. (2025). *European Drought Observatory (EDO) data download portal*. https://drought.emergency.copernicus.eu/tumbo/edo/download/

European Commission, Joint Research Centre. (2025). *ERA5-Land monthly averaged data from 1950 to present*. https://data.jrc.ec.europa.eu/dataset/12a852fe-8a43-4d04-9c75-1d3ef2ac673c

European Organisation for the Exploitation of Meteorological Satellites (EUMETSAT). (2025). *Land Surface Analysis Satellite Application Facility (LSA SAF)*. https://landsaf.ipma.pt/

FLUXNET. (2025). *FLUXNET Data Portal*. https://data.fluxnet.org/data/

Food and Agriculture Organization of the United Nations (FAO). (2025). *Harmonized World Soil Database (HWSD)*. https://www.fao.org/land-water/resources/tools/databases/hwsd/en

Gupta, H. V., Kling, H., Yilmaz, K. K., & Martinez, G. F. (2009). Decomposition of the mean squared error and NSE performance criteria: Implications for improving hydrological modelling. *Journal of Hydrology, 377*(1–2), 80–91.

ICOS ERIC. (2025). *ICOS Carbon Portal*. https://www.icos-cp.eu/

Ionita, M., Caldarescu, D. E., & Nagavciuc, V. (2021). Compound hot and dry events in Europe: Variability and large-scale drivers. *Frontiers in Climate, 3*, Article 688991. https://doi.org/10.3389/fclim.2021.688991

Miralles, D. G., Bonte, O., Koppa, A., et al. (2025). GLEAM4: Global land evaporation and soil moisture dataset at 0.1° resolution from 1980 to near present. *Scientific Data, 12*, 416. https://doi.org/10.1038/s41597-025-04610-y

NASA Goddard Earth Sciences Data and Information Services Center (GES DISC). (2025). *Global Land Data Assimilation System (GLDAS).* https://disc.gsfc.nasa.gov/

Nachtergaele, F. O., van Velthuizen, H., Verelst, L., et al. (2012). *Harmonized World Soil Database (Version 1.2).* FAO & IIASA.

Open Source CNRM. (2025). *ECOCLIMAP-SG project documentation and land-cover class definitions*. https://opensource.umr-cnrm.fr/projects/ecoclimap-sg/wiki

Appendix A1 – A3 Variables per station from 2015 - 2026 (source: Unless otherwise indicated, all figures in this report are based on the data retrieved from Fluxnet.org Download Data)

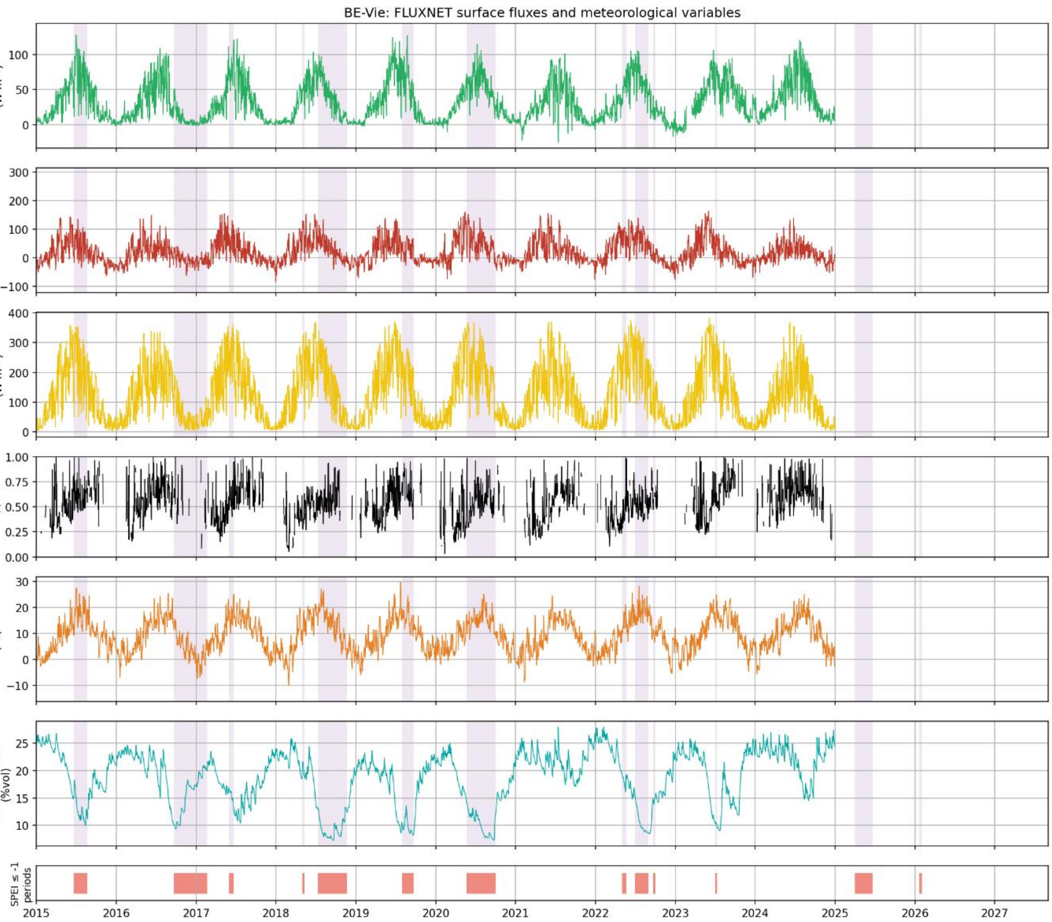

A1. BE Vie, Fluxnet variables and drought periods from 2015 - 2026

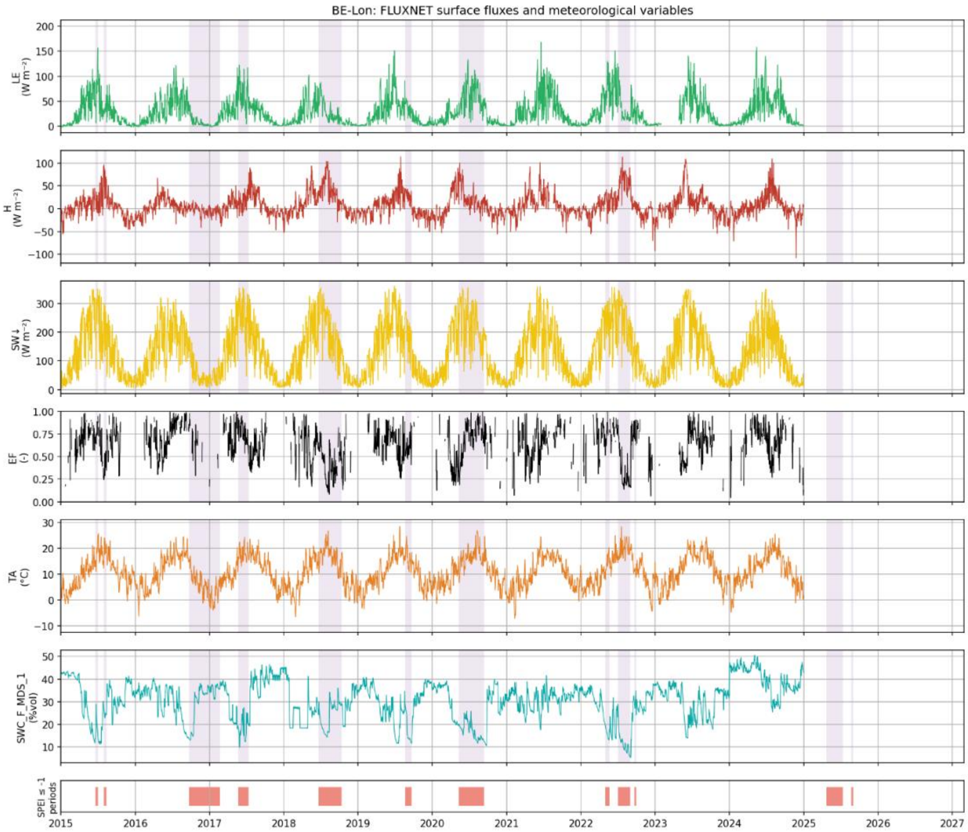

A2. BE Lon, Fluxnet variables and drought periods from 2015 - 2026

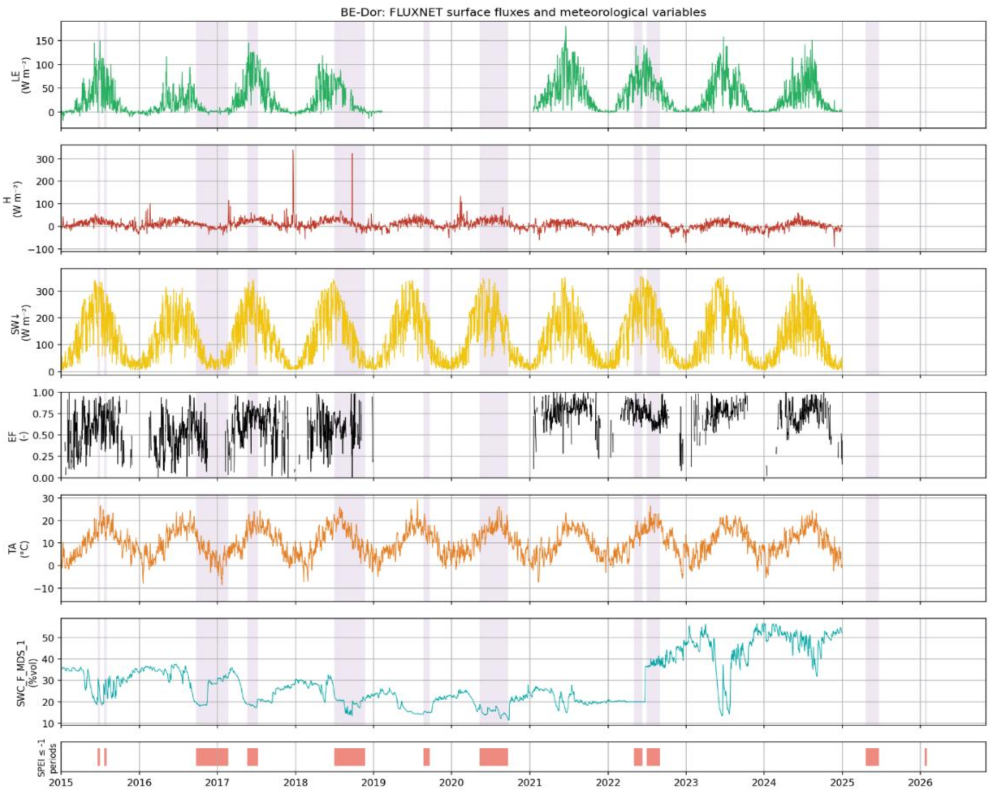

A1. BE Vie, Fluxnet variables and drought periods from 2015 – 2026

Appendix B1 – B8 Variables per station (source: Unless otherwise indicated, all figures in this report are based on the data retrieved from Fluxnet.org Download Data)

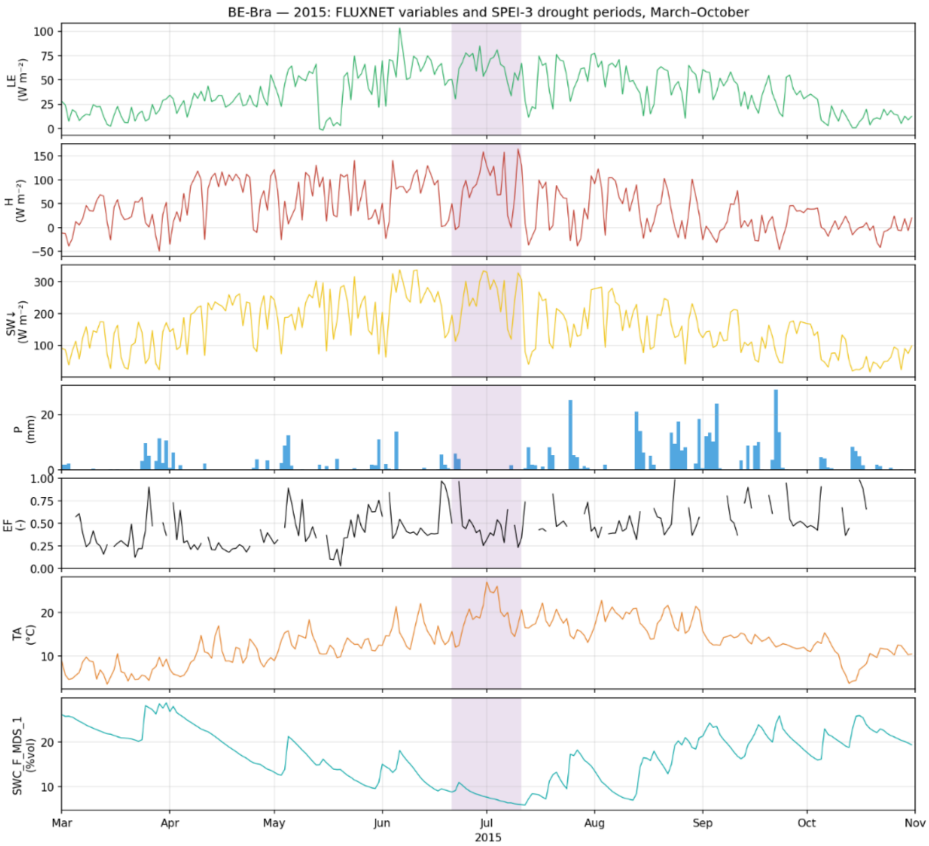

B1. BE Bra, Fluxnet variables throughout observed period 2015

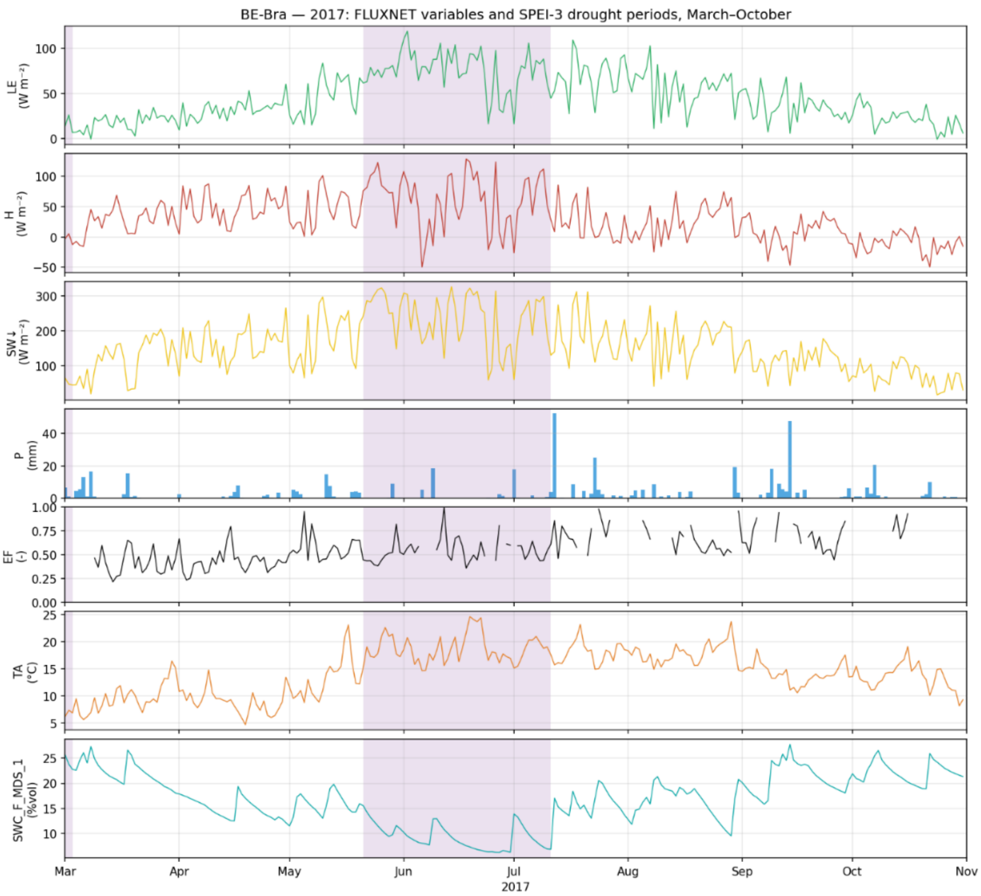

B2. BE Bra, Fluxnet variables throughout observed period 2017

B3. BE Lon, Fluxnet variables throufhout observed period 2017

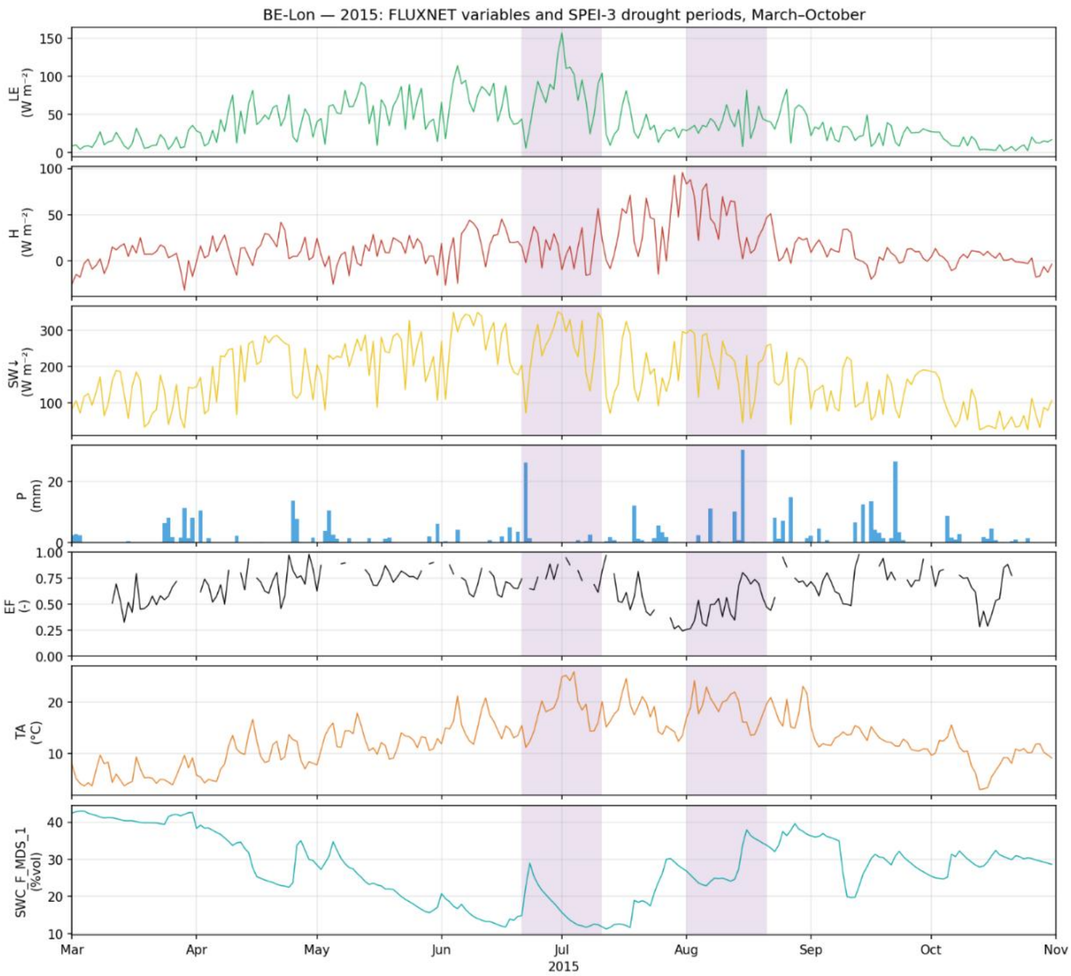

B4. BE Lon, Fluxnet variables throughout observed period 2015

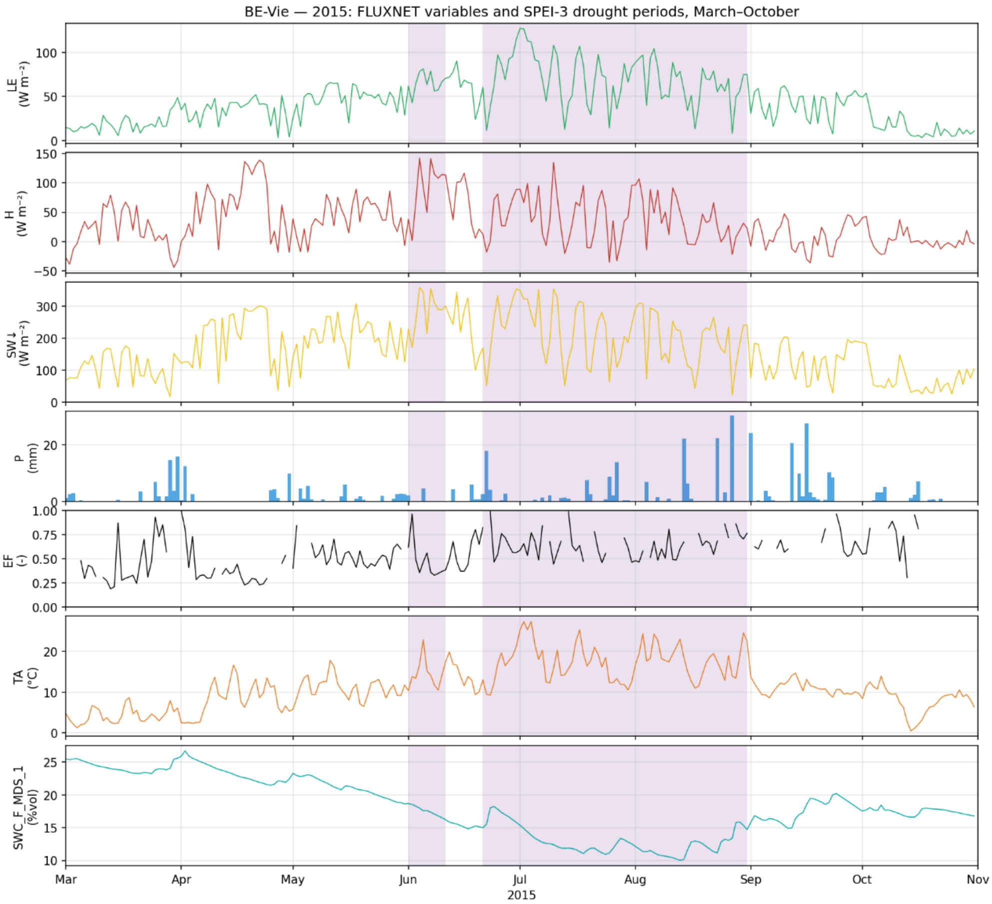

B5. BE Vie, Fluxnet variables throughout observed period 2015

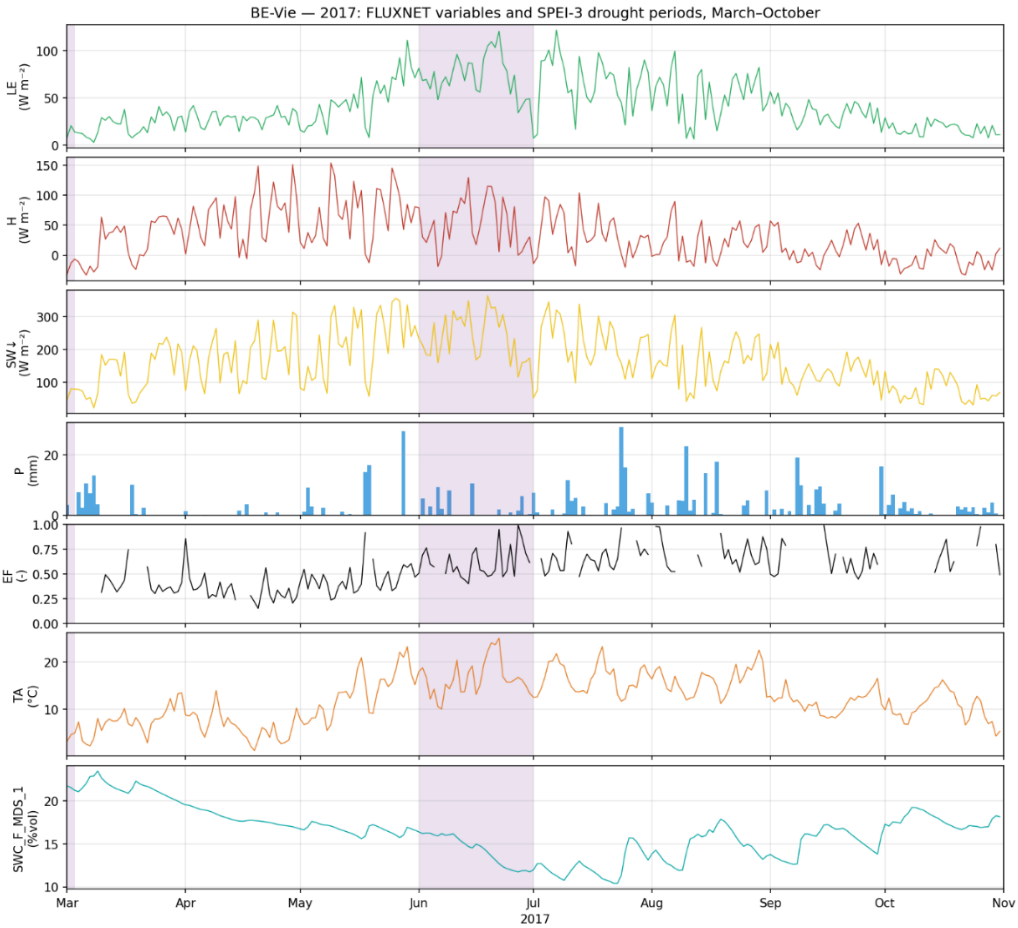

B6. BE Vie, Fluxnet variables throughout observed period 2017

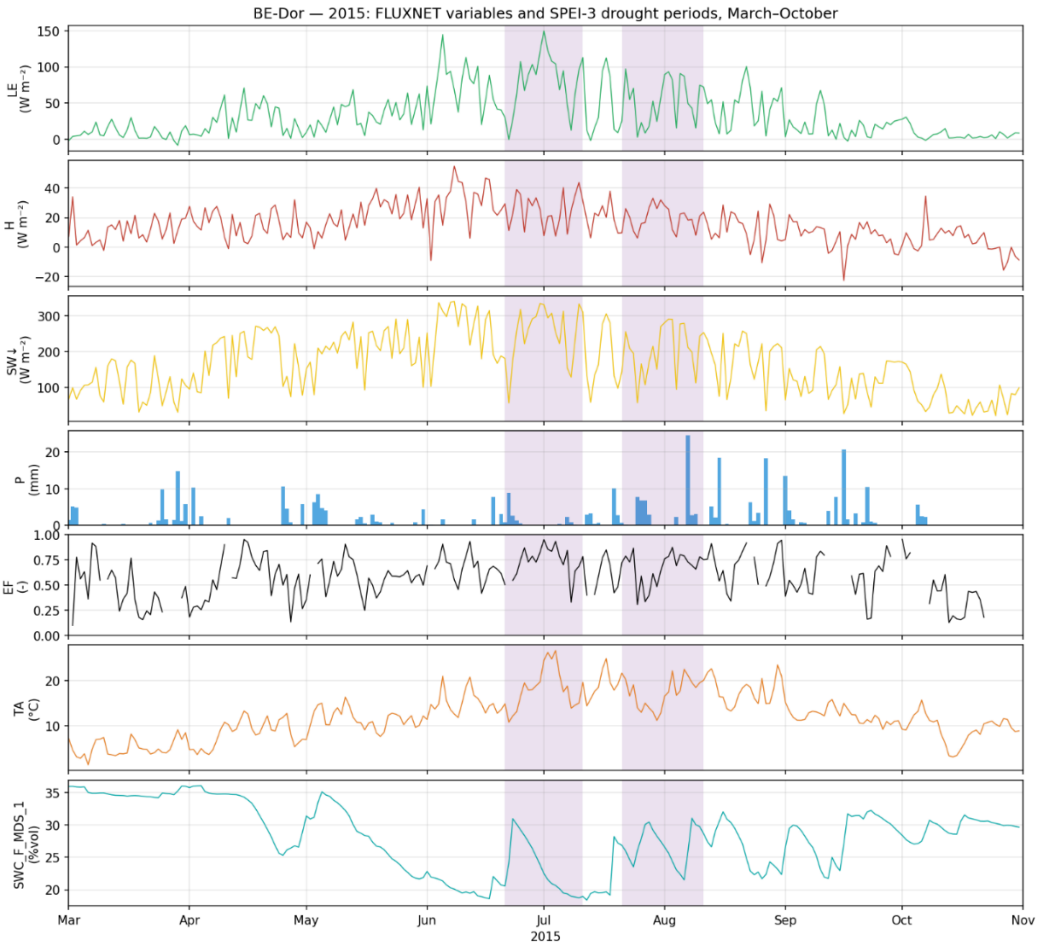

B7. BE Dor, Fluxnet variables throughout observed period 2015

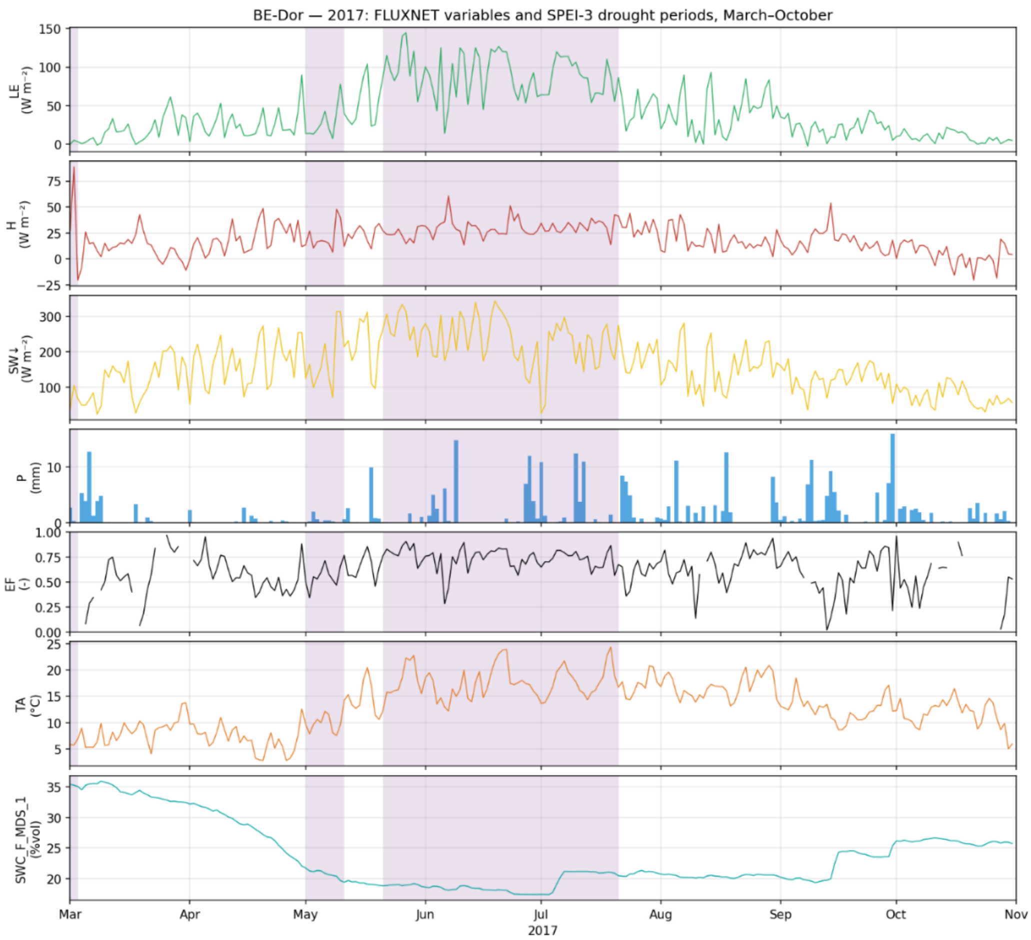

B8. BE Bra, Fluxnet variables throughout observed period 2017

Appendix C1 (source: all figures in this section are based on ICOS Portal, GLEAM, GLDAS, FLUXCOM and LSA SAF)

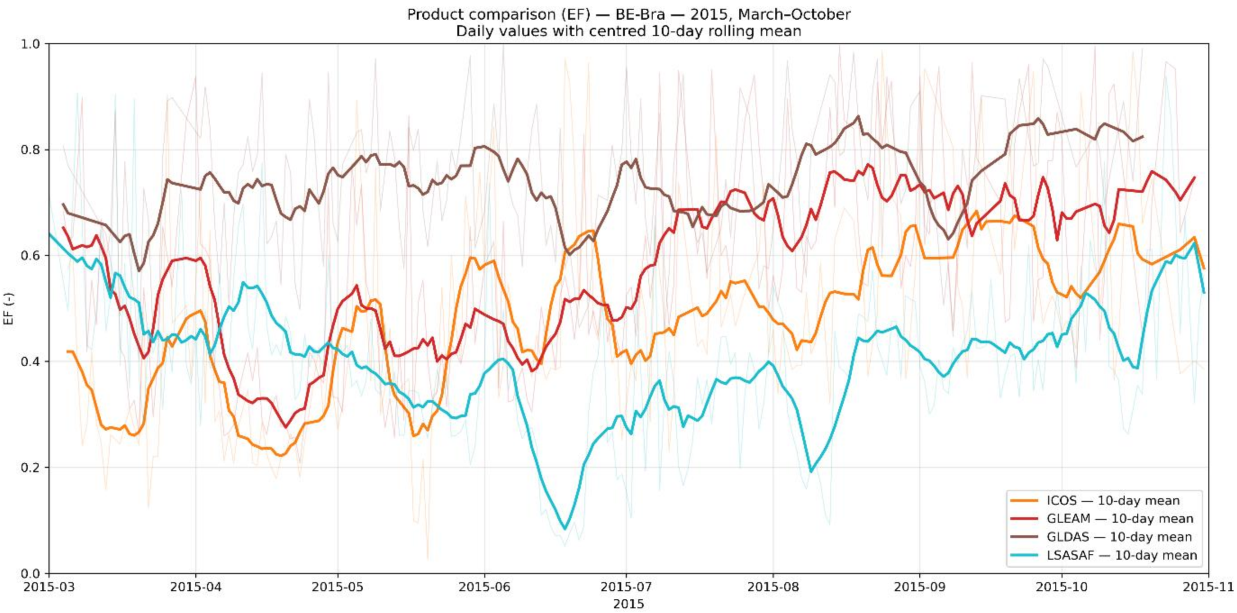

C1. BE Bra, Product comparison (EF) 2015

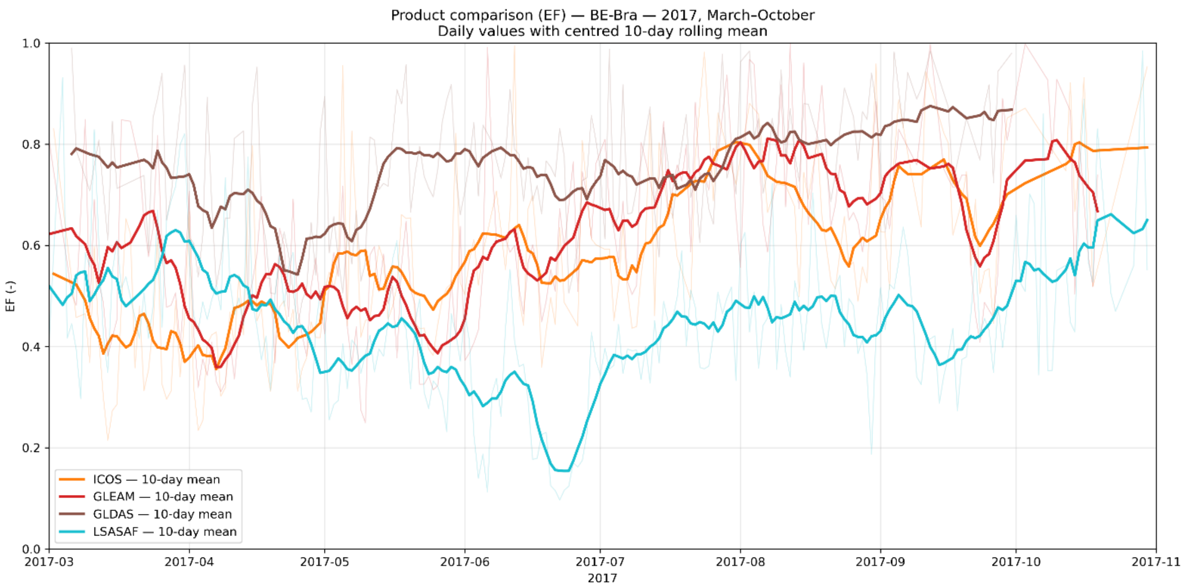

C2. BE Bra, Product comparison (EF) 2017

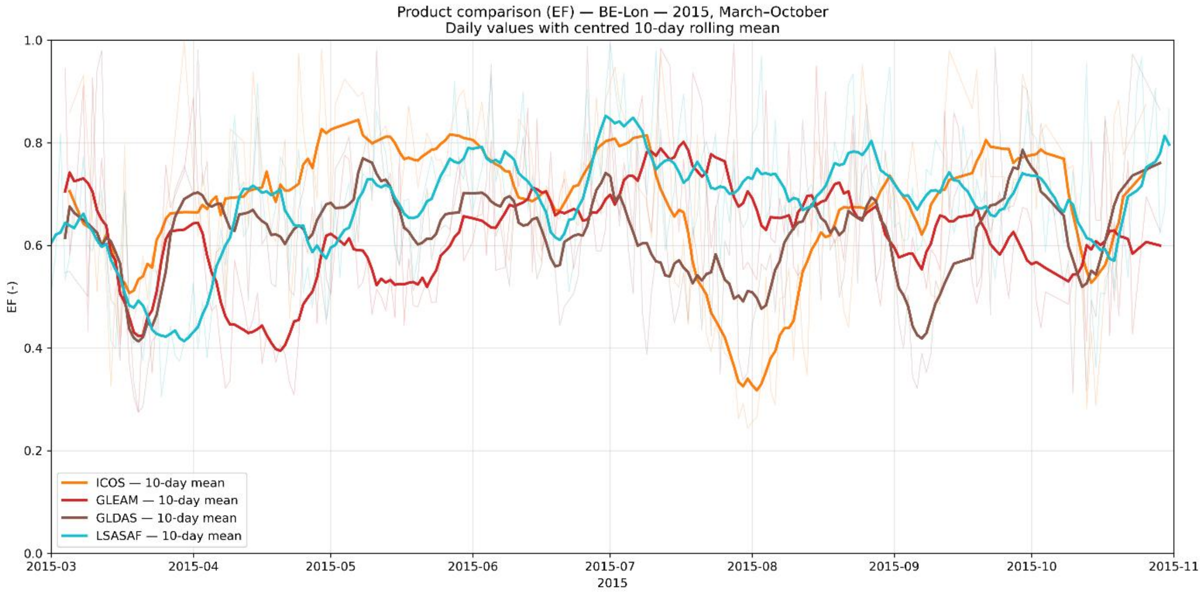

C3. BE Lon, Product comparison (EF) 2015

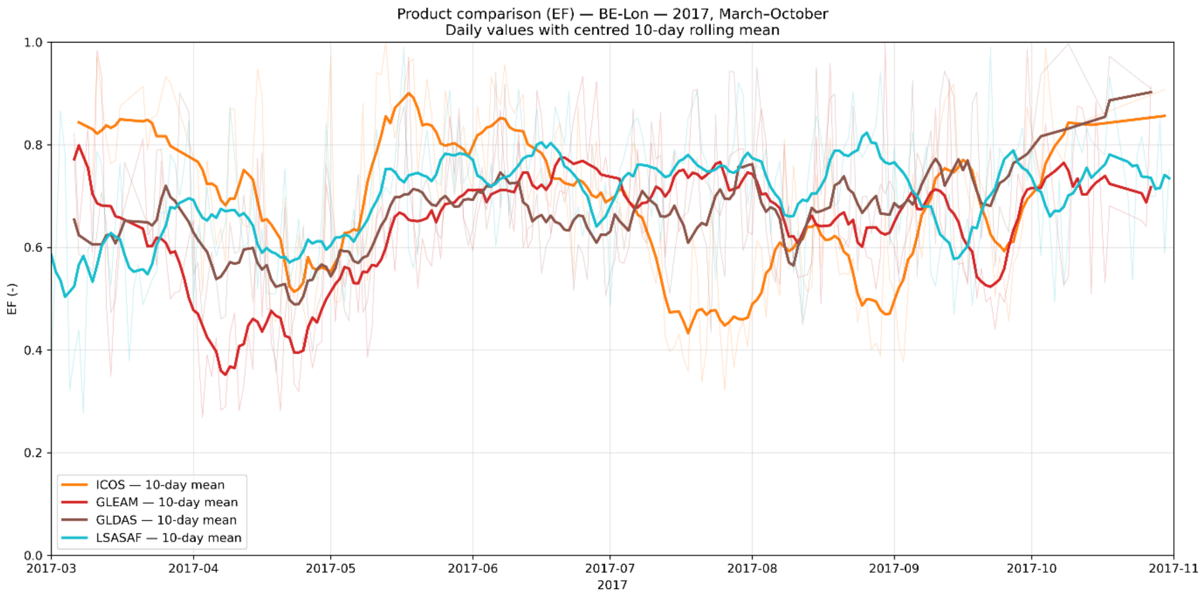

C4. BE Bra, Product comparison (EF) 2017

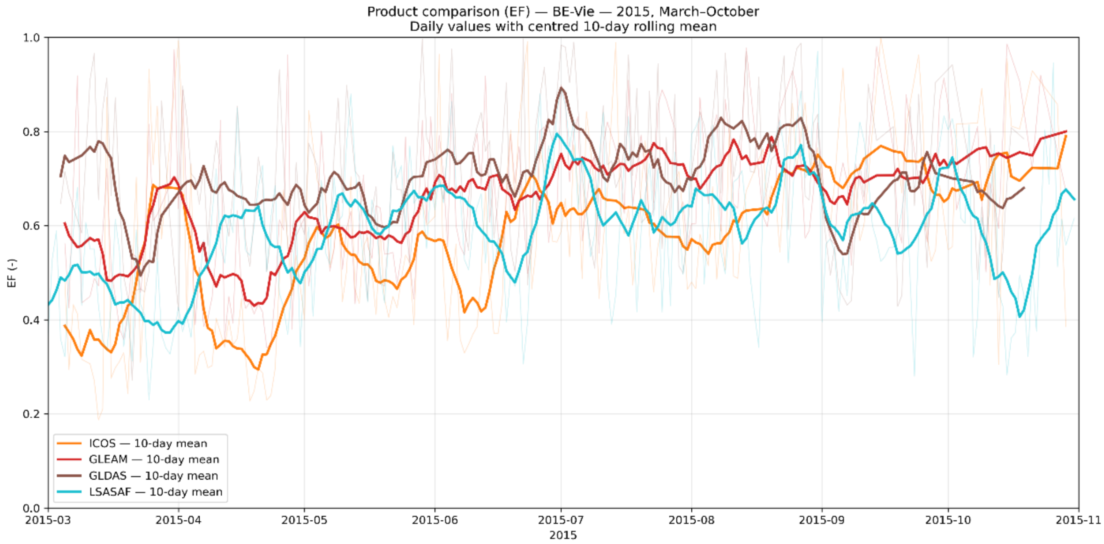

C5. BE , Product comparison (EF) 2015

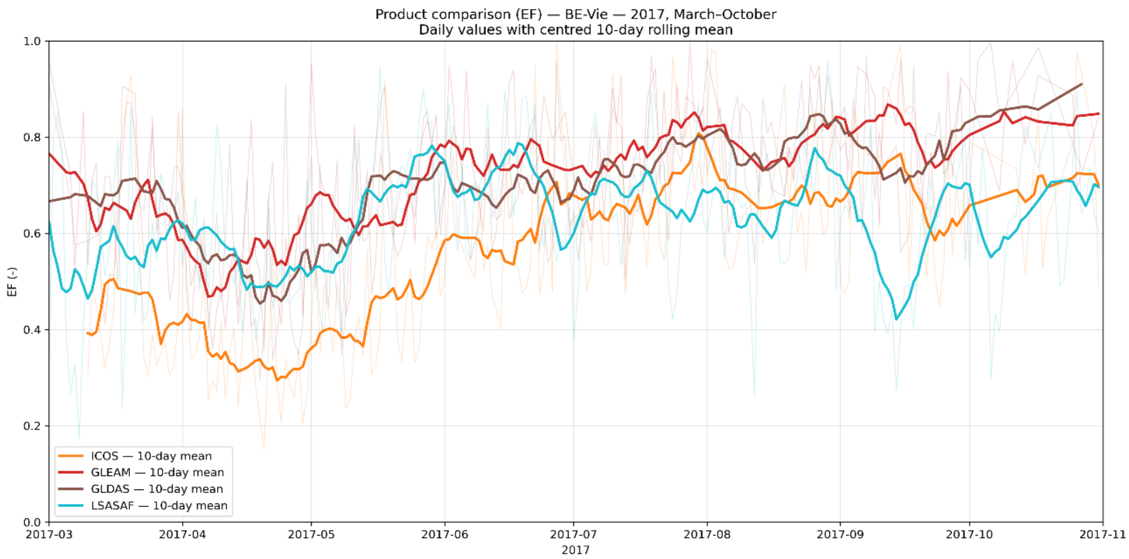

C6. BE Bra, Product comparison (EF) 2017

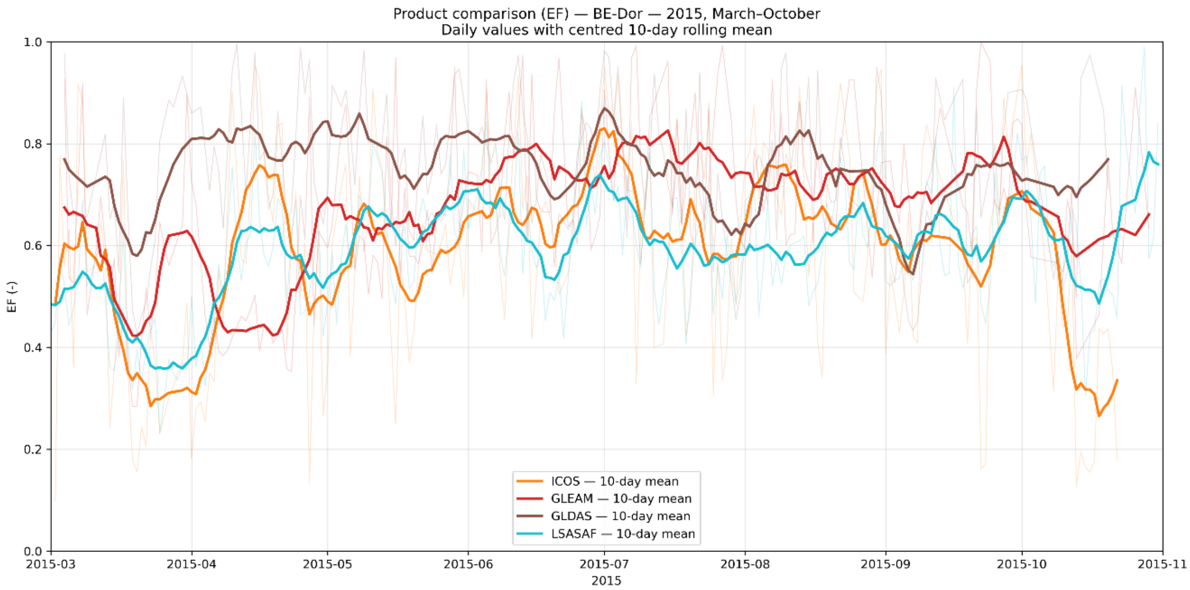

C7. BE Dor, Product comparison (EF) 2015

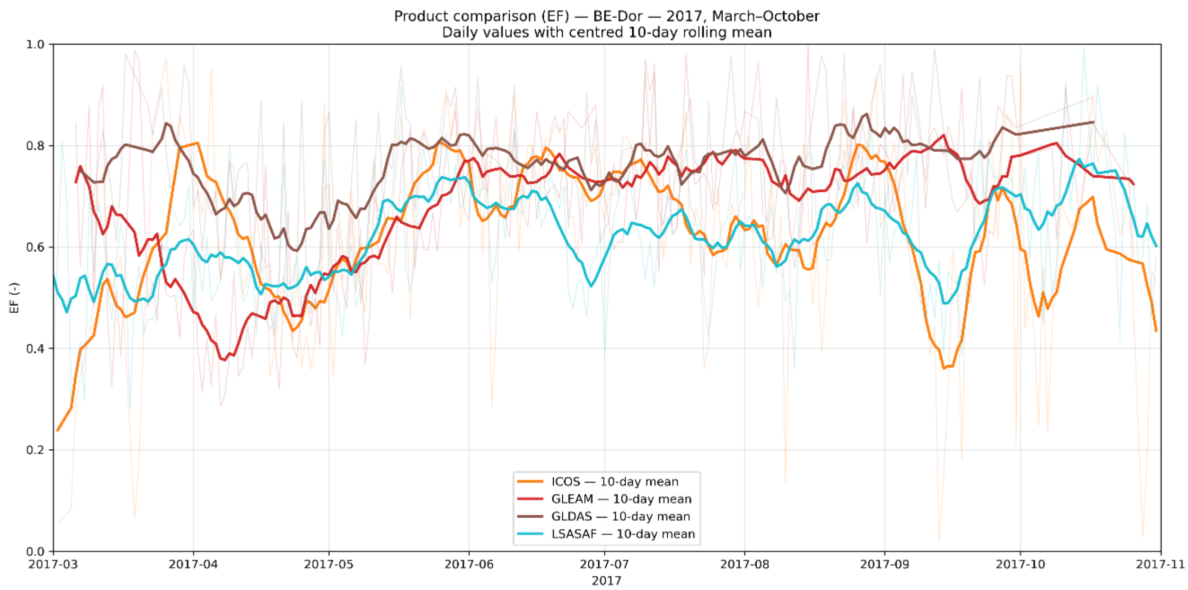

C8. BE Dor, Product comparison (EF) 2017

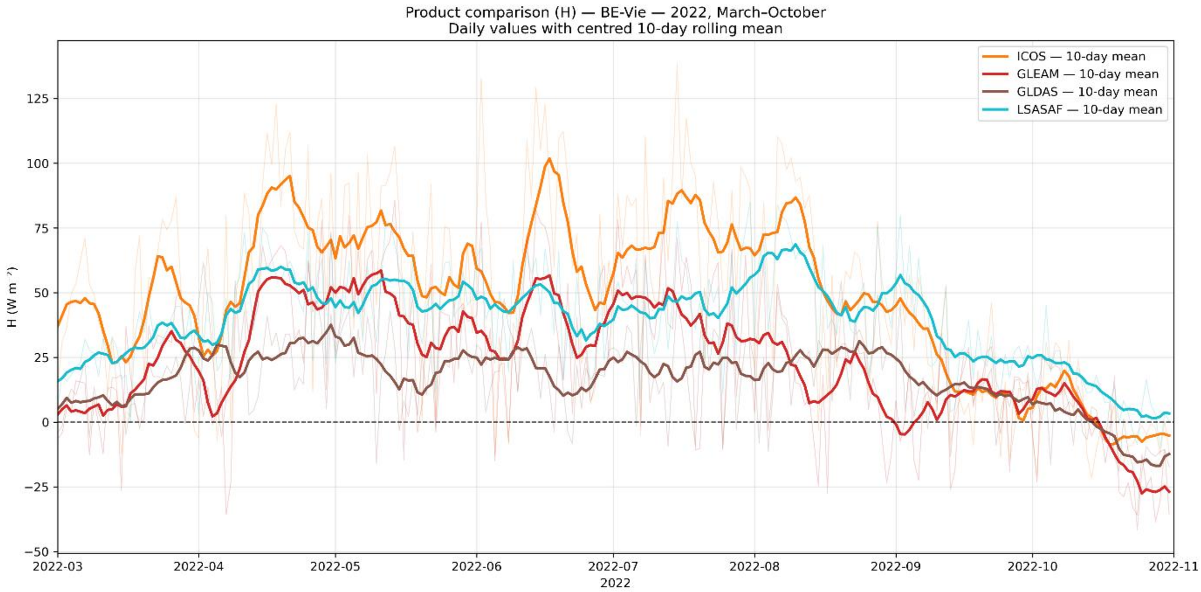

C9. BE Vie, Product comparison (H) 2017

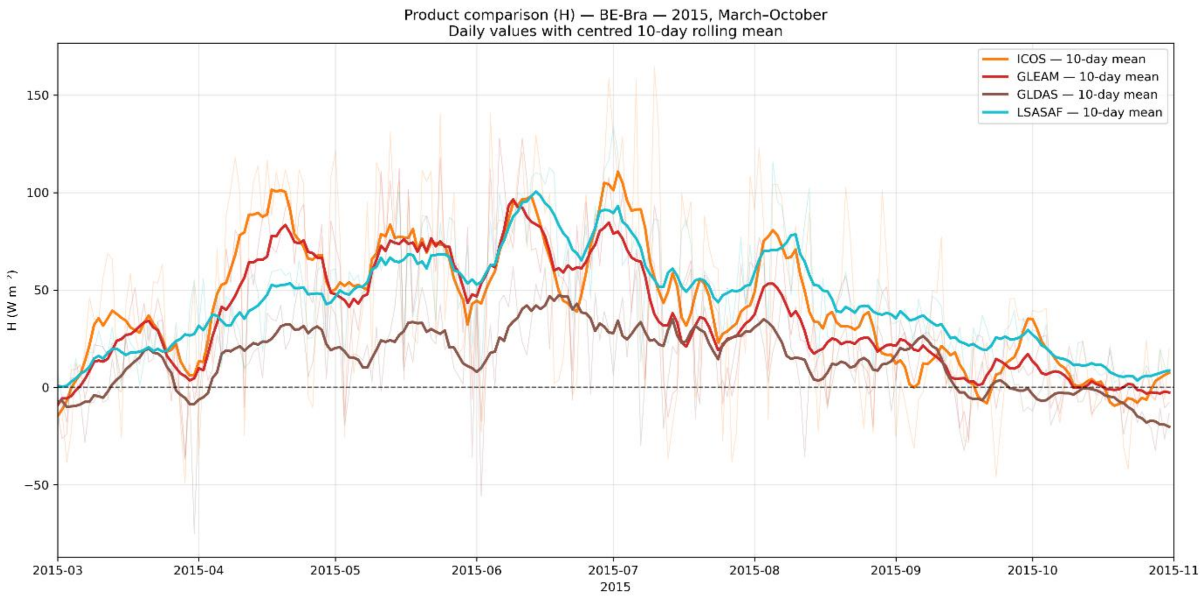

C10. BE Bra, Product comparison (H) 2015

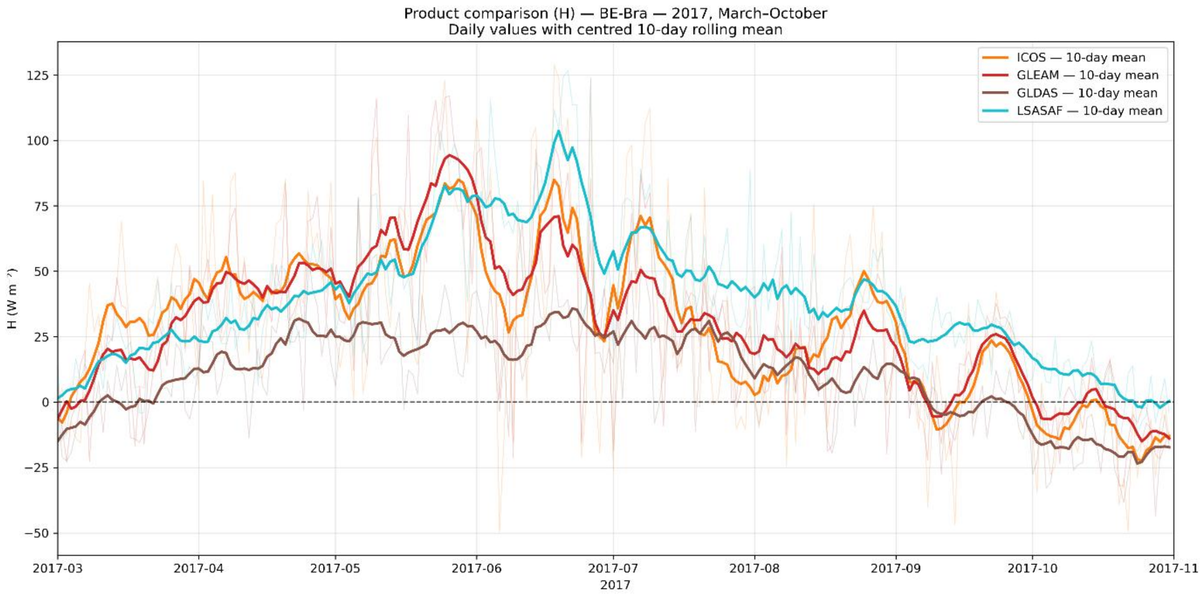

C11. BE Bra, Product comparison (H) 2017

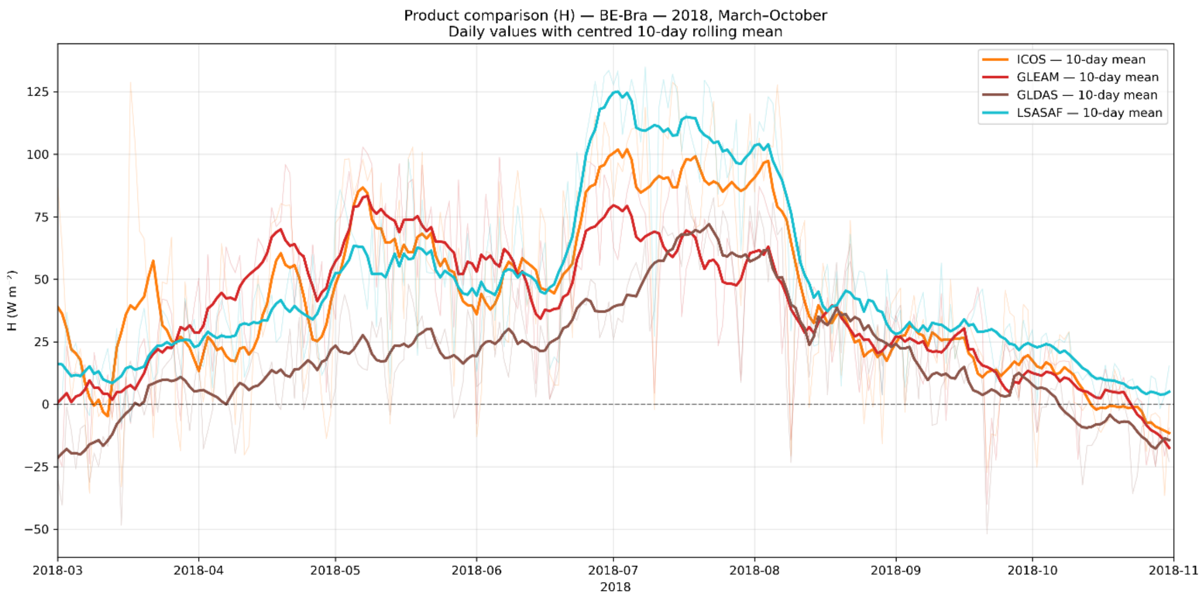

C12. BE Bra, Product comparison (H) 2018

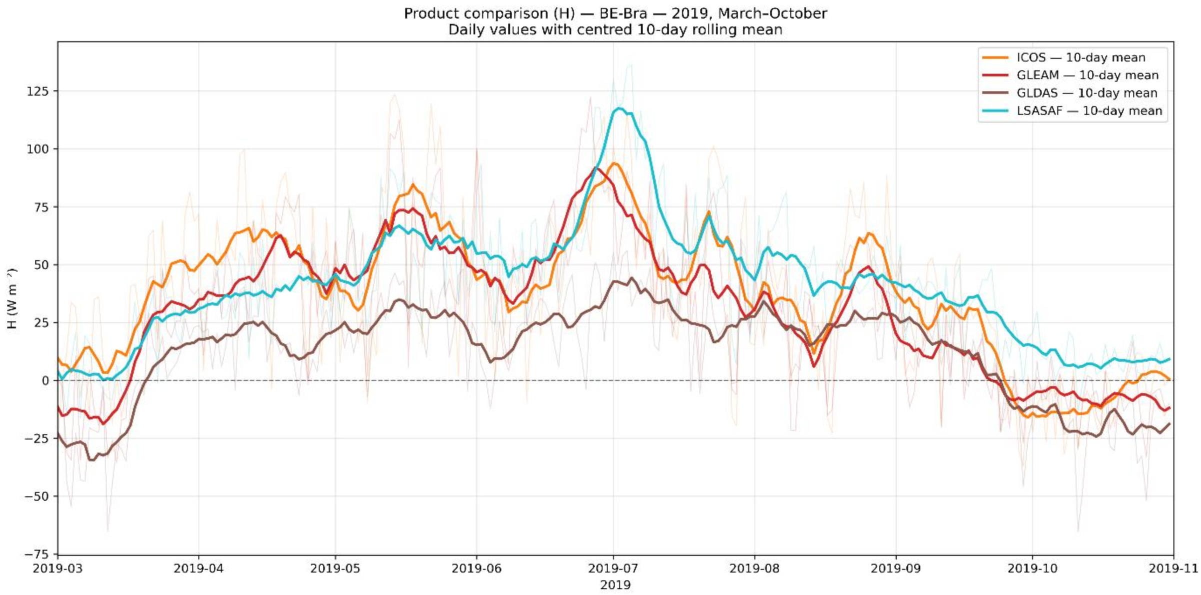

C13. BE Bra, Product comparison (H) 2019

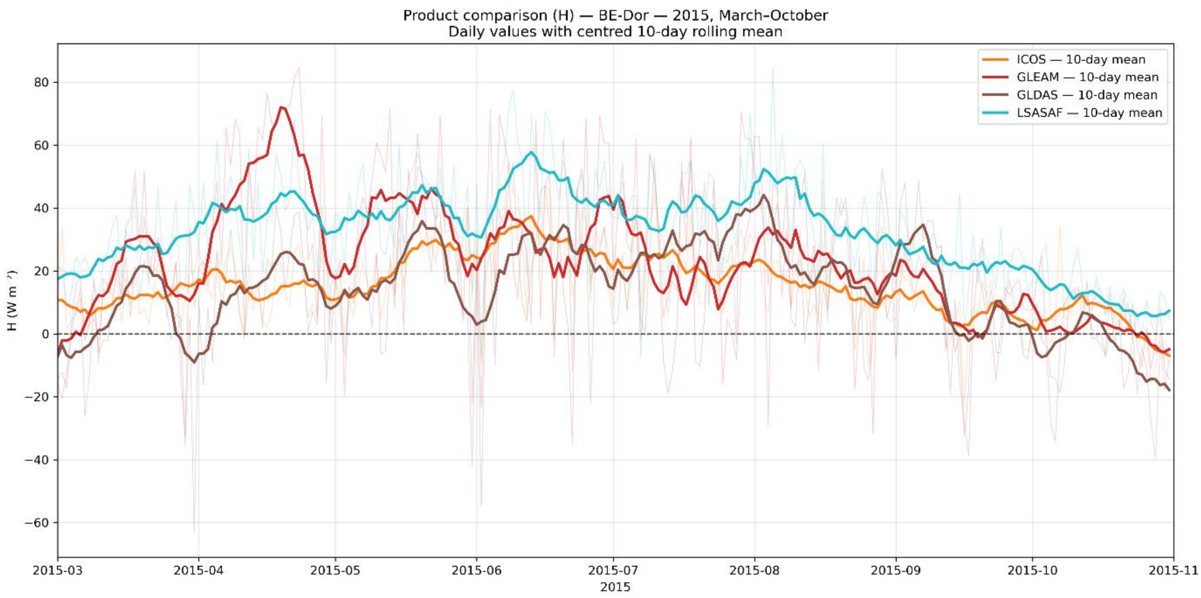

C14. BE Dor, Product comparison (H) 2015

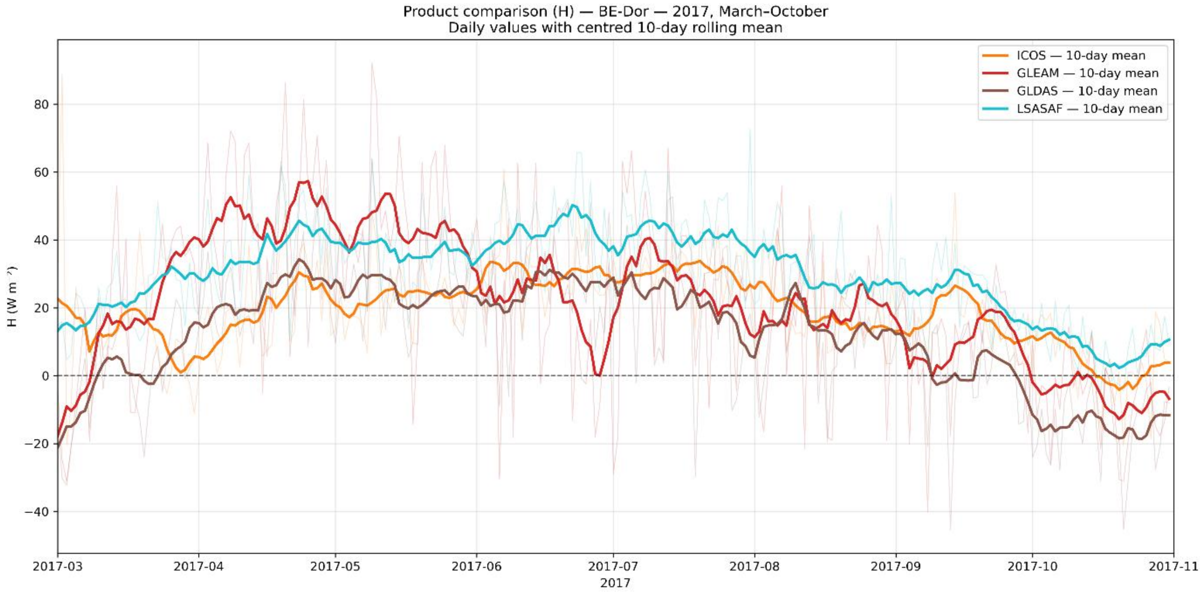

C15. BE Dor, Product comparison (H) 2017

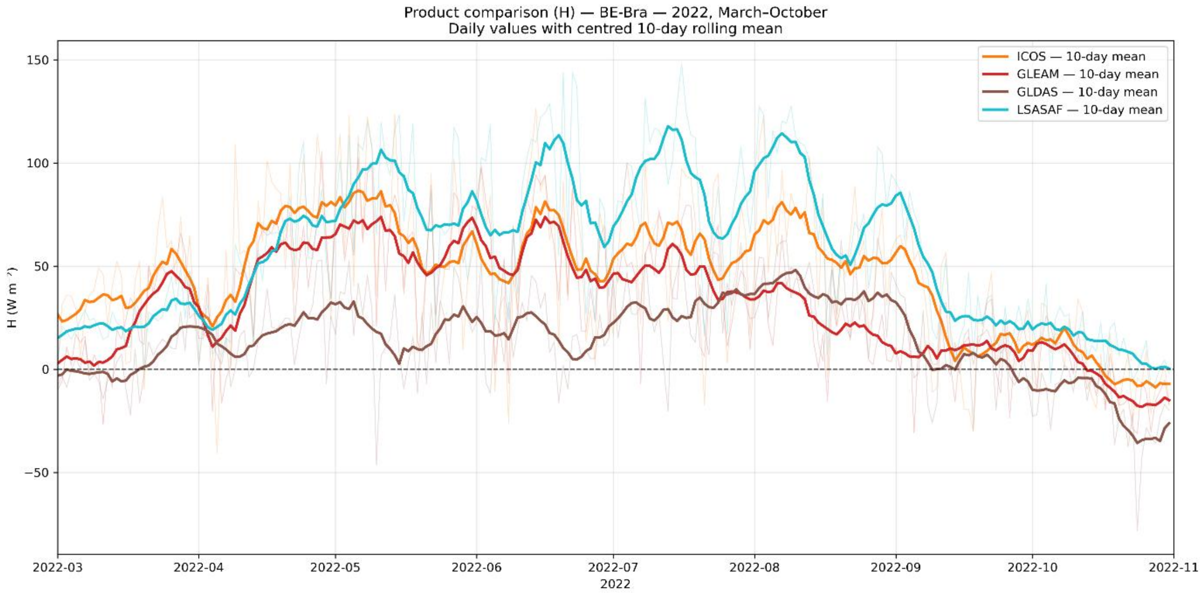

C16. BE Bra, Product comparison (H) 2022

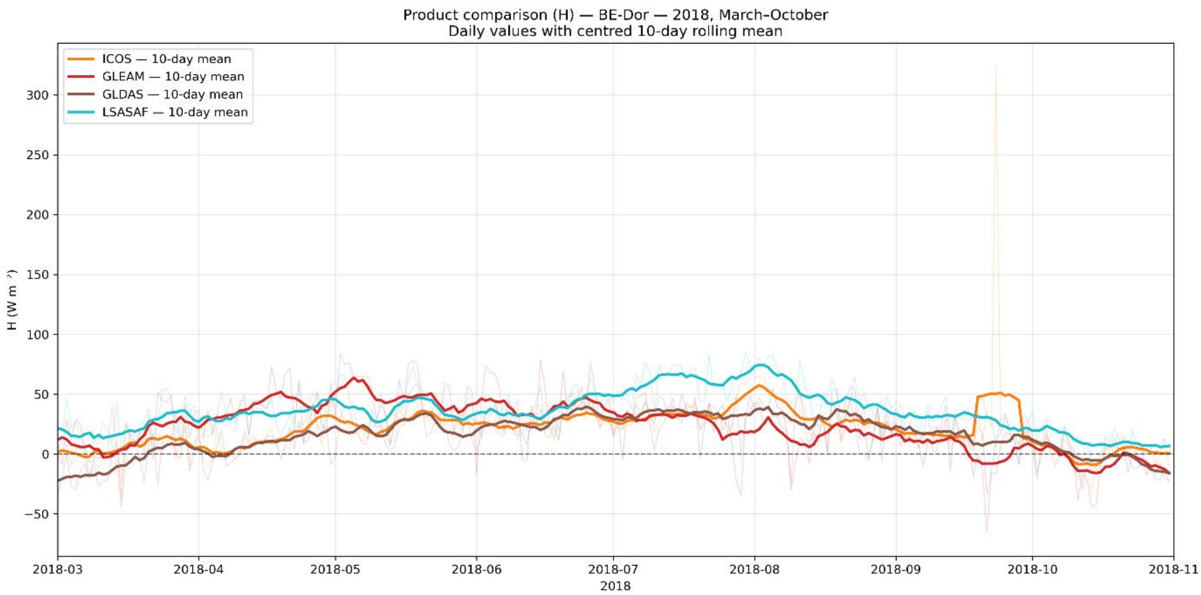

C17. BE Dor, Product comparison (H) 2018

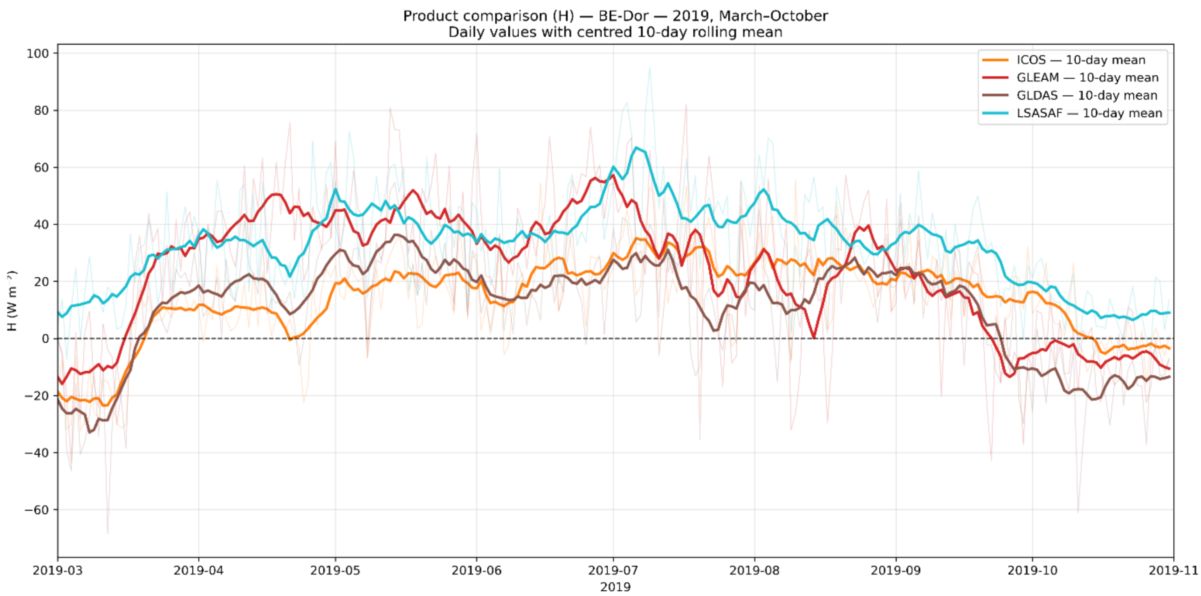

C18. BE Dor, Product comparison (H) 2019

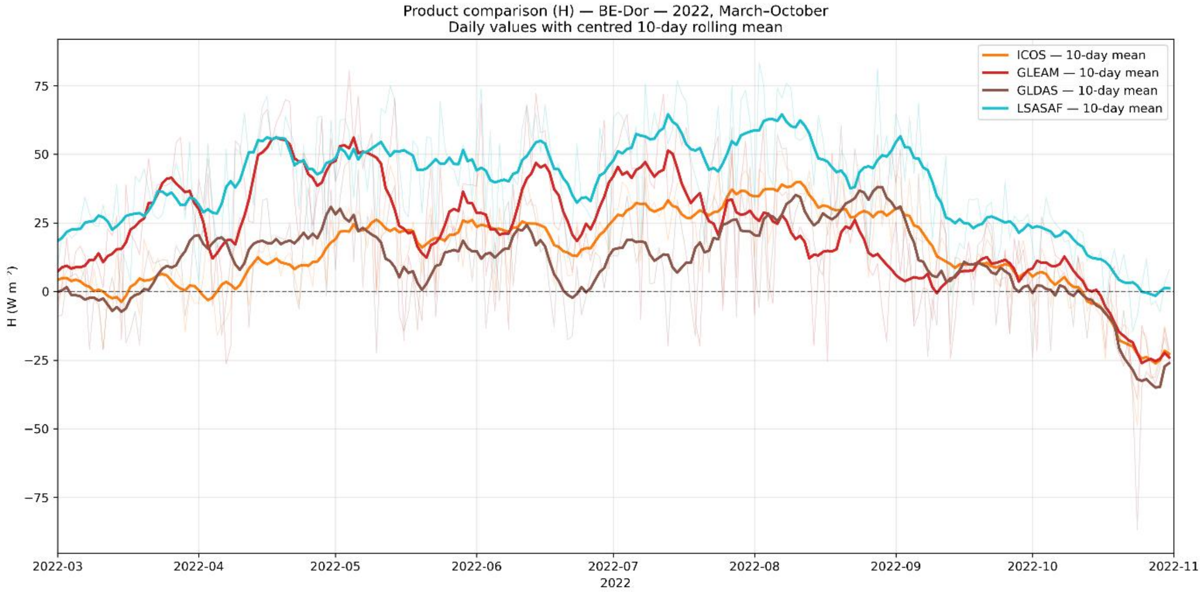

C19. BE Dor, Product comparison (H) 2022

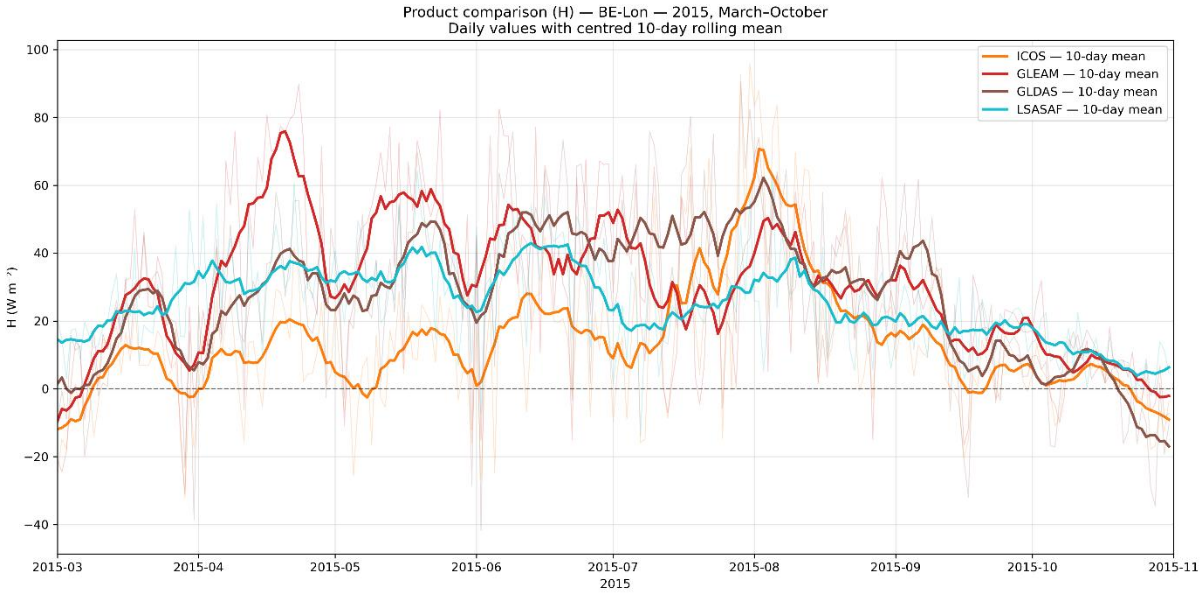

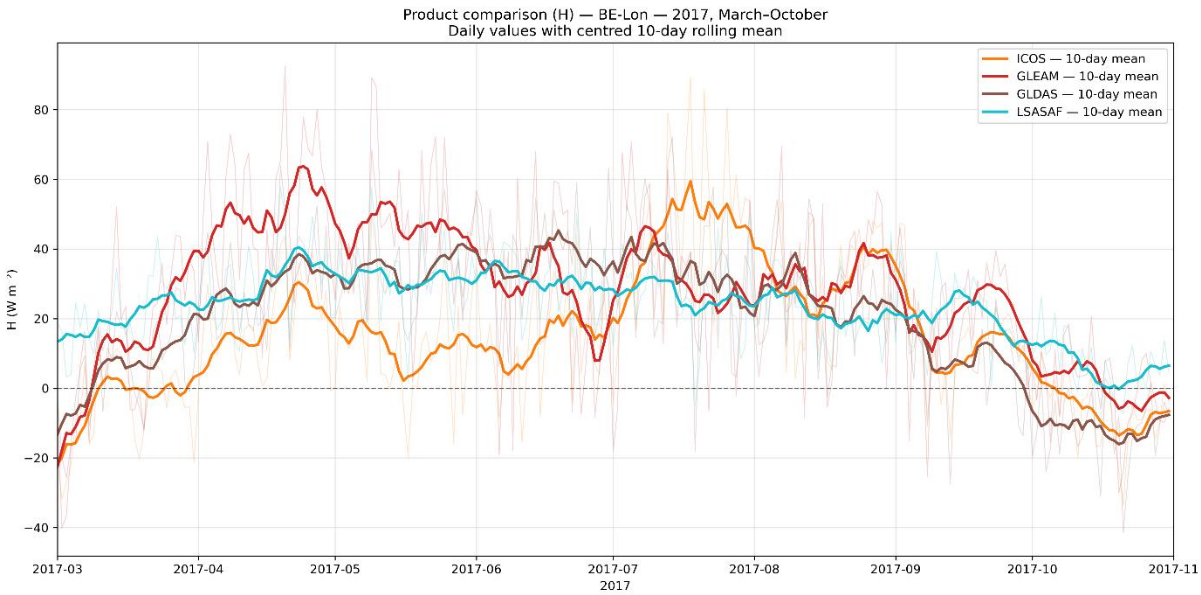

C20. BE Lon, Product comparison (H) 2015

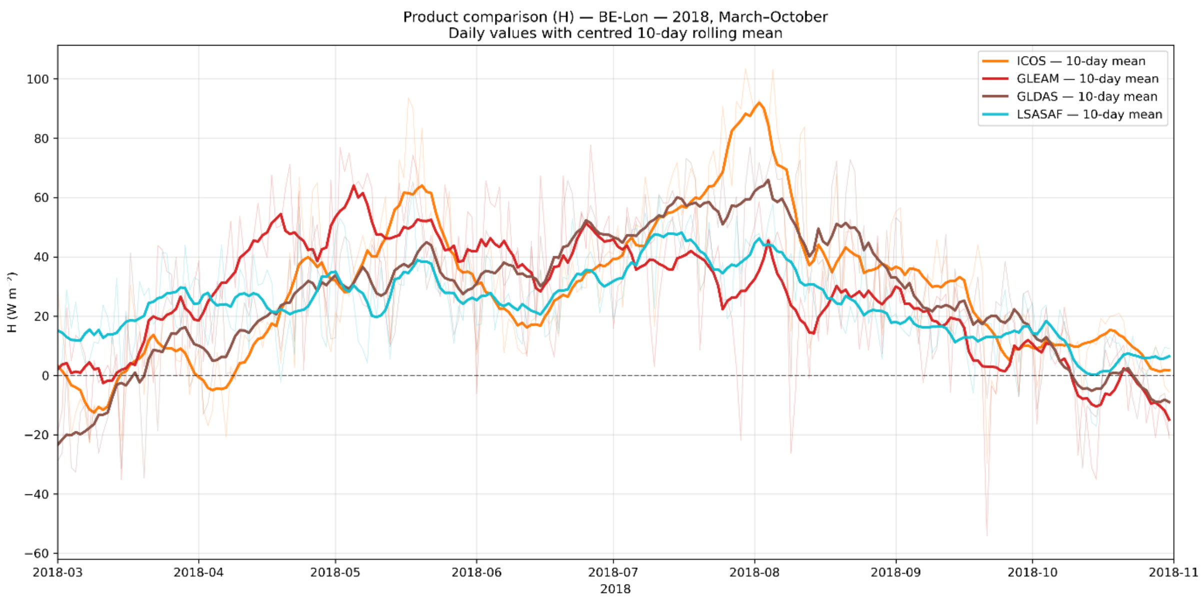

C21. BE Lon, Product comparison (H) 2018

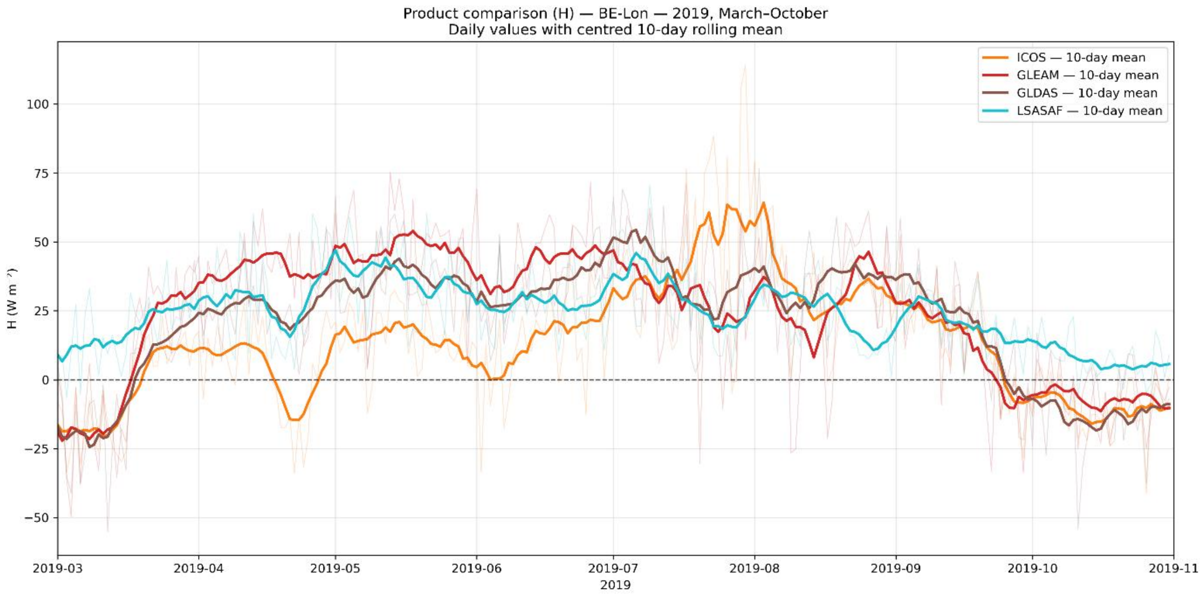

C22. BE Lon, Product comparison (H) 2019

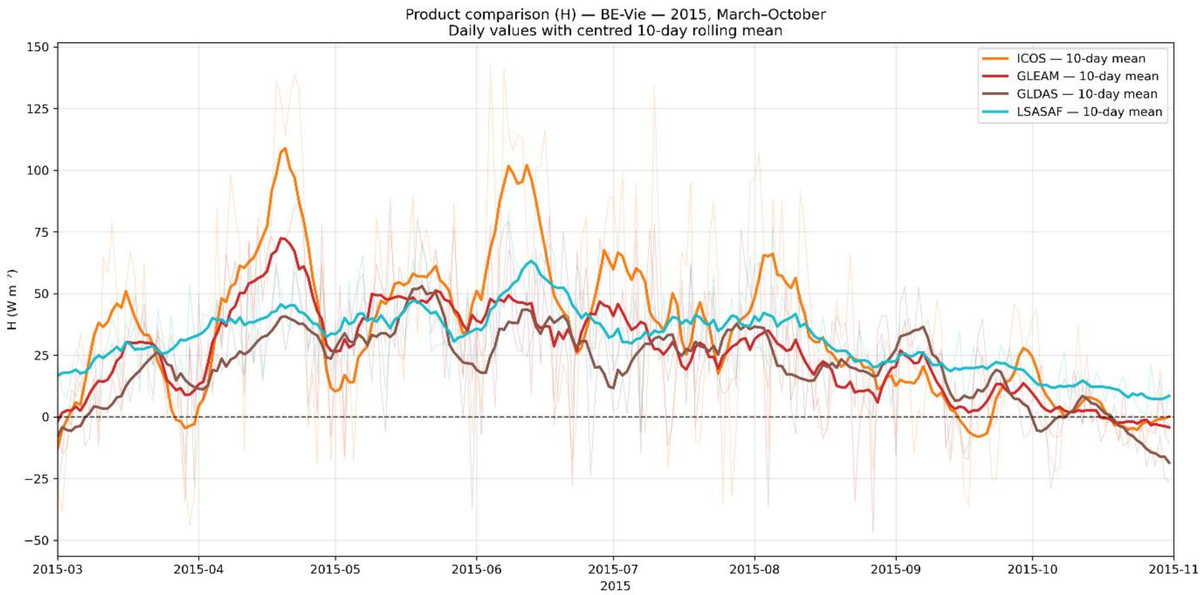

C23. BE Vie, Product comparison (H) 2015

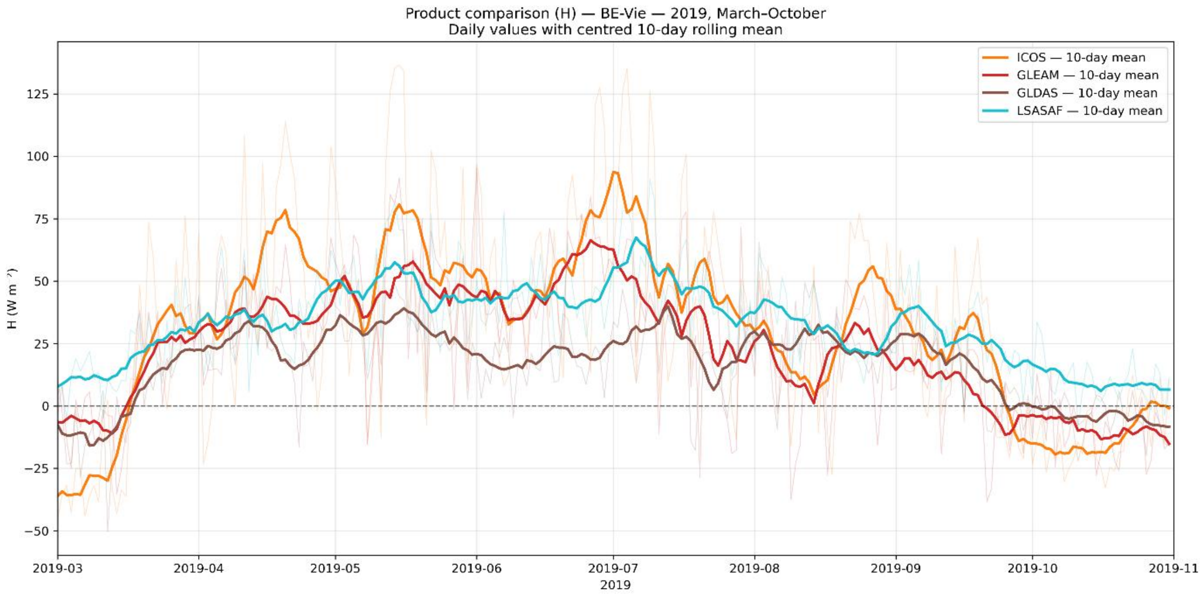

C24. BE Vie, Product comparison (H) 2019

Appendix D Product comparison (LE) (source: all figures in this section are based on ICOS Portal, GLEAM, GLDAS, FLUXCOM and LSA SAF)

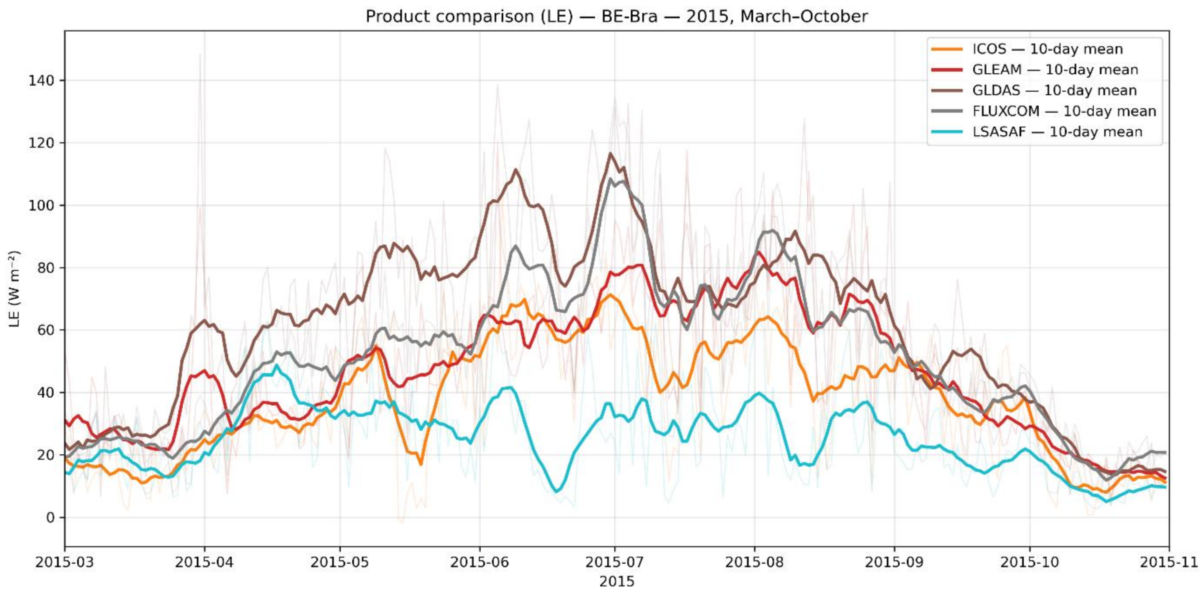

D1. BE Bra, Product comparison (H) 2015

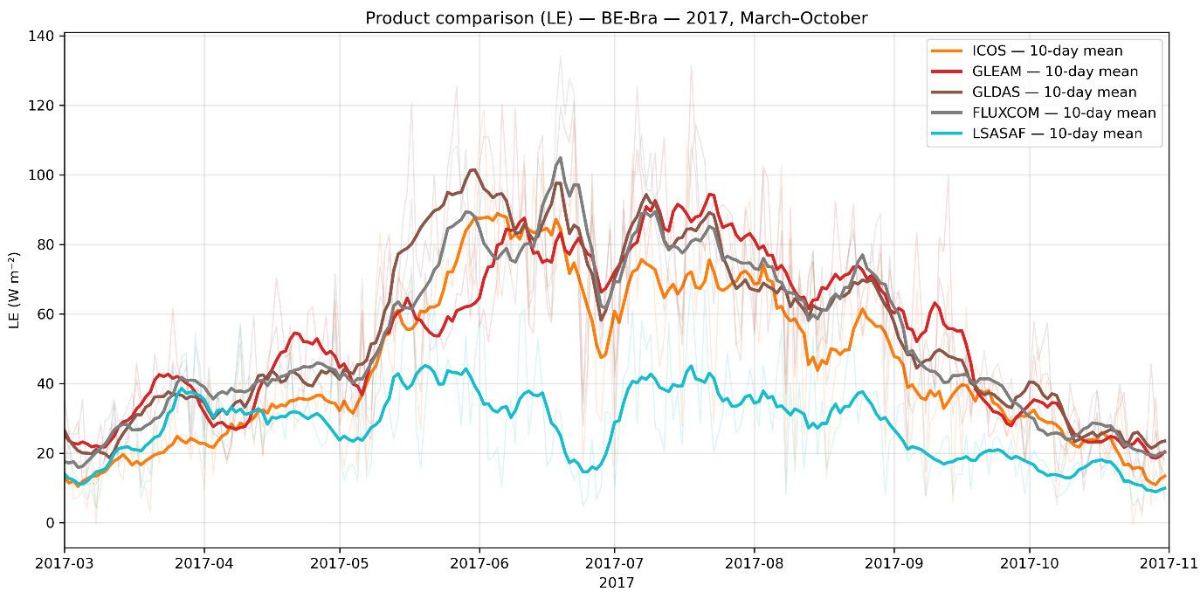

D2. BE Bra, Product comparison (H) 2017

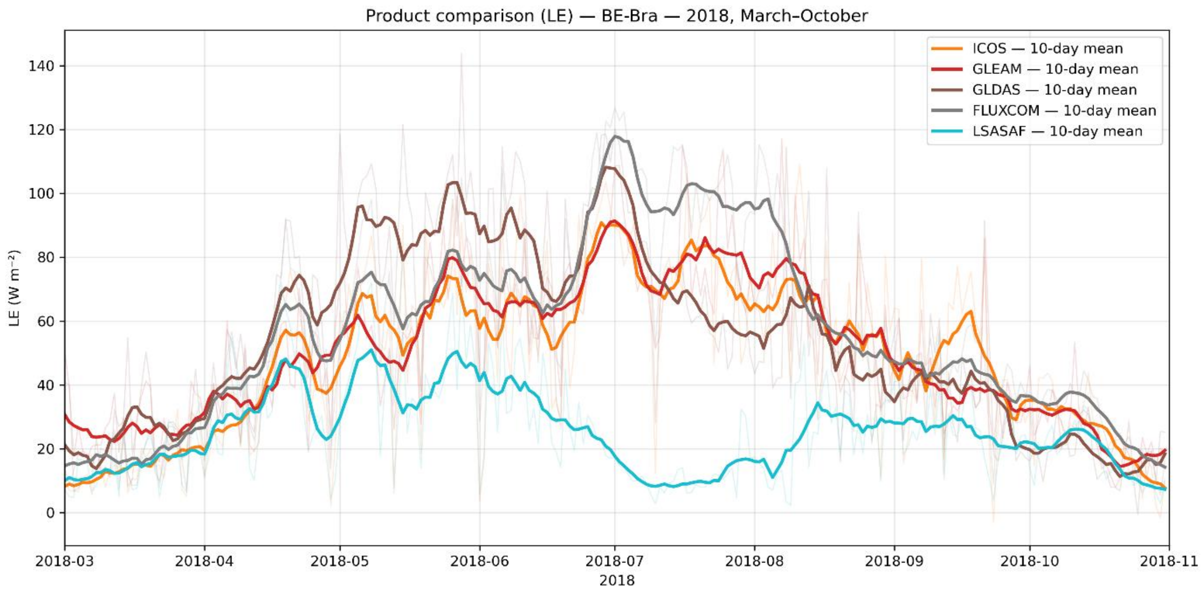

D3. BE Bra, Product comparison (H) 2018

D4. BE Bra, Product comparison (H) 2019

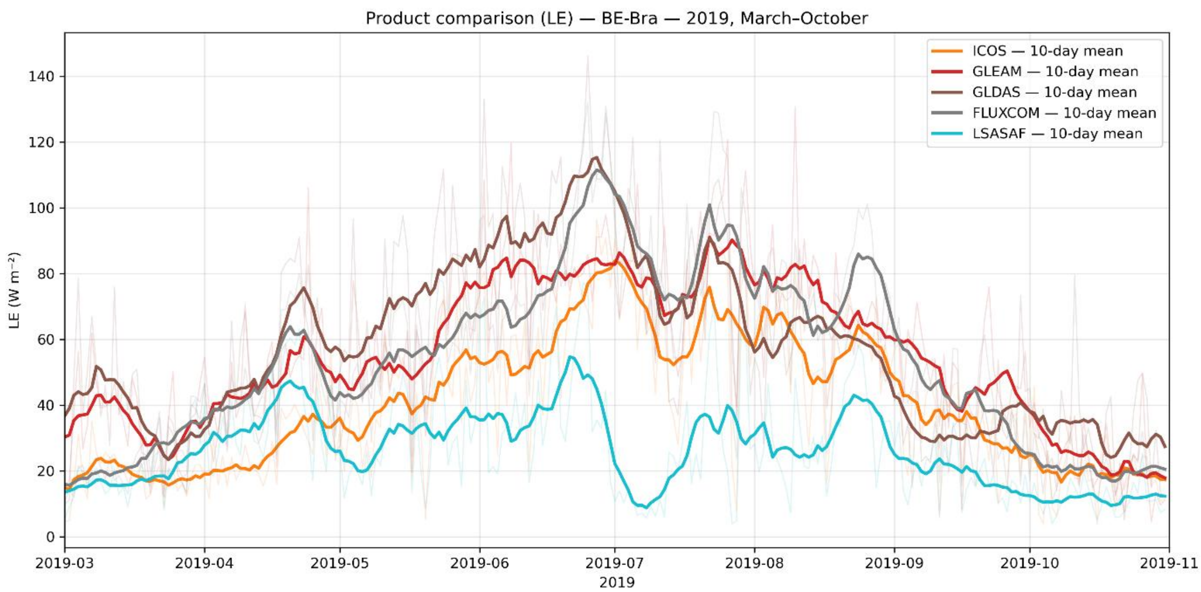

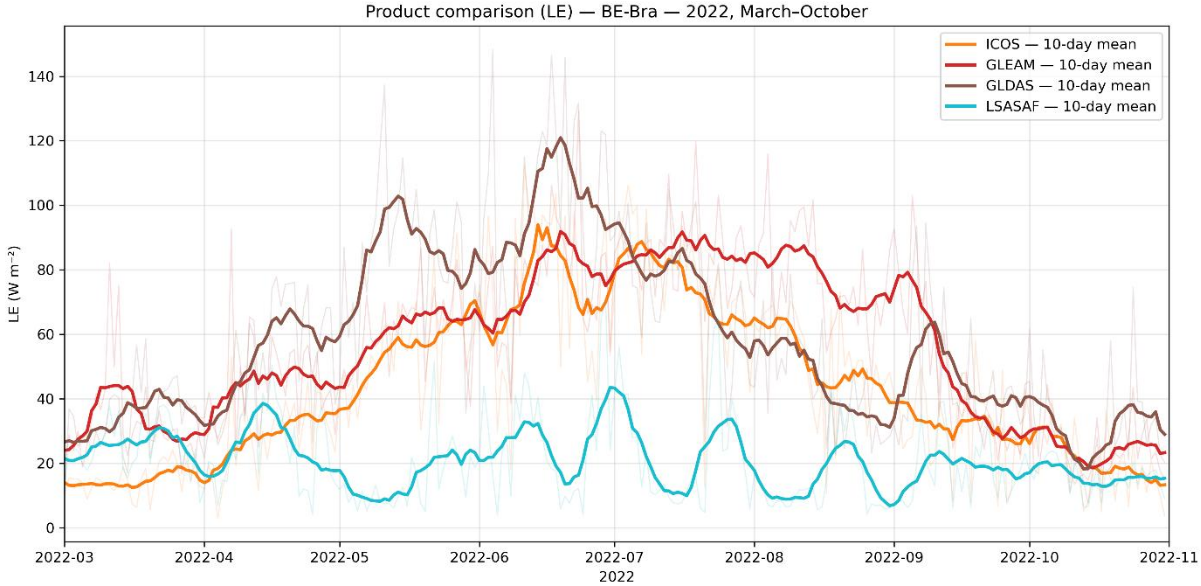

D5. BE Bra, Product comparison (H) 2022

D6. BE Bra, Product comparison (H) 2022

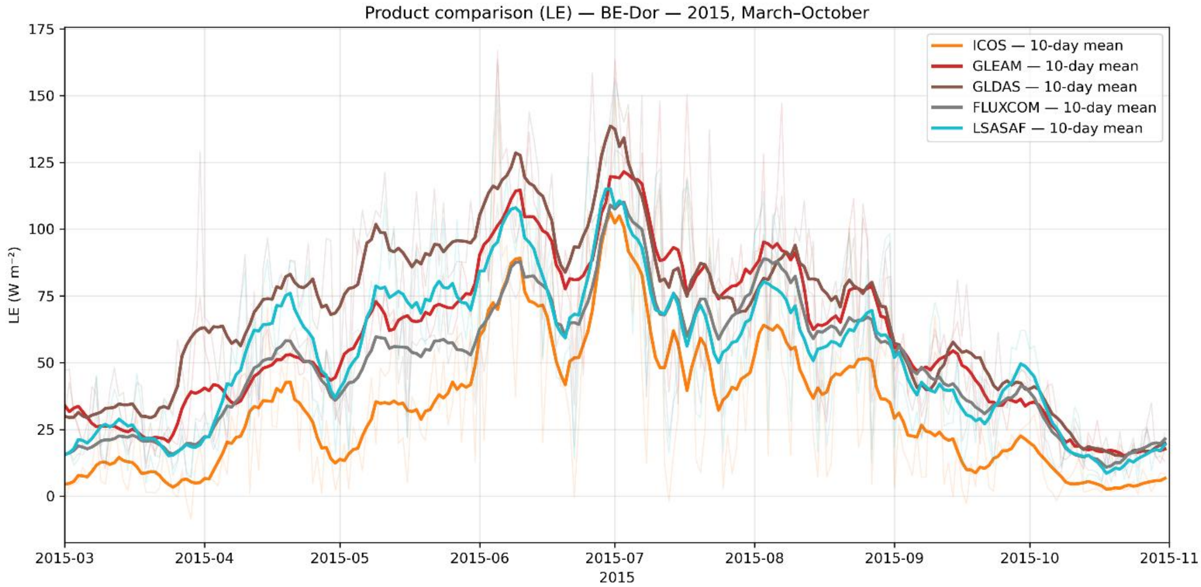

D4. BE Bra, Product comparison (H) 2019hjj

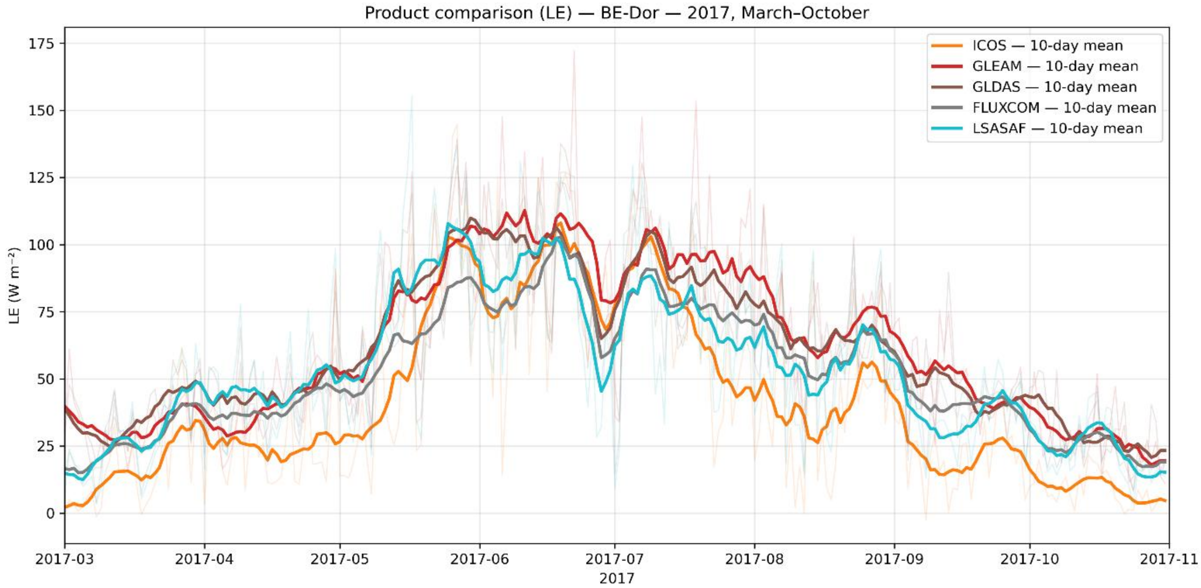

D6. BE Dor, Product comparison (L) 2017

D7. BE Dor, Product comparison (L) 2018

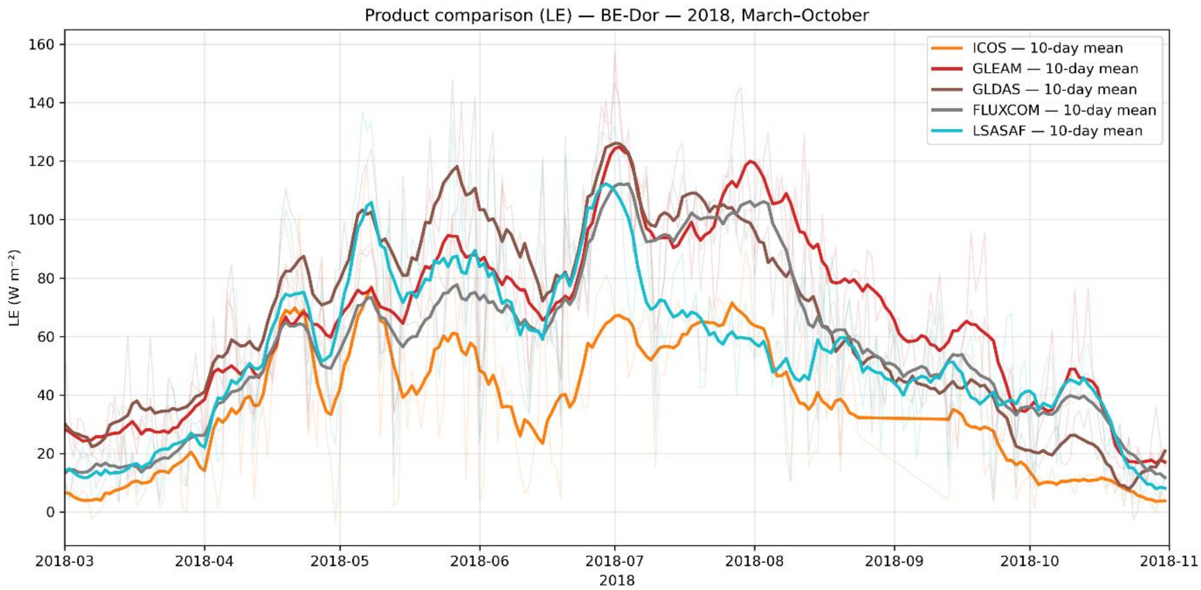

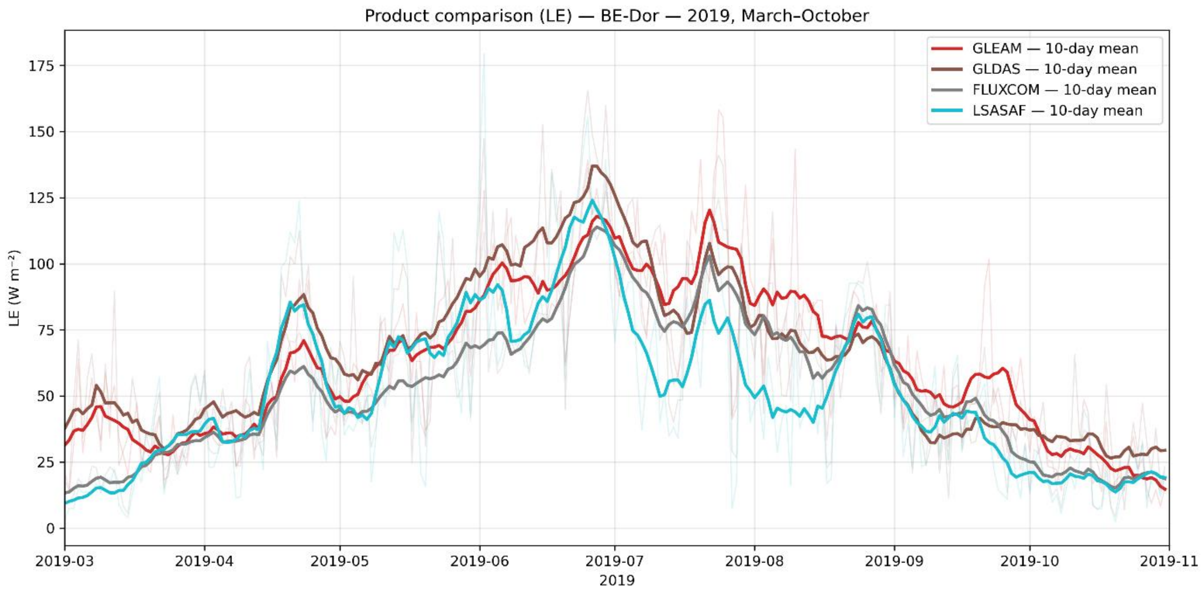

D7. BE Dor, Product comparison (LE) 2019

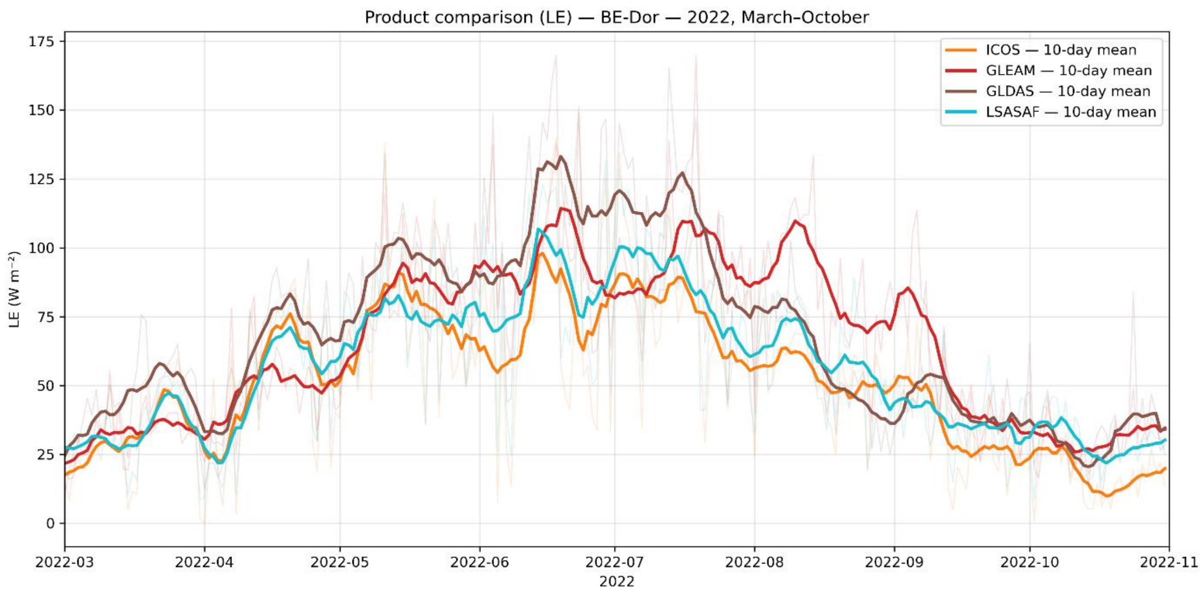

D8. BE Dor, Product comparison (LE) 2022

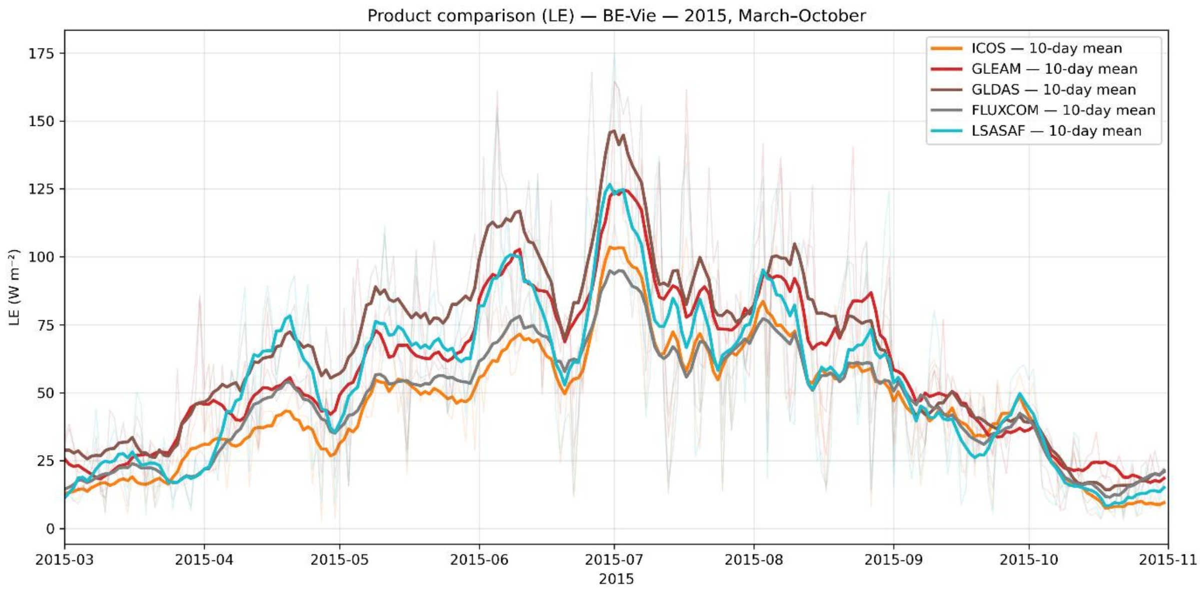

D10. BE Vie, Product comparison (LE) 2015

D11. BE Vie, Product comparison (LE) 2017

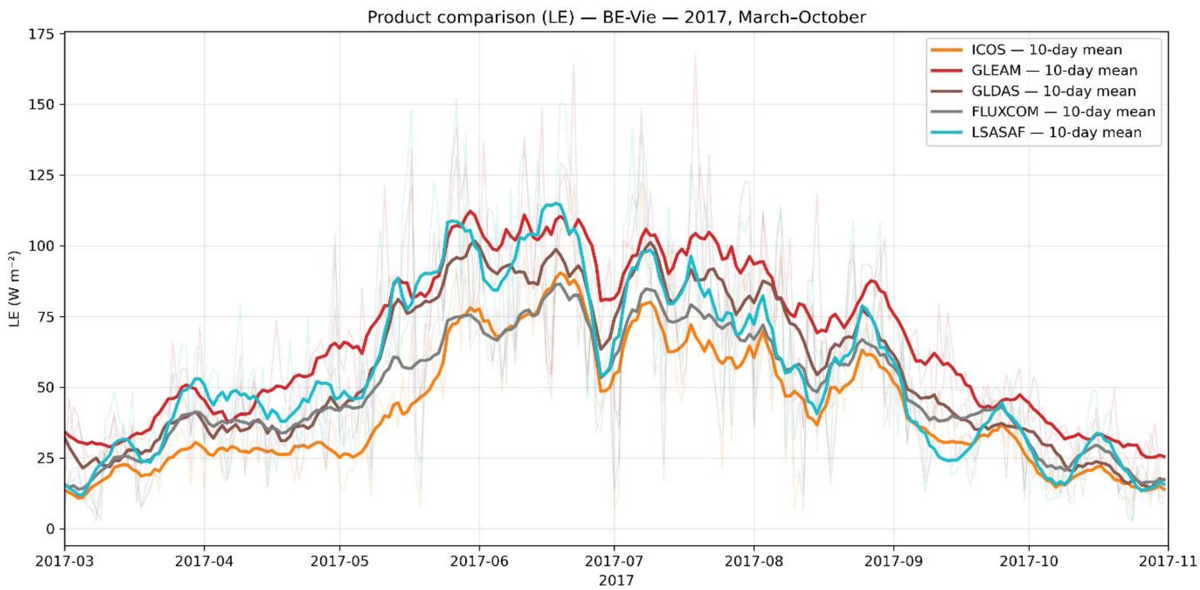

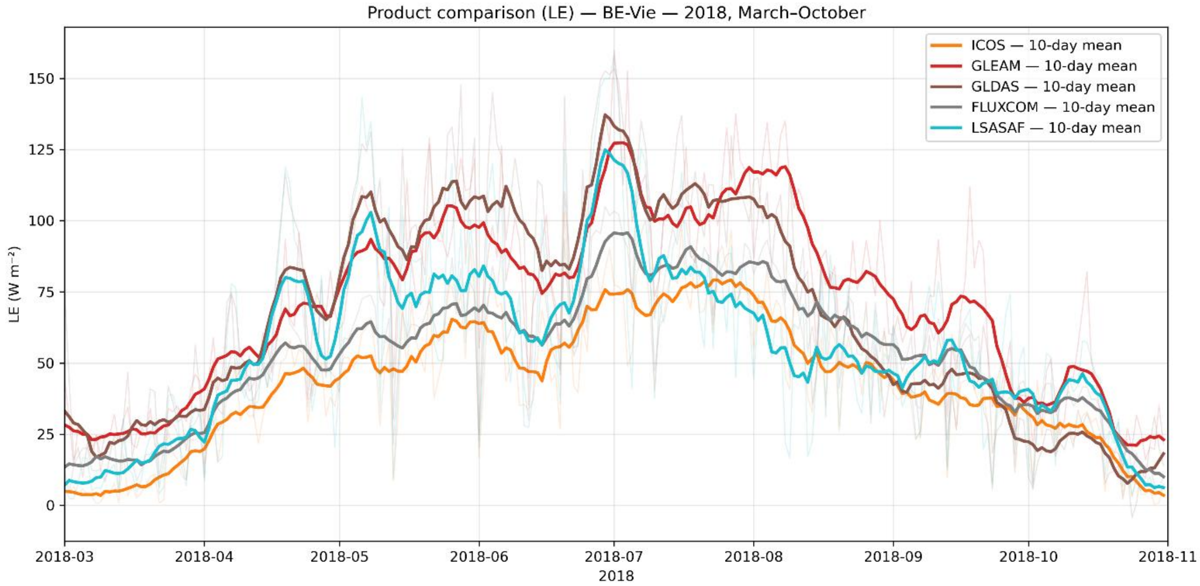

D12. BE Vie, Product comparison (LE) 2018

D13. BE Vie, Product comparison (LE) 2019

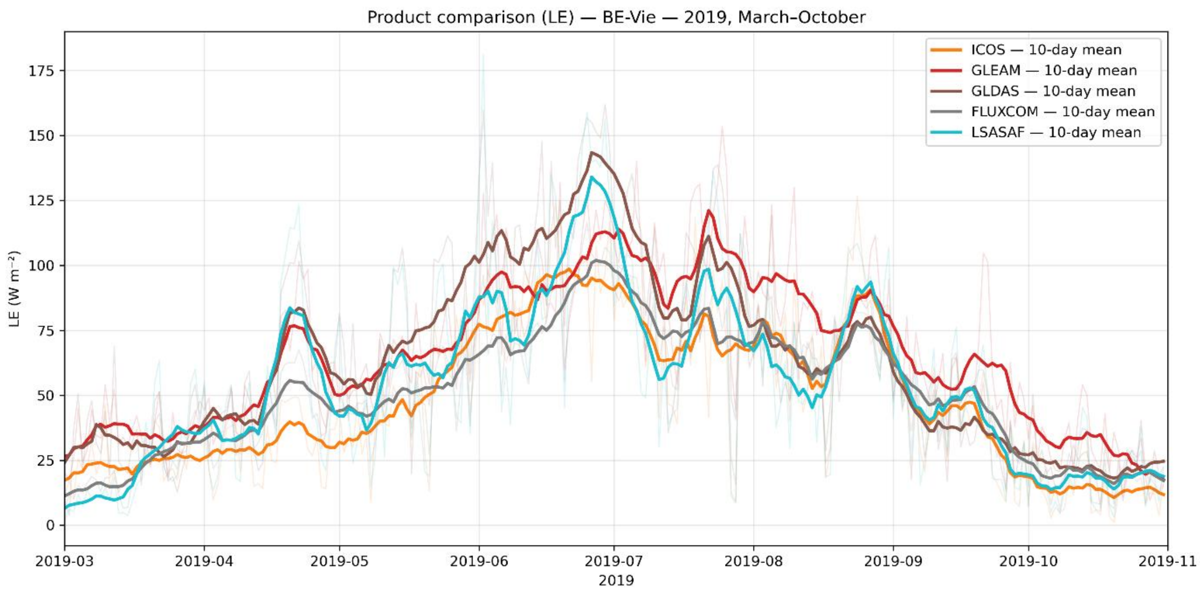

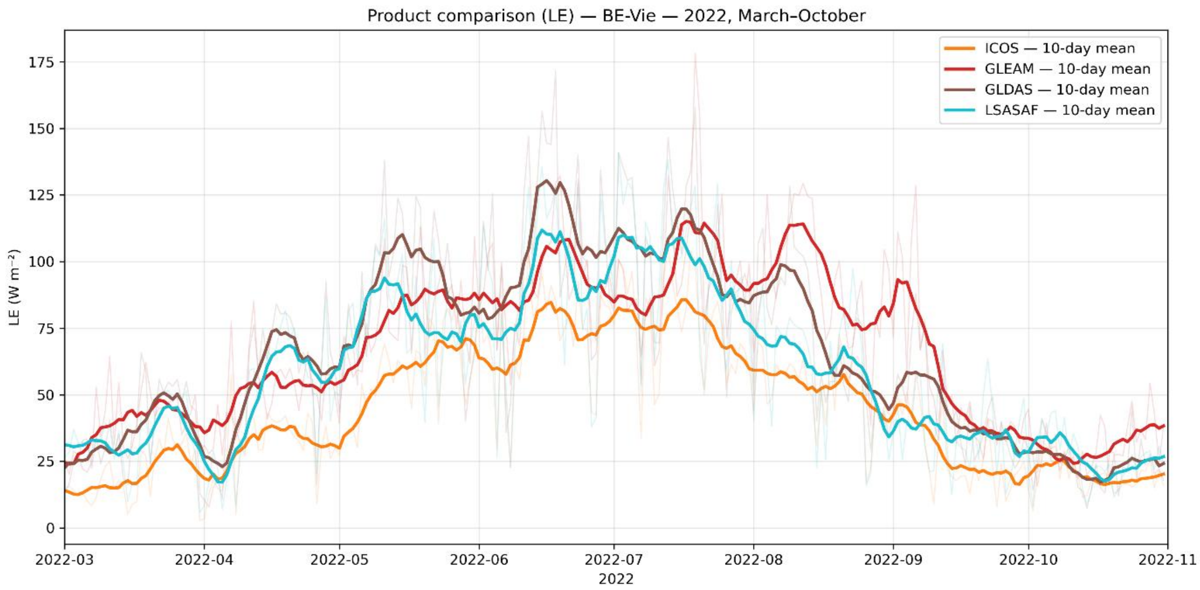

D14. BE Vie, Product comparison (LE) 20

D15. BE Lon, Product comparison (LE) 201

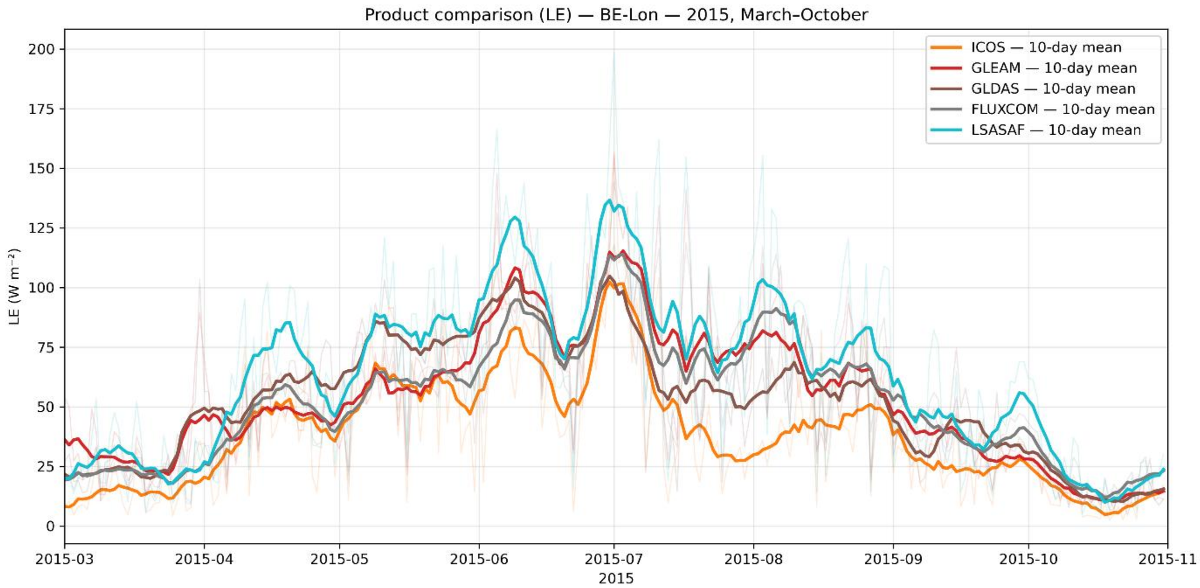

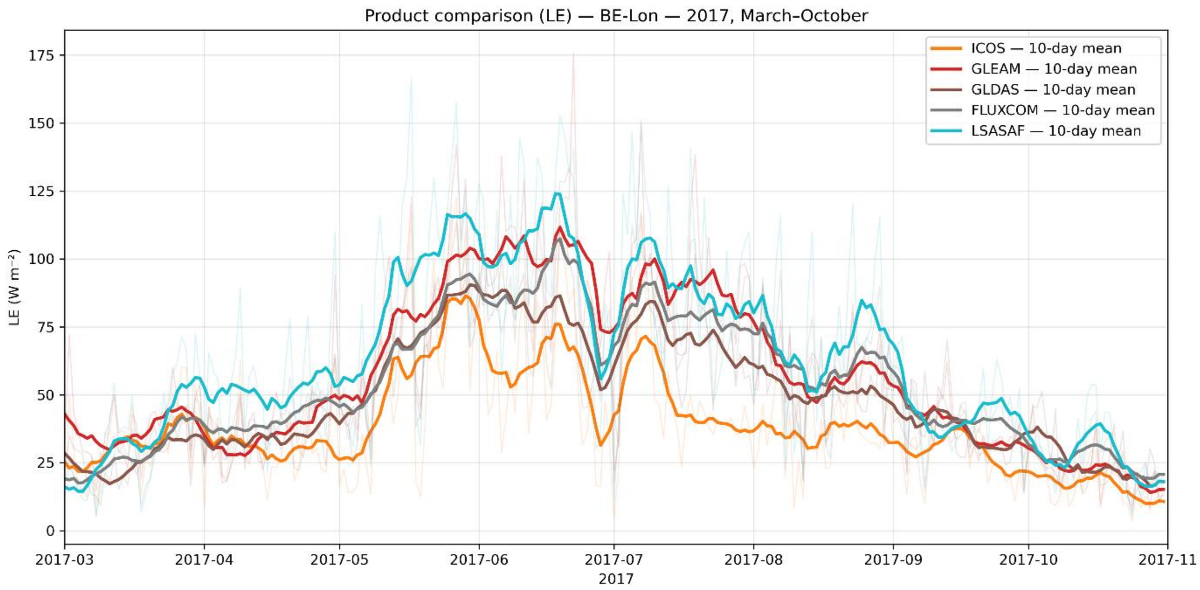

D16. BE Lon, Product comparison (LE) 2017

D17. BE Lon, Product comparison (LE) 2017

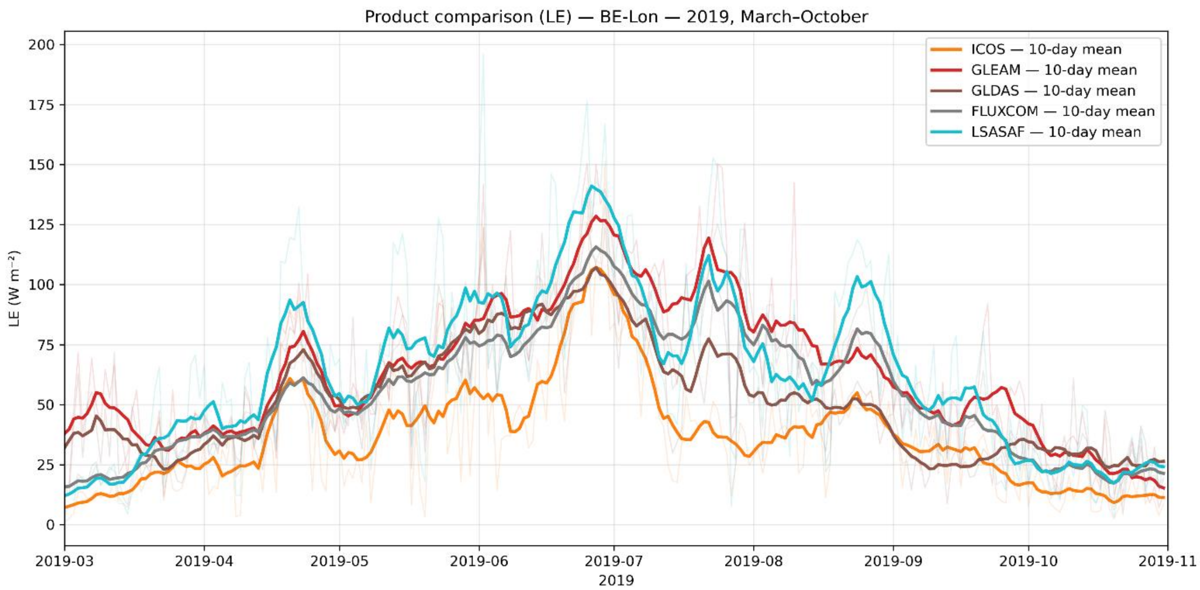

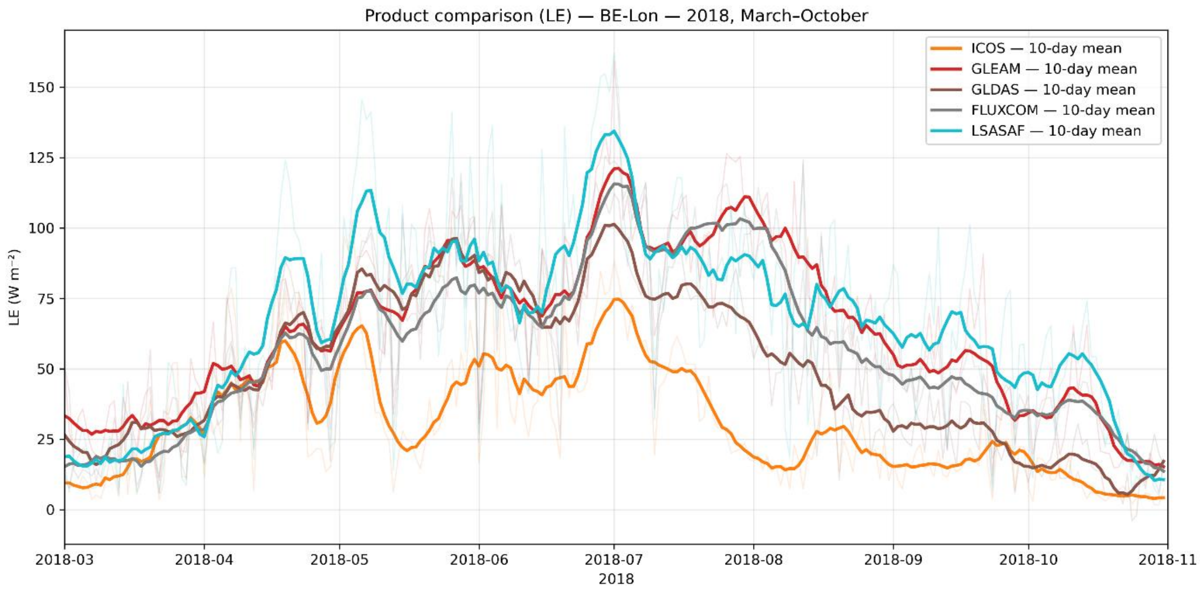

D18. BE Lon, Product comparison (LE) 2018

E1 – E4 Product metrics (Performance was evaluated using the Kling-Gupta Efficiency(KGE; Gupta et al., 2009) together with the root mean square error(RMSE), mean absolute error(MAE), bias, absolute bias, Pearson correlation coefficient® and the KGE components alpha and beta)

	site	year	product	KGE	RMSE	MAE	bias	absolute_bias	pearson_r	alpha	beta
0	BE-Bra	2015	GLDAS	-0.117	0.359	0.322	0.275	0.275	0.131	0.654	1.611
1	BE-Bra	2015	GLEAM	0.416	0.208	0.158	0.083	0.083	0.450	0.939	1.185
2	BE-Bra	2015	LSASAF	-0.216	0.275	0.217	-0.083	0.083	-0.164	0.695	0.822
3	BE-Bra	2017	GLDAS	0.206	0.255	0.222	0.192	0.192	0.329	0.762	1.351
4	BE-Bra	2017	GLEAM	0.631	0.140	0.112	0.027	0.027	0.635	0.974	1.049
5	BE-Bra	2017	LSASAF	-0.046	0.254	0.205	-0.135	0.135	0.007	0.774	0.763
6	BE-Bra	2018	GLDAS	0.085	0.248	0.206	0.152	0.152	0.153	1.191	1.288
7	BE-Bra	2018	GLEAM	0.385	0.163	0.123	0.014	0.014	0.391	0.912	1.026
8	BE-Bra	2018	LSASAF	0.333	0.244	0.203	-0.161	0.161	0.413	1.116	0.705
9	BE-Bra	2019	GLDAS	-0.045	0.295	0.251	0.218	0.218	0.073	0.801	1.439
10	BE-Bra	2019	GLEAM	0.555	0.169	0.132	0.094	0.094	0.606	0.912	1.189
11	BE-Bra	2019	LSASAF	-0.041	0.261	0.215	-0.120	0.120	-0.004	0.849	0.768
12	BE-Bra	2022	GLDAS	-0.048	0.323	0.276	0.243	0.243	0.089	0.998	1.518
13	BE-Bra	2022	GLEAM	0.392	0.217	0.162	0.126	0.126	0.450	0.978	1.259
14	BE-Bra	2022	LSASAF	0.045	0.307	0.265	-0.182	0.182	0.127	1.118	0.629

Figure E1 – Performance metrics BE Bra

	site	year	product	KGE	RMSE	MAE	bias	absolute_bias	pearson_r	alpha	beta
0	BE-Lon	2015	GLDAS	0.393	0.181	0.147	-0.066	0.066	0.433	0.807	0.901
1	BE-Lon	2015	GLEAM	0.048	0.227	0.195	-0.070	0.070	0.076	0.796	0.896
2	BE-Lon	2015	LSASAF	0.065	0.205	0.154	0.001	0.001	0.109	0.716	1.002
3	BE-Lon	2017	GLDAS	0.205	0.184	0.155	-0.014	0.014	0.242	0.762	0.979
4	BE-Lon	2017	GLEAM	0.205	0.208	0.173	-0.050	0.050	0.212	0.933	0.925
5	BE-Lon	2017	LSASAF	-0.146	0.209	0.167	0.026	0.026	-0.090	0.649	1.038
6	BE-Lon	2018	GLDAS	0.392	0.218	0.176	0.111	0.111	0.499	0.739	1.226
7	BE-Lon	2018	GLEAM	-0.322	0.321	0.268	0.180	0.180	-0.208	0.602	1.363
8	BE-Lon	2018	LSASAF	-0.191	0.331	0.282	0.221	0.221	-0.035	0.618	1.450
9	BE-Lon	2019	GLDAS	0.283	0.169	0.129	-0.023	0.023	0.307	0.818	0.964
10	BE-Lon	2019	GLEAM	0.003	0.202	0.157	0.003	0.003	0.021	0.816	1.005
11	BE-Lon	2019	LSASAF	0.081	0.190	0.140	0.044	0.044	0.124	0.732	1.068
12	BE-Lon	2022	GLDAS	0.470	0.205	0.158	0.023	0.023	0.586	0.671	1.038
13	BE-Lon	2022	GLEAM	-0.290	0.312	0.244	0.041	0.041	-0.212	0.564	1.067
14	BE-Lon	2022	LSASAF	-0.097	0.270	0.202	0.075	0.075	0.098	0.387	1.122

Figure E2 – Performance metrics BE Lon

	site	year	product	KGE	RMSE	MAE	bias	absolute_bias	pearson_r	alpha	beta
0	BE-Vie	2015	GLDAS	0.014	0.276	0.239	0.149	0.149	0.071	0.811	1.270
1	BE-Vie	2015	GLEAM	0.511	0.177	0.142	0.081	0.081	0.579	0.798	1.146
2	BE-Vie	2015	LSASAF	-0.026	0.242	0.203	0.047	0.047	0.010	0.742	1.084
3	BE-Vie	2017	GLDAS	0.418	0.226	0.192	0.156	0.156	0.538	0.797	1.290
4	BE-Vie	2017	GLEAM	0.534	0.214	0.187	0.171	0.171	0.713	0.825	1.323
5	BE-Vie	2017	LSASAF	0.109	0.234	0.196	0.100	0.100	0.199	0.652	1.179
6	BE-Vie	2018	GLDAS	-0.167	0.309	0.268	0.247	0.247	-0.040	0.804	1.490
7	BE-Vie	2018	GLEAM	0.354	0.266	0.235	0.232	0.232	0.564	1.040	1.474
8	BE-Vie	2018	LSASAF	0.153	0.212	0.166	0.091	0.091	0.173	1.011	1.180
9	BE-Vie	2019	GLDAS	0.168	0.253	0.211	0.156	0.156	0.243	0.795	1.276
10	BE-Vie	2019	GLEAM	0.502	0.175	0.145	0.101	0.101	0.596	0.773	1.181
11	BE-Vie	2019	LSASAF	0.041	0.217	0.177	0.039	0.039	0.082	0.730	1.068
12	BE-Vie	2022	GLDAS	0.026	0.323	0.289	0.265	0.265	0.204	0.949	1.557
13	BE-Vie	2022	GLEAM	0.244	0.253	0.208	0.192	0.192	0.360	0.948	1.399
14	BE-Vie	2022	LSASAF	0.210	0.193	0.166	0.103	0.103	0.292	0.722	1.211

Figure E3 – Performance metrics BE Vie

	site	year	product	KGE	RMSE	MAE	bias	absolute_bias	pearson_r	alpha	beta
0	BE-Dor	2015	GLDAS	0.251	0.249	0.188	0.152	0.152	0.364	0.698	1.256
1	BE-Dor	2015	GLEAM	0.179	0.234	0.177	0.051	0.051	0.201	0.830	1.084
2	BE-Dor	2015	LSASAF	0.502	0.141	0.112	0.000	0.000	0.761	0.563	1.001
3	BE-Dor	2017	GLDAS	0.260	0.189	0.130	0.101	0.101	0.317	0.763	1.155
4	BE-Dor	2017	GLEAM	0.064	0.230	0.171	0.025	0.025	0.066	0.952	1.039
5	BE-Dor	2017	LSASAF	0.389	0.159	0.116	-0.004	0.004	0.543	0.594	0.994
6	BE-Dor	2018	GLDAS	0.206	0.234	0.171	0.147	0.147	0.298	0.723	1.248
7	BE-Dor	2018	GLEAM	-0.003	0.219	0.177	0.066	0.066	0.012	0.862	1.108
8	BE-Dor	2018	LSASAF	0.385	0.175	0.137	-0.013	0.013	0.432	0.764	0.978
9	BE-Dor	2022	GLDAS	0.176	0.147	0.116	0.029	0.029	0.360	1.517	1.040
10	BE-Dor	2022	GLEAM	-0.205	0.193	0.158	-0.048	0.048	-0.093	1.504	0.935
11	BE-Dor	2022	LSASAF	0.267	0.193	0.159	-0.157	0.157	0.314	0.856	0.788

Figure E4 – Performance metrics BE Dor

F1- Soil groups computed based on HWSD data (https://www.fao.org/land-water/resources/tools/databases/hwsd/en?utm_)

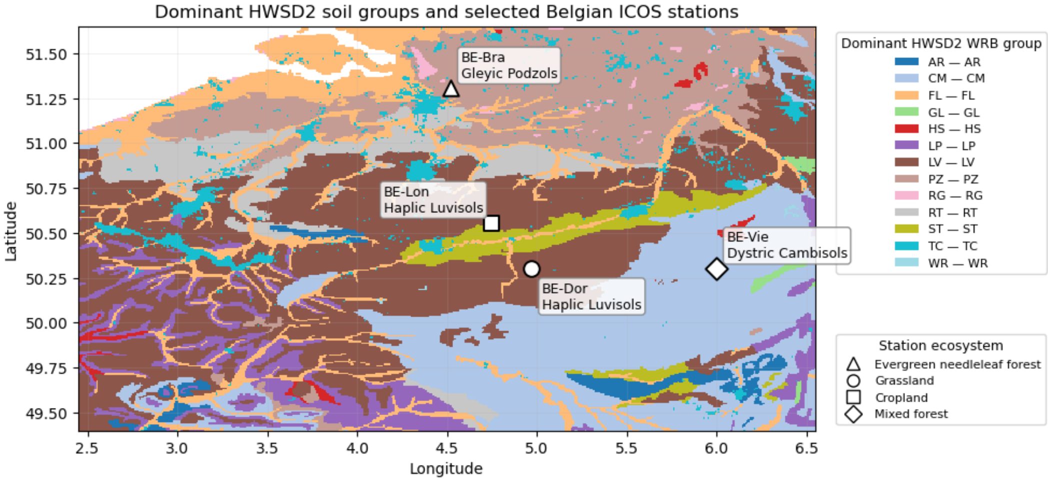

G Main codes used for figure creation (several online tutorials used together with AI)

```
# STATION-LEVEL DROUGHT AND ECOSYSTEM FIGURES
# This script creates two figures for each station:
# 1. Combined overview figure
#    - Left column: drought indices
#    - Right column: ecosystem fluxes and environmental drivers
#    - Shaded periods: SPEI-3 EDO values less than or equal to -1
# 2. Drought-index comparison figure
#    - EDDI
#    - SSI
#    - CDI from the European Drought Observatory
#    - SPEI-3 from the European Drought Observatory
#    - SPEI-3 derived from ERA5
#    - Raw soil-moisture observations and annual medians
#    - Shaded periods: simultaneous EDDI and SSI drought conditions
# Required objects expected to exist before running this script:
# DATA
#     Dictionary containing one pandas DataFrame per station.
# SITES
```

```
#     Dictionary containing station coordinates under:
#     SITES[station]["lat_deg"]
#     SITES[station]["lon_deg"]
# CFG
#     Configuration dictionary containing the soil-moisture column name under:
#     CFG["swc_depth"]
# spi
#     xarray Dataset containing SPI-3 under the variable name "SPI3".
# spei_edo
#     xarray Dataset containing EDO SPEI-3 under the variable name "spe03".
# cdi_edo
#     xarray Dataset containing EDO CDI under the variable name "cdinx".
# era5spei
#     xarray Dataset containing ERA5-derived SPEI-3 under the variable name
#     "SPEI3".
# Each station DataFrame is expected to contain at least:
# date
# EDDI
# SSI
# drought_EDDI
# drought_SSI
# drought_BOTH
# LE_F_MDS
# H_F_MDS
# SW_IN_F
# TA_F
# year
# the soil-moisture column specified by CFG["swc_depth"]
```

```
# IMPORTS

import os

import matplotlib.dates as mdates
import matplotlib.pyplot as plt
import numpy as np
import pandas as pd

from IPython.display import display

# GENERAL SETTINGS

# Directory used for all generated figures.
OUT_DIR = "outputs"

# Earliest date displayed in the figures.
START_DATE = pd.Timestamp("2015-01-01")

# SPEI-3 threshold used to define drought periods.
SPEI_DROUGHT_THRESHOLD = -1.0

# Create the output directory when it does not already exist.
os.makedirs(OUT_DIR, exist_ok=True)

# DATA EXTRACTION AND PREPARATION FUNCTIONS

def extract_station_gridded_series(station):
    """
```

```
Extract gridded drought-index time series for one station.

The nearest available grid cell is selected independently from each
gridded dataset using the station latitude and longitude.

Parameters
----------
station : str
    Station identifier used as a key in the SITES dictionary.

Returns
-------
dict
    Dictionary containing the extracted SPI, EDO SPEI, EDO CDI, and
    ERA5-derived SPEI series.
"""
latitude = SITES[station]["lat_deg"]
longitude = SITES[station]["lon_deg"]

spi_series = (
    spi["SPI3"]
    .sel(lat=latitude, lon=longitude, method="nearest")
    .squeeze()
)

spei_edo_series = (
    spei_edo["spe03"]
    .sel(lat=latitude, lon=longitude, method="nearest")
    .squeeze()
```

```
    )

    cdi_series = (
        cdi_edo["cdinx"]
        .sel(lat=latitude, lon=longitude, method="nearest")
        .squeeze()
    )

    era5_spei_series = (
        era5spei["SPEI3"]
        .sel(lat=latitude, lon=longitude, method="nearest")
        .squeeze()
    )

    return {
        "spi": spi_series,
        "spei_edo": spei_edo_series,
        "cdi": cdi_series,
        "spei_era5": era5_spei_series,
    }


def prepare_station_dataframe(df):
    """
    Prepare a copy of a station DataFrame for plotting.

    The date column is converted to pandas datetime format and evaporative
    fraction is calculated from latent and sensible heat fluxes.
```

```
Evaporative fraction is defined as:

    EF = LE / (LE + H)

Values are set to missing when:
- the sum of LE and H is zero or negative;
- the calculated EF is below 0;
- the calculated EF is above 1.

Parameters
----------
df : pandas.DataFrame
    Original station DataFrame.

Returns
-------
pandas.DataFrame
    Prepared copy containing a cleaned EF column.
"""
prepared = df.copy()

prepared["date"] = pd.to_datetime(prepared["date"])

denominator = prepared["LE_F_MDS"] + prepared["H_F_MDS"]

prepared["EF"] = prepared["LE_F_MDS"] / denominator

invalid_ef = (
    (denominator <= 0)
```

```
        | (prepared["EF"] < 0)
        | (prepared["EF"] > 1)
    )

    prepared.loc[invalid_ef, "EF"] = np.nan

    return prepared


# DROUGHT-PERIOD IDENTIFICATION FUNCTIONS


def get_boolean_periods(dates, condition):
    """
    Convert a Boolean time series into continuous start and end periods.

    Consecutive True values are grouped into one period. Each returned tuple
    contains the first and final date of a continuous period.

    Parameters
    ----------
    dates : array-like
        Dates corresponding to the Boolean condition.
    condition : array-like of bool
        Boolean values indicating whether the condition is satisfied.

    Returns
    -------
    list of tuple
```

```
    List of (start_date, end_date) tuples.
"""
dates = pd.to_datetime(np.asarray(dates))
condition = np.asarray(condition, dtype=bool)

periods = []
start_index = 0
number_of_values = len(condition)

while start_index < number_of_values:

    if condition[start_index]:
        end_index = start_index

        while (
            end_index < number_of_values
            and condition[end_index]
        ):
            end_index += 1

        periods.append(
            (
                dates[start_index],
                dates[end_index - 1],
            )
        )

        start_index = end_index
```

```
        else:
            start_index += 1

    return periods


def get_spei_drought_periods(
    spei_series,
    threshold=SPEI_DROUGHT_THRESHOLD,
):
    """
    Identify continuous EDO SPEI-3 drought periods.

    A drought period is defined as one or more consecutive SPEI-3 values
    less than or equal to the selected threshold.

    Missing SPEI values are treated as non-drought observations.

    Parameters
    ----------
    spei_series : xarray.DataArray
        SPEI-3 time series with a time coordinate.
    threshold : float, default SPEI_DROUGHT_THRESHOLD
        SPEI value used to define drought conditions.

    Returns
    -------
    list of tuple
        Continuous drought periods represented by start and end dates.
```

```
    """
    dates = pd.to_datetime(spei_series["time"].values)
    values = np.asarray(spei_series.values).squeeze()

    drought_condition = (
        np.isfinite(values)
        & (values <= threshold)
    )

    return get_boolean_periods(
        dates=dates,
        condition=drought_condition,
    )


def get_combined_eddi_ssi_periods(df):
    """
    Identify periods during which both EDDI and SSI indicate drought.

    The drought_BOTH column is expected to contain a Boolean condition
    identifying simultaneous EDDI and SSI drought conditions.

    Parameters
    ----------
    df : pandas.DataFrame
        Station DataFrame containing date and drought_BOTH columns.

    Returns
    -------
```

```
    list of tuple
        Continuous combined-drought periods represented by start and end
        dates.
    """
    return get_boolean_periods(
        dates=df["date"],
        condition=df["drought_BOTH"].fillna(False),
    )


# GENERAL PLOTTING HELPERS

def shade_periods(
    ax,
    periods,
    color="#7d3c98",
    alpha=0.12,
):
    """
    Add vertical shading for a collection of time periods.

    Parameters
    ----------
    ax : matplotlib.axes.Axes
        Axis receiving the shaded periods.
    periods : list of tuple
        Collection of (start_date, end_date) tuples.
    color : str, default "#7d3c98"
        Colour used for the shaded periods.
```

```
    alpha : float, default 0.12
        Transparency of the shaded periods.
    """
    for start_date, end_date in periods:
        ax.axvspan(
            start_date,
            end_date,
            color=color,
            alpha=alpha,
            linewidth=0,
        )


def plot_period_bar(
    ax,
    periods,
    label="SPEI ≤ -1\nperiods",
):
    """
    Plot drought periods as horizontal blocks on a compact timeline axis.

    Parameters
    ----------
    ax : matplotlib.axes.Axes
        Axis receiving the drought-period blocks.
    periods : list of tuple
        Collection of (start_date, end_date) tuples.
    label : str
        Axis label describing the represented drought condition.
```

```
    """
    ax.set_ylim(0, 1)
    ax.set_yticks([])
    ax.set_ylabel(label, fontsize=9)

    for start_date, end_date in periods:
        ax.axvspan(
            start_date,
            end_date,
            ymin=0.2,
            ymax=0.8,
            color="#e74c3c",
            alpha=0.65,
            linewidth=0,
        )

    ax.grid(True, axis="x")


def format_shared_time_axis(
    axes,
    start_date=START_DATE,
):
    """
    Apply common annual date formatting to a vertically stacked axis group.

    X-axis labels are hidden for all panels except the final panel.

    Parameters
```

```
    ----------
    axes : sequence of matplotlib.axes.Axes
        Ordered collection of axes sharing the same x-axis.
    start_date : pandas.Timestamp
        Earliest date displayed in the figure.
    """
    for ax in axes[:-1]:
        plt.setp(
            ax.get_xticklabels(),
            visible=False,
        )

    axes[-1].xaxis.set_major_locator(
        mdates.YearLocator()
    )

    axes[-1].xaxis.set_major_formatter(
        mdates.DateFormatter("%Y")
    )

    axes[-1].set_xlim(
        left=start_date
    )


def save_display_close(
    fig,
    file_path,
    dpi=150,
```

```
):
    """
    Save, display, and close a Matplotlib figure.

    Closing the figure after display prevents unnecessary memory use when
    figures are generated for many stations.

    Parameters
    ----------
    fig : matplotlib.figure.Figure
        Figure to save and display.
    file_path : str
        Complete output path.
    dpi : int, default 150
        Resolution used for the saved image.
    """
    fig.savefig(
        file_path,
        dpi=dpi,
        bbox_inches="tight",
    )

    display(fig)
    plt.close(fig)

    print(f"Saved: {file_path}")


# INDIVIDUAL PANEL-PLOTTING FUNCTIONS
```

```
def plot_eddi_panel(
    ax,
    df,
    shaded_periods=None,
):
    """
    Plot EDDI values and highlight observations classified as drought.

    Positive EDDI values represent relatively dry evaporative-demand
    conditions. Horizontal dotted lines indicate selected drought-intensity
    reference levels.
    """
    values = df["EDDI"].to_numpy()

    ax.fill_between(
        df["date"],
        0,
        values,
        where=values >= 0,
        color="#c0392b",
        alpha=0.55,
    )

    ax.fill_between(
        df["date"],
        0,
        values,
        where=values < 0,
```

```
    color="#2980b9",
    alpha=0.40,
)

drought_mask = (
    df["drought_EDDI"]
    .fillna(False)
    .to_numpy(dtype=bool)
)

ax.plot(
    df.loc[drought_mask, "date"],
    values[drought_mask],
    ".",
    markersize=3,
    color="black",
)

for reference_level in (0.8, 1.3, 1.6):
    ax.axhline(
        reference_level,
        color="grey",
        linestyle=":",
        linewidth=0.7,
    )

ax.axhline(
    0,
    color="black",
```

```
        linewidth=0.6,
    )

    ax.set_ylabel("EDDI\n(+ = dry)")
    ax.set_ylim(-3.2, 3.2)
    ax.grid(True)

    if shaded_periods is not None:
        shade_periods(
            ax,
            shaded_periods,
        )


def plot_ssi_panel(
    ax,
    df,
    shaded_periods=None,
):
    """
    Plot SSI values and highlight observations classified as drought.

    Negative SSI values represent relatively dry soil-moisture conditions.
    Horizontal dotted lines indicate selected drought-intensity reference
    levels.
    """
    values = df["SSI"].to_numpy()

    ax.fill_between(
```

```
    df["date"],
    0,
    values,
    where=values <= 0,
    color="#8c5a2b",
    alpha=0.55,
)

ax.fill_between(
    df["date"],
    0,
    values,
    where=values > 0,
    color="#2980b9",
    alpha=0.40,
)

drought_mask = (
    df["drought_SSI"]
    .fillna(False)
    .to_numpy(dtype=bool)
)

ax.plot(
    df.loc[drought_mask, "date"],
    values[drought_mask],
    ".",
    markersize=3,
    color="black",
```

```
    )

    for reference_level in (-0.8, -1.3, -1.6):
        ax.axhline(
            reference_level,
            color="grey",
            linestyle=":",
            linewidth=0.7,
        )

    ax.axhline(
        0,
        color="black",
        linewidth=0.6,
    )

    ax.set_ylabel("SSI\n(- = dry)")
    ax.set_ylim(-3.2, 3.2)
    ax.grid(True)

    if shaded_periods is not None:
        shade_periods(
            ax,
            shaded_periods,
        )


def plot_standardized_index_panel(
    ax,
```

```
    series,
    ylabel,
    color,
    shaded_periods=None,
    drought_threshold=None,
):
    """
    Plot a standardized drought-index time series.

    Parameters
    ----------
    ax : matplotlib.axes.Axes
        Axis receiving the time series.
    series : xarray.DataArray
        Time series containing a time coordinate.
    ylabel : str
        Y-axis label.
    color : str
        Line colour.
    shaded_periods : list of tuple, optional
        Time periods added as vertical shading.
    drought_threshold : float, optional
        Optional horizontal drought threshold.
    """
    ax.plot(
        series["time"].values,
        np.asarray(series.values).squeeze(),
        color=color,
        linewidth=1,
```

```
    )

    ax.axhline(
        0,
        color="black",
        linewidth=0.6,
    )

    if drought_threshold is not None:
        ax.axhline(
            drought_threshold,
            color="grey",
            linestyle=":",
            linewidth=0.8,
        )

    ax.set_ylabel(ylabel)
    ax.set_ylim(-3.2, 3.2)
    ax.grid(True)

    if shaded_periods is not None:
        shade_periods(
            ax,
            shaded_periods,
        )


def plot_cdi_panel(
    ax,
```

```
    cdi_series,
    shaded_periods=None,
):
    """
    Plot the categorical EDO Combined Drought Indicator time series.
    """
    ax.step(
        cdi_series["time"].values,
        np.asarray(cdi_series.values).squeeze(),
        where="post",
        color="black",
        linewidth=1,
    )

    ax.set_ylabel("CDI\nEDO")
    ax.set_yticks([0, 1, 2, 3])
    ax.set_ylim(-0.2, 3.2)
    ax.grid(True)

    if shaded_periods is not None:
        shade_periods(
            ax,
            shaded_periods,
        )


# FIGURE 1: COMBINED INDICES, FLUXES, AND ENVIRONMENTAL DRIVERS

def create_combined_station_figure(
```

```
    station,
    df,
    gridded_series,
    output_dir=OUT_DIR,
):
    """
    Create a two-column station overview figure.

    The left column contains drought indices. The right column contains
    ecosystem fluxes and environmental drivers. Purple shading and the
    bottom timeline bars indicate EDO SPEI-3 periods less than or equal
    to -1.

    Parameters
    ----------
    station : str
        Station identifier.
    df : pandas.DataFrame
        Prepared station DataFrame containing EF.
    gridded_series : dict
        Dictionary returned by extract_station_gridded_series().
    output_dir : str
        Directory used for the saved figure.
    """
    spei_periods = get_spei_drought_periods(
        gridded_series["spei_edo"],
        threshold=SPEI_DROUGHT_THRESHOLD,
    )
```

```python
fig = plt.figure(
    figsize=(18, 12)
)

# Independent GridSpec objects allow different numbers of rows in the
# left and right columns while preserving aligned figure boundaries.
left_grid = fig.add_gridspec(
    nrows=6,
    ncols=1,
    left=0.06,
    right=0.48,
    top=0.90,
    bottom=0.10,
    height_ratios=[
        1,
        1,
        0.7,
        1,
        1,
        0.28,
    ],
    hspace=0.08,
)

right_grid = fig.add_gridspec(
    nrows=7,
    ncols=1,
    left=0.55,
    right=0.98,
```

```
    top=0.90,
    bottom=0.10,
    height_ratios=[
        1,
        1,
        1,
        0.8,
        1,
        1,
        0.28,
    ],
    hspace=0.08,
)

left_axes = [
    fig.add_subplot(left_grid[row, 0])
    for row in range(6)
]

right_axes = [
    fig.add_subplot(right_grid[row, 0])
    for row in range(7)
]

# All panels in each column share a common time axis.
for ax in left_axes[1:]:
    ax.sharex(left_axes[0])

for ax in right_axes[1:]:
```

```
    ax.sharex(right_axes[0])

# Left column: drought indices

plot_standardized_index_panel(
    ax=left_axes[0],
    series=gridded_series["spi"],
    ylabel="SPI-3\n(-)",
    color="#1f77b4",
    shaded_periods=spei_periods,
    drought_threshold=-1,
)

plot_standardized_index_panel(
    ax=left_axes[1],
    series=gridded_series["spei_edo"],
    ylabel="SPEI-3\nEDO",
    color="#34495e",
    shaded_periods=spei_periods,
    drought_threshold=-1,
)

plot_cdi_panel(
    ax=left_axes[2],
    cdi_series=gridded_series["cdi"],
    shaded_periods=spei_periods,
)

plot_eddi_panel(
```

```
    ax=left_axes[3],
    df=df,
    shaded_periods=spei_periods,
)

plot_ssi_panel(
    ax=left_axes[4],
    df=df,
    shaded_periods=spei_periods,
)

plot_period_bar(
    ax=left_axes[5],
    periods=spei_periods,
    label="SPEI ≤ -1\nperiods",
)

left_axes[0].set_title(
    "Drought indices"
)

# Right column: ecosystem fluxes and environmental drivers

right_axes[0].plot(
    df["date"],
    df["LE_F_MDS"],
    color="#27ae60",
    linewidth=0.7,
)
```

```
right_axes[0].set_ylabel(
    "LE\n(W m⁻²)"
)

right_axes[1].plot(
    df["date"],
    df["H_F_MDS"],
    color="#c0392b",
    linewidth=0.7,
)

right_axes[1].set_ylabel(
    "H\n(W m⁻²)"
)

right_axes[2].plot(
    df["date"],
    df["SW_IN_F"],
    color="#f1c40f",
    linewidth=0.7,
)

right_axes[2].set_ylabel(
    "SW↓\n(W m⁻²)"
)

right_axes[3].plot(
    df["date"],
```

```
    df["EF"],
    color="black",
    linewidth=0.7,
)

right_axes[3].set_ylabel(
    "EF\n(-)"
)

right_axes[3].set_ylim(
    0,
    1,
)

right_axes[4].plot(
    df["date"],
    df["TA_F"],
    color="#e67e22",
    linewidth=0.7,
)

right_axes[4].set_ylabel(
    "TA\n(°C)"
)

soil_moisture_column = CFG["swc_depth"]

right_axes[5].plot(
    df["date"],
```

```
    df[soil_moisture_column],
    color="#00a6a6",
    linewidth=0.7,
)

right_axes[5].set_ylabel(
    f"{soil_moisture_column}\n(%vol)"
)

# Apply grids and identical SPEI drought shading to all continuous
# right-column data panels.
for ax in right_axes[:6]:
    ax.grid(True)

    shade_periods(
        ax,
        spei_periods,
    )

plot_period_bar(
    ax=right_axes[6],
    periods=spei_periods,
    label="SPEI ≤ -1\nperiods",
)

right_axes[0].set_title(
    "Fluxes and environmental drivers"
)
```

```
# Shared formatting

format_shared_time_axis(
    left_axes,
    start_date=START_DATE,
)

format_shared_time_axis(
    right_axes,
    start_date=START_DATE,
)

fig.suptitle(
    f"{station}: drought indices and ecosystem fluxes\n"
    "Purple bands and bottom bars indicate EDO SPEI-3 ≤ -1 periods",
    fontsize=14,
    y=0.98,
)

output_path = os.path.join(
    output_dir,
    f"{station}_combined_indices_left_fluxes_right.png",
)

save_display_close(
    fig=fig,
    file_path=output_path,
)
```

```
# FIGURE 2: DETAILED DROUGHT-INDEX COMPARISON

def create_drought_comparison_figure(
    station,
    df,
    gridded_series,
    output_dir=OUT_DIR,
):
    """
    Create a detailed comparison of station-level drought indicators.

    Purple shading indicates continuous periods during which both EDDI and
    SSI classify drought conditions. The soil-moisture panel includes the
    original daily observations and one median value per year.

    Parameters
    ----------
    station : str
        Station identifier.
    df : pandas.DataFrame
        Prepared station DataFrame.
    gridded_series : dict
        Dictionary returned by extract_station_gridded_series().
    output_dir : str
        Directory used for the saved figure.
    """
    combined_drought_periods = (
        get_combined_eddi_ssi_periods(df)
```

```
)

fig, axes = plt.subplots(
    nrows=6,
    ncols=1,
    figsize=(14, 13),
    sharex=True,
    gridspec_kw={
        "height_ratios": [
            1,
            1,
            0.7,
            1,
            1,
            0.8,
        ]
    },
)

# EDDI

plot_eddi_panel(
    ax=axes[0],
    df=df,
    shaded_periods=combined_drought_periods,
)

# SSI
```

```
plot_ssi_panel(
    ax=axes[1],
    df=df,
    shaded_periods=combined_drought_periods,
)

# EDO Combined Drought Indicator

plot_cdi_panel(
    ax=axes[2],
    cdi_series=gridded_series["cdi"],
    shaded_periods=combined_drought_periods,
)

# EDO SPEI-3

plot_standardized_index_panel(
    ax=axes[3],
    series=gridded_series["spei_edo"],
    ylabel="SPEI-3\nEDO",
    color="#34495e",
    shaded_periods=combined_drought_periods,
)

# ERA5-derived SPEI-3

plot_standardized_index_panel(
    ax=axes[4],
    series=gridded_series["spei_era5"],
```

```
    ylabel="SPEI-3\nERA5",
    color="#16a085",
    shaded_periods=combined_drought_periods,
)

# ----------------------------------------------------------------------
# Raw soil moisture and annual median
# ----------------------------------------------------------------------

soil_moisture_column = CFG["swc_depth"]

axes[5].plot(
    df["date"],
    df[soil_moisture_column],
    color="#27ae60",
    linewidth=0.6,
    alpha=0.8,
    label="Daily soil moisture",
)

# The annual median is positioned on 1 July of the corresponding year.
# This date is used only for visual placement and does not represent the
# exact date at which the median occurred.
annual_median = (
    df.groupby("year")[soil_moisture_column]
    .median()
    .dropna()
)
```

```
annual_median_dates = pd.to_datetime(
    annual_median.index
    .astype(str)
    + "-07-01"
)

axes[5].plot(
    annual_median_dates,
    annual_median.values,
    "o-",
    color="black",
    markersize=4,
    label="Annual median",
)

axes[5].set_ylabel(
    f"{soil_moisture_column}\n(%vol)"
)

axes[5].legend(
    fontsize=8,
    loc="upper right",
)

axes[5].grid(True)

shade_periods(
    axes[5],
    combined_drought_periods,
```

```
)

# ------------------------------------------------------------------------
# Shared formatting and annotation
# ------------------------------------------------------------------------

axes[0].set_title(
    f"{station}: drought indices comparison"
)

# Empty plotted data create a legend entry explaining the shaded regions.
axes[0].plot(
    [],
    [],
    linestyle="none",
    marker=None,
    label="Purple shading = simultaneous EDDI and SSI drought",
)

axes[0].legend(
    fontsize=8,
    loc="upper left",
)

axes[-1].xaxis.set_major_locator(
    mdates.YearLocator()
)

axes[-1].xaxis.set_major_formatter(
```

```
        mdates.DateFormatter("%Y")
    )

    axes[-1].set_xlim(
        left=START_DATE
    )

    fig.tight_layout()

    output_path = os.path.join(
        output_dir,
        f"{station}_drought_indices_comparison.png",
    )

    save_display_close(
        fig=fig,
        file_path=output_path,
    )


#
# OPTIONAL SINGLE-STATION WRAPPER
#

def plot_station_figures(
    station,
    create_combined=True,
    create_comparison=True,
):
```

```
"""
Create the selected figure types for one station.

Parameters
----------
station : str
    Station identifier.
create_combined : bool, default True
    Create the two-column indices and fluxes overview.
create_comparison : bool, default True
    Create the detailed drought-index comparison.
"""
if station not in DATA:
    raise KeyError(
        f"Station '{station}' was not found in DATA."
    )

if station not in SITES:
    raise KeyError(
        f"Station '{station}' was not found in SITES."
    )

station_df = prepare_station_dataframe(
    DATA[station]
)

gridded_series = extract_station_gridded_series(
    station
)
```

```
    if create_combined:
        create_combined_station_figure(
            station=station,
            df=station_df,
            gridded_series=gridded_series,
        )

    if create_comparison:
        create_drought_comparison_figure(
            station=station,
            df=station_df,
            gridded_series=gridded_series,
        )


#
# CREATE BOTH FIGURES FOR EVERY STATION
#

for station in DATA:
    plot_station_figures(
        station=station,
        create_combined=True,
        create_comparison=True,
    )
```

F2 Performance metrics

```
def calculate_metrics(observed, predicted):
    """
    Calculate performance metrics for one product against ICOS.

    Bias is defined as:
        product - ICOS

    Therefore:
        positive bias = product overestimates ICOS
        negative bias = product underestimates ICOS

    KGE 2009:
        KGE = 1 - sqrt(
            (r - 1)^2
            + (alpha - 1)^2
            + (beta - 1)^2
        )

    where:
        r = Pearson correlation

        alpha =
            standard deviation of product
            divided by standard deviation of ICOS

        beta =
            mean of product
            divided by mean of ICOS
    """
```

```
pair = pd.DataFrame(
    {
        "observed": pd.to_numeric(
            observed,
            errors="coerce"
        ),

        "predicted": pd.to_numeric(
            predicted,
            errors="coerce"
        ),
    }
).dropna()

n = len(pair)

empty_result = {
    "N": n,
    "bias": np.nan,
    "absolute_bias": np.nan,
    "RMSE": np.nan,
    "MAE": np.nan,
    "pearson_r": np.nan,
    "KGE": np.nan,
    "alpha": np.nan,
    "beta": np.nan,
}
```

```
if n < 2:
    return empty_result

obs = pair["observed"]
sim = pair["predicted"]

error = sim - obs

bias = error.mean()

absolute_bias = abs(
    bias
)

rmse = np.sqrt(
    np.mean(
        error ** 2
    )
)

mae = np.mean(
    np.abs(
        error
    )
)

# Correlation requires variation in both series.
if (
    obs.nunique() > 1
```

```
    and sim.nunique() > 1
):
    pearson_r = obs.corr(
        sim,
        method="pearson"
    )
else:
    pearson_r = np.nan

obs_mean = obs.mean()
sim_mean = sim.mean()

obs_std = obs.std(
    ddof=1
)

sim_std = sim.std(
    ddof=1
)

# KGE cannot be calculated when:
# - Pearson correlation is unavailable
# - the observed mean is zero
# - the observed standard deviation is zero
if (
    pd.isna(pearson_r)
    or np.isclose(obs_mean, 0)
    or np.isclose(obs_std, 0)
):
```

```
    alpha = np.nan
    beta = np.nan
    kge = np.nan

else:

    alpha = (
        sim_std
        / obs_std
    )

    beta = (
        sim_mean
        / obs_mean
    )

    kge = 1 - np.sqrt(
        (pearson_r - 1) ** 2
        + (alpha - 1) ** 2
        + (beta - 1) ** 2
    )

return {
    "N": n,
    "bias": bias,
    "absolute_bias": absolute_bias,
    "RMSE": rmse,
    "MAE": mae,
```

```
        "pearson_r": pearson_r,
        "KGE": kge,
        "alpha": alpha,
        "beta": beta,
    }
```

F3 ECOCLIMAP footprints

```
# ECOCLIMAP-SG LAND COVER, ICOS STATIONS AND PRODUCT GRID-CELL FOOTPRINTS

import numpy as np
import matplotlib.pyplot as plt
import xarray as xr

from matplotlib.colors import ListedColormap, BoundaryNorm
from matplotlib.patches import Patch
from matplotlib.lines import Line2D


plt.close("all")

# 1. ECOCLIMAP CLASS COLOURS

class_colors = {

    # Water
    1: "#00008B",   # Sea and oceans
    2: "#0000FF",   # Lakes
    3: "#66B3FF",   # Rivers
```

```
# Bare
4: "#B8B39A",   # Bare land
5: "#7A7063",   # Bare rock

# Snow
6: "#F2F2F2",   # Permanent snow

# Forest
7: "#1B5E20",   # Boreal broadleaf deciduous
8: "#556B2F",   # Temperate broadleaf deciduous
9: "#7CB342",   # Tropical broadleaf deciduous
10: "#43A047",  # Temperate broadleaf evergreen
11: "#66BB6A",  # Tropical broadleaf evergreen
12: "#0B6623",  # Boreal needleleaf evergreen
13: "#2ECC71",  # Temperate needleleaf evergreen
14: "#D8A7B1",  # Boreal needleleaf deciduous

# Shrubs
15: "#C68642",

# Grass
16: "#9CCC65",  # Boreal grassland
17: "#66BB33",  # Temperate grassland
18: "#00C853",  # Tropical grassland

# Crops
19: "#C5C8BC",  # Winter C3 crops
20: "#B2FF59",  # Summer C3 crops
```

```
    21: "#C0CA33",  # C4 crops

    # Flooded vegetation
    22: "#8B6B1F",  # Flooded trees
    23: "#2F6F6F",  # Flooded grassland

    # Urban
    24: "#7F0000",  # LCZ1 compact high-rise
    25: "#C00000",  # LCZ2 compact mid-rise
    26: "#FF0000",  # LCZ3 compact low-rise
    27: "#FF6600",  # LCZ4 open high-rise
    28: "#FF9933",  # LCZ5 open mid-rise
    29: "#FFCC33",  # LCZ6 open low-rise
    30: "#FFD966",  # LCZ7 lightweight low-rise
    31: "#CCCC00",  # LCZ8 large low-rise
    32: "#999999",  # LCZ9 sparsely built
    33: "#555555",  # LCZ10 heavy industry
}


# 2. PRODUCT FOOTPRINT STYLES

product_styles = {

    "GLDAS": {
        "color": "#D7191C",      # bright red
        "linestyle": "--",       # solid
        "linewidth": 2.8,
        "zorder": 15,
```

```
    },

    "GLEAM": {
        "color": "#6B3E06",      # darker brown
        "linestyle": "--",        # dotted
        "linewidth": 3.4,
        "zorder": 16,
    },

    "FLUXCOM": {
        "color": "#002D72",      # dark navy
        "linestyle": "-",        # solid
        "linewidth": 3.0,
        "zorder": 17,
    },

    "LSA SAF": {
        "color": "#FF5A00",      # neon orange
        "linestyle": "-",        # dotted
        "linewidth": 4.2,
        "zorder": 20,
    },

}

# 3. MAP SETTINGS

LANDCOVER_ALPHA = 0.68
```

```
MAP_XLIM = (3.95, 6.45)
MAP_YLIM = (49.95, 51.48)

OUTPUT_FILE = (
    "/data/gent/vo/002/gvo00202/vsc50144/"
    "ecoclimap_gridcell_footprints_zoomed_transparent.png"
)

# 4. FIND LAND-COVER CLASSES PRESENT IN THE RASTER

classes_present = np.unique(
    landcover.values
)

classes_present = classes_present[
    ~np.isnan(classes_present)
].astype(int)

print(
    "Classes present:",
    classes_present
)

# 5. CONVERT ORIGINAL CLASS CODES TO COLOUR-MAP POSITIONS
#
# Example:
# [1, 2, 5, 8] -> [0, 1, 2, 3]

class_to_position = {
```

```
    code: position
    for position, code in enumerate(classes_present)
}


mapped_values = np.full(
    landcover.shape,
    np.nan,
    dtype=float
)


for code, position in class_to_position.items():

    mapped_values[
        landcover.values == code
    ] = position


mapped_landcover = xr.DataArray(
    mapped_values,
    coords=landcover.coords,
    dims=landcover.dims,
    name="landcover_classes"
)


# 6. BUILD DISCRETE ECOCLIMAP COLOUR MAP
```

```
colors_present = [
    class_colors[code]
    for code in classes_present
]


cmap = ListedColormap(
    colors_present
)


bounds = (
    np.arange(
        len(classes_present) + 1
    )
    - 0.5
)


norm = BoundaryNorm(
    bounds,
    cmap.N
)


# 7. STANDARDISE PRODUCT NAMES

def standardise_product_name(product):
    """
```

```
    Convert different LSA-SAF spellings to one consistent product name.
    """

    product = str(
        product
    ).strip().upper()

    product_name_map = {
        "GLDAS": "GLDAS",
        "GLEAM": "GLEAM",
        "FLUXCOM": "FLUXCOM",
        "LSASAF": "LSA SAF",
        "LSA-SAF": "LSA SAF",
        "LSA SAF": "LSA SAF",
    }

    return product_name_map.get(
        product,
        product
    )


# 8. CHECK REQUIRED FOOTPRINT COLUMNS

required_footprint_columns = {
    "product",
    "polygon_geometry",
}
```

```
missing_footprint_columns = (
    required_footprint_columns
    .difference(
        footprints.columns
    )
)


if missing_footprint_columns:

    raise ValueError(
        "The footprints dataframe is missing these columns: "
        f"{sorted(missing_footprint_columns)}\n\n"
        f"Available columns are:\n{footprints.columns.tolist()}"
    )


# 9. DETECT STATION COORDINATE COLUMNS

possible_lon_columns = [
    "station_lon",
    "station_longitude",
    "lon_station",
    "longitude",
    "lon",
]
```

```
possible_lat_columns = [
    "station_lat",
    "station_latitude",
    "lat_station",
    "latitude",
    "lat",
]


station_lon_column = next(
    (
        column
        for column in possible_lon_columns
        if column in footprints.columns
    ),
    None
)


station_lat_column = next(
    (
        column
        for column in possible_lat_columns
        if column in footprints.columns
    ),
    None
)
```

```
if station_lon_column is None:

    raise ValueError(
        "No station-longitude column was found.\n"
        f"Available footprint columns:\n{footprints.columns.tolist()}"
    )


if station_lat_column is None:

    raise ValueError(
        "No station-latitude column was found.\n"
        f"Available footprint columns:\n{footprints.columns.tolist()}"
    )


print(
    "Station longitude column:",
    station_lon_column
)

print(
    "Station latitude column:",
    station_lat_column
)

# 10. DETECT STATION LABEL COLUMN
#
# Prefer site_id, for labels such as BE-Bra, BE-Lon, etc.
```

```python
if "site_id" in footprints.columns:

    station_label_column = "site_id"

elif "station" in footprints.columns:

    station_label_column = "station"

else:

    raise ValueError(
        "Neither `site_id` nor `station` exists in footprints."
    )


# Keep one coordinate record for each station
station_points = (
    footprints[
        [
            station_label_column,
            station_lon_column,
            station_lat_column,
        ]
    ]
    .dropna()
    .drop_duplicates(
        subset=station_label_column
    )
```

```
    .copy()
)


# 11. CREATE FIGURE
#
# Important:
# - The legends remain within the figure canvas.
# - No tight_layout is used.
# - The map itself keeps the requested geographic extent.

fig, ax = plt.subplots(
    figsize=(14, 9)
)


# Reserve space for the legends on the right.
# This prevents clipping without changing longitude/latitude limits.
fig.subplots_adjust(
    left=0.08,
    right=0.72,
    bottom=0.10,
    top=0.92
)

# 12. PLOT ECOCLIMAP LAND COVER

mapped_landcover.plot(
    ax=ax,
```

```
    x="lon",
    y="lat",
    cmap=cmap,
    norm=norm,
    add_colorbar=False,
    alpha=LANDCOVER_ALPHA,
    rasterized=True,
    zorder=1,
)


# 13. PLOT PRODUCT GRID-CELL FOOTPRINTS

products_plotted = set()

for _, footprint_row in footprints.iterrows():

    product = standardise_product_name(
        footprint_row["product"]
    )

    if product not in product_styles:
        continue

    polygon = footprint_row[
        "polygon_geometry"
    ]

    if polygon is None:
```

```
    continue

if getattr(
    polygon,
    "is_empty",
    False
):
    continue

style = product_styles[
    product
]

products_plotted.add(
    product
)

# Support Polygon and MultiPolygon geometries
if polygon.geom_type == "MultiPolygon":

    polygon_parts = list(
        polygon.geoms
    )

else:

    polygon_parts = [
        polygon
    ]
```

```
    for polygon_part in polygon_parts:

        x_coordinates, y_coordinates = (
            polygon_part.exterior.xy
        )

        ax.plot(
            x_coordinates,
            y_coordinates,
            color=style["color"],
            linestyle=style["linestyle"],
            linewidth=style["linewidth"],
            zorder=style["zorder"],
            solid_capstyle="butt",
            dash_capstyle="butt",
        )

# 14. PLOT ICOS STATIONS

for _, station_row in station_points.iterrows():

    station_lon = float(
        station_row[
            station_lon_column
        ]
    )
```

```
station_lat = float(
    station_row[
        station_lat_column
    ]
)

station_label = str(
    station_row[
        station_label_column
    ]
)


# Black dot with white edge
ax.scatter(
    station_lon,
    station_lat,
    s=48,
    facecolor="black",
    edgecolor="white",
    linewidth=1.1,
    zorder=30,
)


# Station label
ax.annotate(
    station_label,
    xy=(
```

```
            station_lon,
            station_lat
        ),
        xytext=(
            7,
            7
        ),
        textcoords="offset points",
        fontsize=8,
        fontweight="bold",
        color="black",
        ha="left",
        va="bottom",
        zorder=31,
    )

# 15. MAP EXTENT AND LABELS

ax.set_xlim(
    MAP_XLIM
)

ax.set_ylim(
    MAP_YLIM
)


ax.set_title(
    "ECOCLIMAP-SG land cover, ICOS stations and product grid-cell footprints"
```

```
)

ax.set_xlabel(
    "Longitude (°E)"
)

ax.set_ylabel(
    "Latitude (°N)"
)

# 16. LAND-COVER LEGEND
# Same labels and styling as the original map.
# The legend is attached to the figure rather than outside the axes.

landcover_legend_handles = [
    Patch(
        facecolor=class_colors[code],
        edgecolor="black",
        linewidth=0.3,
        label=f"{code}: {class_names[code]}"
    )
    for code in classes_present
]

landcover_legend = fig.legend(
```

```
    handles=landcover_legend_handles,
    title="Land-cover classes",
    loc="upper left",

    # Coordinates are relative to the full figure canvas.
    # Therefore the legend cannot be clipped at the right.
    bbox_to_anchor=(
        0.735,
        0.92
    ),

    borderaxespad=0,
    fontsize=8,
    title_fontsize=9,
    frameon=True,
)
# 17. PRODUCT FOOTPRINT LEGEND

footprint_legend_handles = [
    Line2D(
        [0],
        [0],
        color=product_styles[product]["color"],
        linestyle=product_styles[product]["linestyle"],
        linewidth=product_styles[product]["linewidth"],
        label=product,
    )
    for product in [
        "GLDAS",
```

```
        "GLEAM",
        "FLUXCOM",
        "LSA SAF",
    ]
]


footprint_legend_handles.append(
    Line2D(
        [0],
        [0],
        marker="o",
        linestyle="None",
        markerfacecolor="black",
        markeredgecolor="white",
        markeredgewidth=1.0,
        markersize=7,
        label="ICOS station",
    )
)


footprint_legend = fig.legend(
    handles=footprint_legend_handles,
    title="Grid-cell footprints",
    loc="upper left",
    bbox_to_anchor=(
        0.735,
        0.36
```

```
    ),
    borderaxespad=0,
    fontsize=8,
    title_fontsize=9,
    frameon=True,
)

# 18. CHECK WHAT WAS PLOTTED

print(
    "Products plotted:",
    sorted(products_plotted)
)


print(
    "Stations plotted:",
    station_points[
        station_label_column
    ].tolist()
)

# 19. SAVE AND OVERWRITE
#
# Deliberately:
# - no plt.tight_layout()
# - no bbox_inches="tight"
#
# The legends are already inside the 14 × 9 inch figure canvas.
```

```
# This prevents both the map and legends from being cropped.

fig.savefig(
    OUTPUT_FILE,
    dpi=300,
    facecolor="white",
)



plt.show()



print(
    "Figure overwritten:",
    OUTPUT_FILE
)
```

Diurnal cycles

```
# MEAN DIURNAL CYCLES FOR STATION-SPECIFIC TWO-MONTH PERIODS
# ICOS, GLDAS AND LSA-SAF — LE AND H

import numpy as np
import pandas as pd
import matplotlib.pyplot as plt
from pathlib import Path



# 1. STATION-SPECIFIC YEARS AND PERIODS

station_config = {
```

"BE-Bra": {
"years": [2017, 2018, 2022],
"periods": {
"March–April": [3, 4],
"June–July": [6, 7],
"August–September": [8, 9],
},
},

"BE-Lon": {
"years": [2018, 2019, 2022],
"periods": {
"April–May": [4, 5],
"June–July": [6, 7],
"August–September": [8, 9],
},
},

"BE-Vie": {
"years": [2018, 2019, 2022],
"periods": {
"May–June": [5, 6],
"July–August": [7, 8],
"September–October": [9, 10],
},
},

"BE-Dor": {

```
        "years": [2017, 2022],
        "periods": {
            "May–June": [5, 6],
            "July–August": [7, 8],
            "September–October": [9, 10],
        },
    },
}


# Names that may occur in GLDAS or LSA-SAF
STATION_NAME_MAP = {
    "Brasschaat": "BE-Bra",
    "Dorinne": "BE-Dor",
    "Lonzee": "BE-Lon",
    "Vielsalm": "BE-Vie",
    "BE-Bra": "BE-Bra",
    "BE-Dor": "BE-Dor",
    "BE-Lon": "BE-Lon",
    "BE-Vie": "BE-Vie",
}


# 2. HELPER FUNCTIONS

def find_column(df, possible_names, description):
    """
    Return the first matching column from a list of possible names.
    """
```

```
    for column in possible_names:
        if column in df.columns:
            return column

    raise ValueError(
        f"No column found for {description}.\n"
        f"Tried: {possible_names}\n"
        f"Available columns: {df.columns.tolist()}"
    )


def clean_flux(series):
    """
    Convert flux values to numeric and remove FLUXNET missing-value codes.
    """
    values = pd.to_numeric(series, errors="coerce")
    values = values.mask(values <= -9990)

    return values


def standardise_product(product_df, source_name):
    """
    Standardise GLDAS or LSA-SAF to:
    site_id, datetime, source, LE_Wm2, H_Wm2

    Data are resampled to a common 3-hour resolution.
    """
    temp = product_df.copy()
```

```
station_col = find_column(
    temp,
    ["station", "site_id", "site", "Station"],
    f"{source_name} station",
)

time_col = find_column(
    temp,
    ["datetime", "time", "date", "timestamp"],
    f"{source_name} datetime",
)

le_col = find_column(
    temp,
    ["LE_Wm2", "LE", "LE_F_MDS"],
    f"{source_name} LE",
)

h_col = find_column(
    temp,
    ["H_Wm2", "H", "H_F_MDS"],
    f"{source_name} H",
)

temp["datetime"] = pd.to_datetime(
    temp[time_col],
    errors="coerce",
)
```

```
temp["site_id"] = (
    temp[station_col]
    .astype(str)
    .str.strip()
    .map(STATION_NAME_MAP)
)

temp["LE_Wm2"] = clean_flux(temp[le_col])
temp["H_Wm2"] = clean_flux(temp[h_col])

temp = (
    temp[
        [
            "site_id",
            "datetime",
            "LE_Wm2",
            "H_Wm2",
        ]
    ]
    .dropna(subset=["site_id", "datetime"])
    .sort_values(["site_id", "datetime"])
    .drop_duplicates(subset=["site_id", "datetime"])
    .copy()
)

product_parts = []

for site, sub in temp.groupby("site_id"):
```

```
        sub = (
            sub
            .set_index("datetime")
            .sort_index()
        )

        flux_3h = (
            sub[["LE_Wm2", "H_Wm2"]]
            .resample("3h")
            .mean()
            .reset_index()
        )

        flux_3h["site_id"] = site
        flux_3h["source"] = source_name

        product_parts.append(flux_3h)

    if not product_parts:
        return pd.DataFrame(
            columns=[
                "site_id",
                "datetime",
                "source",
                "LE_Wm2",
                "H_Wm2",
            ]
        )
```

```
    return (
        pd.concat(product_parts, ignore_index=True)
        .sort_values(["site_id", "datetime"])
        .reset_index(drop=True)
    )


# 3. PREPARE ICOS AT 3-HOURLY RESOLUTION

icos_parts = []

for site, original_df in ICOS_HH.items():

    if site not in station_config:
        continue

    temp = original_df.copy()

    time_col = find_column(
        temp,
        [
            "datetime",
            "TIMESTAMP_START",
            "date",
            "time",
        ],
        f"ICOS datetime for {site}",
    )
```

```
if time_col == "TIMESTAMP_START":
    temp["datetime"] = pd.to_datetime(
        temp[time_col].astype(str),
        format="%Y%m%d%H%M",
        errors="coerce",
    )
else:
    temp["datetime"] = pd.to_datetime(
        temp[time_col],
        errors="coerce",
    )

temp["LE_Wm2"] = clean_flux(temp["LE_F_MDS"])
temp["H_Wm2"] = clean_flux(temp["H_F_MDS"])

temp = (
    temp[
        [
            "datetime",
            "LE_Wm2",
            "H_Wm2",
        ]
    ]
    .dropna(subset=["datetime"])
    .sort_values("datetime")
    .drop_duplicates(subset=["datetime"])
    .set_index("datetime")
)
```

```
# Mean of the half-hourly ICOS observations in every 3-hour block
means_3h = (
    temp[["LE_Wm2", "H_Wm2"]]
    .resample("3h")
    .mean()
)

# Six half-hour observations are theoretically available per 3-hour block.
# Retain a block only when at least four valid observations are present.
counts_3h = (
    temp[["LE_Wm2", "H_Wm2"]]
    .resample("3h")
    .count()
)

means_3h.loc[
    counts_3h["LE_Wm2"] < 4,
    "LE_Wm2",
] = np.nan

means_3h.loc[
    counts_3h["H_Wm2"] < 4,
    "H_Wm2",
] = np.nan

means_3h = means_3h.reset_index()
means_3h["site_id"] = site
means_3h["source"] = "ICOS"
```

```
    icos_parts.append(means_3h)


ICOS_3H = (
    pd.concat(icos_parts, ignore_index=True)
    .sort_values(["site_id", "datetime"])
    .reset_index(drop=True)
)


# 4. PREPARE GLDAS AND LSA-SAF

GLDAS_3H = standardise_product(
    gldas,
    source_name="GLDAS",
)

LSASAF_3H = standardise_product(
    lsa,
    source_name="LSA-SAF",
)


# 5. COMBINE ALL PRODUCTS

standard_columns = [
    "site_id",
    "datetime",
```

```python
    "source",
    "LE_Wm2",
    "H_Wm2",
]

ALL_FLUXES_3H = (
    pd.concat(
        [
            ICOS_3H[standard_columns],
            GLDAS_3H[standard_columns],
            LSASAF_3H[standard_columns],
        ],
        ignore_index=True,
    )
    .dropna(subset=["site_id", "datetime"])
    .sort_values(
        [
            "site_id",
            "datetime",
            "source",
        ]
    )
    .reset_index(drop=True)
)

ALL_FLUXES_3H["year"] = ALL_FLUXES_3H["datetime"].dt.year
ALL_FLUXES_3H["month"] = ALL_FLUXES_3H["datetime"].dt.month
ALL_FLUXES_3H["hour"] = ALL_FLUXES_3H["datetime"].dt.hour
```

```
print("Combined dataset created:", ALL_FLUXES_3H.shape)

display(
    ALL_FLUXES_3H.head()
)


# 6. PLOT SETTINGS

PRODUCT_ORDER = [
    "ICOS",
    "GLDAS",
    "LSA-SAF",
]

PRODUCT_STYLE = {
    "ICOS": {
        "color": "black",
        "linestyle": "-",
        "marker": "o",
    },
    "GLDAS": {
        "color": "tab:blue",
        "linestyle": "-",
        "marker": "s",
    },
    "LSA-SAF": {
        "color": "tab:red",
```

```
        "linestyle": "-",
        "marker": "^",
    },
}

VARIABLE_SETTINGS = {
    "LE": {
        "column": "LE_Wm2",
        "label": r"Latent heat flux, LE (W m$^{-2}$)",
        "short_label": "LE",
    },
    "H": {
        "column": "H_Wm2",
        "label": r"Sensible heat flux, H (W m$^{-2}$)",
        "short_label": "H",
    },
}

HOURS = np.arange(0, 24, 3)



# Change this folder when you want the plots somewhere else.
OUTPUT_FOLDER = Path("diurnal_cycle_figures")
OUTPUT_FOLDER.mkdir(parents=True, exist_ok=True)



# 7. PLOTTING FUNCTION

def plot_station_diurnal_cycles(station, variable):
```

```
config = station_config[station]
years = config["years"]
periods = config["periods"]

variable_column = VARIABLE_SETTINGS[variable]["column"]
variable_label = VARIABLE_SETTINGS[variable]["label"]
short_label = VARIABLE_SETTINGS[variable]["short_label"]

n_rows = len(years)
n_columns = len(periods)

fig, axes = plt.subplots(
    nrows=n_rows,
    ncols=n_columns,
    figsize=(5.2 * n_columns, 3.7 * n_rows),
    sharex=True,
    sharey=True,
    squeeze=False,
)

station_data = ALL_FLUXES_3H[
    ALL_FLUXES_3H["site_id"] == station
].copy()

for row_index, year in enumerate(years):

    for column_index, (period_name, months) in enumerate(periods.items()):
```

```
ax = axes[row_index, column_index]

selected = station_data[
    (station_data["year"] == year)
    & (station_data["month"].isin(months))
].copy()

for product in PRODUCT_ORDER:

    product_data = selected[
        selected["source"] == product
    ]

    diurnal_mean = (
        product_data
        .groupby("hour")[variable_column]
        .mean()
        .reindex(HOURS)
    )

    valid_values = diurnal_mean.notna().sum()

    if valid_values == 0:
        continue

    style = PRODUCT_STYLE[product]

    ax.plot(
        HOURS,
```

```
        diurnal_mean.values,
        label=product,
        color=style["color"],
        linestyle=style["linestyle"],
        marker=style["marker"],
        linewidth=1.8,
        markersize=4.5,
    )

ax.axhline(
    0,
    color="grey",
    linewidth=0.8,
    alpha=0.6,
)

ax.grid(
    True,
    alpha=0.25,
)

ax.set_xticks(HOURS)
ax.set_xlim(0, 21)

# Column titles only above the first row
if row_index == 0:
    ax.set_title(
        period_name,
        fontsize=12,
```

```
            fontweight="bold",
        )

    # Year label at the left of every row
    if column_index == 0:
        ax.set_ylabel(
            f"{year}\n\n{variable_label}",
            fontsize=10,
        )

    if row_index == n_rows - 1:
        ax.set_xlabel(
            "Hour of day",
            fontsize=10,
        )

    if selected.empty:
        ax.text(
            0.5,
            0.5,
            "No data",
            transform=ax.transAxes,
            ha="center",
            va="center",
            fontsize=11,
        )

# Obtain one common legend
handles = []
```

```
labels = []

for ax in axes.flat:
    current_handles, current_labels = ax.get_legend_handles_labels()

    for handle, label in zip(current_handles, current_labels):
        if label not in labels:
            handles.append(handle)
            labels.append(label)

if handles:
    fig.legend(
        handles,
        labels,
        loc="upper center",
        bbox_to_anchor=(0.5, 0.985),
        ncol=len(labels),
        frameon=False,
    )

fig.suptitle(
    f"{station} — Mean diurnal cycle of {short_label}",
    fontsize=15,
    fontweight="bold",
    y=1.015,
)

fig.tight_layout(
    rect=[0, 0, 1, 0.96]
```

```
    )

    output_file = (
        OUTPUT_FOLDER
        / f"{station}_{short_label}_mean_diurnal_cycles.png"
    )

    fig.savefig(
        output_file,
        dpi=300,
        bbox_inches="tight",
    )

    plt.show()
    plt.close(fig)

    print("Saved:", output_file)


# 8. CREATE ALL FIGURES

for station in station_config:

    plot_station_diurnal_cycles(
        station=station,
        variable="LE",
    )

    plot_station_diurnal_cycles(
```

```
    station=station,
    variable="H",
)
```